INFORMATION TO USERS

This manuscript has been reproduced from the microfilm master. UMI films the text directly from the original or copy submitted. Thus, some thesis and dissertation copies are in typewriter face, while others may be from any type of computer printer.

The quality of this reproduction is dependent upon the quality of the copy submitted. Broken or indistinct print, colored or poor quality illustrations and photographs, print bleedthrough, substandard margins, and improper alignment can adversely affect reproduction.

In the unlikely event that the author did not send UMI a complete manuscript and there are missing pages, these will be noted. Also, if unauthorized copyright material had to be removed, a note will indicate the deletion.

Oversize materials (e.g., maps, drawings, charts) are reproduced by sectioning the original, beginning at the upper left-hand corner and continuing from left to right in equal sections with small overlaps.

ProQuest Information and Learning
300 North Zeeb Road, Ann Arbor, MI 48106-1346 USA
800-521-0600

UNIVERSITY OF OKLAHOMA

GRADUATE COLLEGE

NEURAL NETWORK AND ANALYTICAL MODELING OF SLOPE STABILITY

A Dissertation

SUBMITTED TO THE GRADUATE FACULTY

in partial fulfillment of the requirements for the

degree of

Doctor of Philosophy

By

JINGGANG CAO
Norman, Oklahoma
2002

UMI Number: 3062579

UMI Microform 3062579

ProQuest Information and Learning Company
300 North Zeeb Road
P.O. Box 1346
Ann Arbor, MI 48106-1346

NEURAL NETWORK AND ANALYTICAL MODELING OF SLOPE STABILITY

A Dissertation APPROVED FOR THE
SCHOOL OF CIVIL ENGINEERING AND ENVIRONMENTAL SCIENCE

BY

Md. Musharraf Hussain 9/18/02

9/18/02

K. K. M 9/20/02

ACKNOWLEDGEMENTS

I wish to express my deepest gratitude and appreciation to my supervisor, Dr. Musharraf M. Zaman, for his personal care, continuous guidance, patience, friendship and support throughout my Ph.D. program. Without his active involvement, encouragement and thoughtful suggestions this work could not be completed.

I would like to acknowledge Dr. Kanthasamy Muraleetharan, Dr. May Yuan, Dr. Luther White and Dr. Mazen Kanj for their time on serving on my dissertation committee, advice and assistance in completion of the dissertation.

My sincerest gratitude is to my wife Chun Bao for her constant encouragement, help and support to achieve this goal. My gratitude also is to our son Charles B. Cao, my parents and parents-in-law and other family members for their moral support. My special appreciation is due to Mr. Fred Balster for his encouragement and assistance during the course of this study.

TABLE OF CONTENTS

LIST OF TABLES

LIST OF FIGURES

LIST OF SYMBOLS

a = output vector

b = bias vector

b = width of slice

c = cohesion of soil

c' = effective cohesion of soil

d = depth of slip block

d = depth of firm base

d_w = depth of phreatic surface above failure plane

E_n, E_{n+1} = vertical interslice forces

E = Young's modulus

F = transfer function

F_s = factor of safety of slope

F_f = force equilibrium

F_m = moment equilibrium

$f(x)$ = function of interslice shear force and normal force

g = acceleration due to gravity

h = height of a soil layer

H = height of slope

H_t = height of tension cracks at crest of slope

H_w = height of water level

I'_s, I'_c = integral functions

k = seismic coefficient

k_h, k_v = horizontal and vertical seismic coefficients

m = mass of soil

LIST OF SYMBOLS (CONTINUED)

m_α = integral function

M_r = resisting moment about the center of circle

M_s = sliding or disturbing moment about the center of circle

n = a given slice

N = resolved forces of normal components

N = shearing resistance when failure occurs

n = vector direction

$O(a, b)$ = center of circular slip surface.

p = input vector

P = a point in an n-dimensional space

q = surcharge on crest of slope

Q = resultant of interslice forces

r = radius

R = resisting force

R = number of inputs

S = number of neurons

T = downslope slide force

tp = training parameters

u = pore water pressure acting on the base of a slice

w = weight matrix

W = weight of slice

X_n, X_{n+1} = horizontal interslice forces

X_l, X_r = interslice forces

ΔX = difference of interslice forces

y_1, y_2, y_3 = line equations in (x, y) plane

LIST OF SYMBOLS (CONTINUED)

$\hat{y}$ = function of weights

Z = resultants of interslice forces

α = inclination of failure surface

β = inclination of slope

γ = _unit weight of soil

γ_w = unit weight of water

ε = Poisson's ratio

θ = inclination of slip surface

ϕ = friction angle of soil

ϕ' = effective friction angle of soil

λ = scaling factor

τ_f = average shear strength of soil

τ_d = average shear stress along potential failure surface

τ_m = shear stress mobilized along failure surface

ABSTRACT

A semi-analytical method is developed for analysis of slope stability involving cohesive and non-cohesive soils. For sandy slopes, a planar slip surface is employed. For clayey slopes, circular slip surfaces are employed including Toe Failure, Face Failure and Base Failure resulting from different locations of a hard stratum. Earthquake effects are considered in an approximate manner in terms of seismic coefficient-dependent forces. The proposed method can be viewed as an extension of the method of slices, but it provides a more accurate treatment of the forces because they are represented in an integral form. Also, the minimum factor of safety is obtained by using the Powell's optimization technique rather than by a trial and error approach used commonly. The results (factor of safety) from the proposed semi-analytical method developed in this study are compared with the solutions by the Bishop method (1952) and the finite element method, and satisfactory agreements are obtained. The proposed method is simpler and more straightforward than the Bishop method and the finite element method. Also, it is found to be as good as or better than traditional slope stability analysis methods.

An artificial neural network is also introduced in this study, as an alternate approach, for modeling slope stability. The proposed neural network model is a two-layer recurrent neural network (RNN) with a sigmoid hidden layer and a linear output layer. The model is developed by using data from 124 slopes collected for this study. The input variables include the parameters that contribute to the failure of

a slope and include the height of a slope, the inclination of slope, the height of water level, the height of tension cracks at crest of slope, the depth of firm base, horizontal and vertical seismic coefficients, the unit weight of soil, the cohesion of soil, the friction angle of soil, the thickness of each layer, and the pore water pressure ratio which is defined as the ratio of the pore water pressure to the overburden pressure for a given layer. The output layer is a single linear neuron – the factor of safety of a slope. Training is performed on the 104 slope data randomly selected from the 124 slopes and prediction or evaluation is based on the remaining 20 slopes. Statistical analyses performed show that the results from the proposed RNN model are closer to the finite element method than to the Bishop method and the proposed semi-analytical method. A separate RNN model is developed to determine circular slip surfaces by retraining the proposed neural network model with three neurons in the output layer, namely the coordinates of the center and the radius of the circular slip surface. In comparison with the proposed semi-analytical method, the proposed RNN model is found to be more effective in representing relatively complex slopes with layered soils and/or pore water pressures.

CHAPTER 1

INTRODUCTION

1.1 Introduction

Slope stability has been a subject of continued concern because of tremendous loss of properties and infrastructure caused annually by slope failures in North America and other places in the world (Bishop and Morgenstern, 1960; Haug et al., 1976; Schuster, 1978; Hansbo et al., 1985; Leshchinsky and Huang, 1992; Gottardi et al., 1998; Shioi and Sutoh, 1999; Zhang, 2001). In the United States of America alone, it is estimated that the direct and indirect costs of slope failures exceed $1 billion per year (Bjerrum, 1967; Brunsden and Prior, 1984; National Research Council, 1985; Fredlund and Scoular, 1999). It is therefore important to develop more effective methods for the assessment of slope failures through evaluation of factor of safety.

Slope failures, also referred to as slides or landslides, whether sudden or gradual, are due to overstress of the slope or foundation materials with respect to their available strength (Morgenstern 1963; Davis, 1968; Ching and Fredlund, 1983; Abramson, 1996; Dai et al., 2000). Overstresses may occur due to the following:

1) factors causing an increase in shear stress (e.g., external loads, steepening of slope, undercutting of a slope at the toe, sudden drawdown, earthquakes);
2) factors causing a decrease in shear strength (e.g., liquefaction triggered by shock or dynamic forces, saturation of a slope particularly in desiccated soils, other factors that increase excess pore water pressure);

3) hydrodynamic forces (such as earthquake-induced waves, seepage forces);

4) hydrostatic forces (such as tension cracks filled with water in fissured clays or desiccated clays, artesian pressures in filled aquifers).

Due to numerous factors affecting slope failures, slope stability analyses have always been a difficult and complex task in geotechnical engineering and geomechanics (Cousins, 1978; Leshchinsky et al., 1985; Wakai and Ugai, 1999). Common practice in slope stability analysis involves either neglecting or over-simplifying more complex soil behaviors and properties as well as seismic forces (in case of earthquake-induced slope failures) (Ishihara, 1985; Seed and De Alba, 1986; Liu, 1990; Fredlund and Scoular, 1999).

Traditional methods currently available for analyzing slope stability problems include the Fellenius Method (also called Ordinary Method of Slices or Swedish Method of Slices) (Fellenius, 1927), Bishop Method (Bishop, 1955), Janbu's Method (Janbu, 1968, 1973), Morgenstern and Price Method (Morgenstern and Price, 1965), and Spencer's Method (Spencer, 1967, 1968, 1973). These methods share some common features and limitations. All limit equilibrium methods employ assumptions to render a slope stability problem determinate. The methods that consider side forces between slices (e.g., Janbu's method) are generally subjected to numerical instability problems under certain conditions (Duncan, 1996). When numerical instability problems arise, the solution may fail to converge, or the calculated values may be unreasonable (Ching and Fredlund, 1983). The procedure

using the sums of the terms (forces) for all slices makes the hand-calculation of factor of safety a repetitive and laborious process (Brunsden and Prior, 1984). Fortunately, a handful of computer codes based on the limit equilibrium methods are now available. These computer codes (such as GeoSlope, Stabl for Windows, and XSLOPE) simplify the process of finding the factor of safety and the most critical slip surface with a direct graphical view (Cheng, 2002).

In recent years, numerical methods have been widely used in slope stability analyses with the unprecedented development of computer hardware and software (Kohgo and Yamashita, 1988; Huang and Yamasaki, 1993; Fredlund and Scoular, 1999; Cheng et al., 2000). Both finite difference methods and finite element methods may be used for the solution of non-linear problems. As pointed out by Cundall (1976) and Leshchinsky et al. (1985), the equations which result from using a particular finite difference scheme can be same as those from a finite element scheme, if a particular integration method is employed. Although these numerical methods are more complex to use than the conventional limit equilibrium methods, they nevertheless can provide an insight into the way a slope will deform and fail (Snitbahn and Chen, 1976, 1978; Booker and Small, 1981; Leshchinsky and Huang, 1992; Cheng et al., 2000). Such information is quite valuable in addition to the information (factor of safety, slip surface) obtained from traditional methods. Although finite element analyses are capable of modeling field conditions (complex geometry, soil properties) realistically, they usually require significant effort and

cost that may not be justified in some cases (Chen and Chameau, 1982; Duncan, 1996).

In this study, semi-analytical and artificial neural network (ANN) models are developed for slope stability analysis. The semi-analytical solutions simplify the process of calculating and finding the minimum factors of safety. The proposed semi-analytical method can be viewed as an extension of the method of slices, but it provides a more accurate treatment of the associated forces because they are represented in an integral form. Also, the factor of safety is obtained by using a minimization technique rather than by a trial and error approach used commonly. The semi-analytical solutions presented here may be useful for analyzing simple slopes. They could also be used for validating results obtained from other approaches and providing initial estimates for complex slopes before more rigorous and costly analyses such as finite element method are adopted.

Since many factors are involved in modeling slope stability, physics-based models can have difficulties in representing real-life situations and in considering such important factors as slope geometry and soil properties affecting the stability of slopes (Bishop, 1971, Pentz, 1982; Bernander and Gustass, 1984; Jiao et al., 2000). Additionally, physics-based models usually require data pertaining to geometric and soil properties that may not be available and/or justified in some cases (Booker and Davis, 1972; Hunt, 1986; Liu et al., 1988). The neural network approach can be a useful modeling tool in such situations. Among important attributes, neural network

models are based on laboratory and/or field data and thus it is easier to include the factors affecting slope stability in such models. Because artificial neural network models have learning capability that physics-based models do not have, they can model slopes with a reasonable accuracy even when some data pertaining to geometric and/or soil properties are unavailable. The neural network method as adopted in this study is based on the field and laboratory data including geometry, soil properties (e.g., shear-strength), and actual failure or slip surface data collected from field. Field case history data available at geotechnical engineering firms as well as case studies that have been reported in the literature were collected in this study to develop a database for the neural network modeling (architecture, training) effort. Slope stability analyses using finite element methods that are available in the literature contributed to the database. Also, they provided a basis for comparison of the neural network model performance.

1.2 Objectives

In this study, semi-analytical method and artificial neural network modeling approach are used for analyses of slopes. Two different modeling approaches are pursued because for certain class of problems (e.g., slopes with some data unavailable) one method may be more preferable than the other. The specific goals of this study include the following:

(i) Develop semi-analytical solutions for slope stability analysis;

(ii) Develop an artificial neural network (recurrent network)-based model for analysis of slope stability;

(iii) Explore the strengths and weaknesses of each method (Semi-analytical method, ANN-based method) with respect to physics-based methods, namely the finite element method and the traditional limit equilibrium methods (e.g., the Bishop method).

1.3 Format of the Dissertation

Following the introduction to slope stability problems in Chapter 1, a detailed literature review of the methods of slope stability analysis is provided in Chapter 2. Chapter 3 presents the proposed semi-analytical method for calculating the factor of safety in which an integral approach is used to accurately represent the forces in various slices and an optimization technique is used to obtain the critical slip surface. Chapter 4 presents the proposed neural network method for modeling slope stability. Finally, in Chapter 5 summary and conclusions of this study are presented and, recommendations for further studies are discussed.

CHAPTER 2

LITERATURE REVIEW

2.1 Introduction

Different analytical techniques have been developed in the past that may be used by engineers when assessing whether a particular natural or man-made slope is stable under a given state of conditions (e.g., short-term, long-term). One of the earliest analyses, which is still used today in many applications involving earth pressure, was proposed by Coulomb in 1773. Coulomb's approach for earth pressures against retaining walls used plane sliding surfaces, that was extended to analysis of slopes in 1820 by Francis. By about 1840, experience with cuttings and embankments for railways and canals in England and France began to show that many failure surfaces in clay were not plane, but significantly curved (Brunsden and Prior, 1984). In 1916, curved failure surfaces were again reported from the failure of quay structures in Sweden (Petterson, 1956). In analyzing these failures, cylindrical surfaces were used and the sliding soil mass was divided into a number of vertical slices. The procedure is still sometimes referred to as the 'Swedish Method of Slices' (Walker and Fell, 1987). The practice of dividing a sliding mass into a number of slices is still in use, and it forms the basis of many modern analyses (Duncan, 1996). By mid-1950s further attention was given to the methods of analysis using circular and non-circular sliding surfaces (Bishop, 1955; Petterson, 1956). In carrying out such analyses, an appropriate means needs to be selected. Table 2–1 presents a summary of typical traditional methods of slope stability analysis.

Table 2-1 Features of Traditional Methods

Method	Features
Sliding Block	Can be used for typical planar failure surfaces. Well-suited to many rock slopes and some soil slopes. Graphical solutions possible in simple cases.
Fellenius Method (Fellenius, 1927)	Inter-slice forces ignored. Normal force on base of slice obtained by resolving total forces normal to base. Underestimates factor of safety. Errors (on the safe side) large for deep failure masses with high pore pressures. Effective normal stresses on the bases of some slices can become negative. F_s is defined as the ratio of resisting to disturbing moments or forces. Calculation simple, no iteration required. Applicable to circular failure surfaces.
Bishop Method (Bishop, 1955)	Inter-slice forces ignored. Normal force on slice base obtained by resolving forces on slice vertically. Gives fairly accurate results but is restricted to slip surfaces of circular shape. Iterative procedure required for solution but rapid convergence usually obtained. Useful for hand calculations. Errors possible where portion of slip surface has steep negative slope near toe. Calculation of normal forces on slip surface possible.
Janbu Method (Janbu, 1968)	Requires assumption of inter-slice forces. Iterations made with successive sets of inter-slice forces till convergence reached. Suitable for slip surfaces of arbitrary shape. Convergence generally rapid but sometimes slow due to large changes in inter-slice forces between iterations. Necessary to check acceptability of solution in terms of position of line of thrust. Any implied tension or violation of failure criterion of solution to be regarded as rigorous.
Morgenstern-Price Method (Morgenstern and Price, 1965)	Versatile method which satisfies both force equilibrium and moment equilibrium and accounts for inter-slice forces which must be assumed. Side force inclinations assumed to vary linearly across each slice. Applicable to failure surfaces of arbitrary shape and arbitrary boundary conditions but computer is essential. F_s determined by numerical methods. Acceptability of solution must be checked. Considerable experience and judgment required.
Spencer Method (Spencer, 1967)	Originally devised for circular failure surfaces, but adapted for non-circular failure surfaces. Assumes inter-slice forces to be parallel. Accuracy acceptable. Satisfies both force and moment equilibria. Use of computer desirable. Specially devised in relation to embankment stability problems, but may used for other problems.

Note: In all methods except the Fellenius Method above, factor of safety, F_s, is defined as the ratio of unit shear strength available at a point to unit shear strength mobilized or required at the same point. F_s is assumed constant along a slip surface.

In selecting a particular method of analysis, the reliability and quantity of soil data, the knowledge of the slope geology and the consequences of failure should all be considered (Anderson and Richards, 1987). The results of an analysis are usually presented as a "factor of safety" (i.e. the ratio of available strength to mobilized strength). One must decide whether to use "total stress parameters" or "effective stress parameters" based on field conditions with respect to pore water, drainage, and duration of loading.

The limiting equilibrium methods are still very popular methods of slope stability analysis in use today; this popularity is partly due to the simplicity and ease of use of such methods (Duncan, 1996). Computer codes based on the limiting equilibrium methods further simplify the process of finding the solution for a given slope. Also, the geotechnical engineering profession has gained significant experience in their use (Brunsden and Prior, 1984). Of these methods, the method of slices used with a circular failure surface is probably the most popular one, as circles are convenient for analysis and often approximate the observed failure surface (Abramson, 1996).

In the past three decades, there has been a growing awareness of the applications of numerical methods (finite difference method, finite element method) to engineering slope designs (Tavenas et al., 1980; Ching and Fredlund 1983; Donald and Giam 1988; Huang et al., 1989). Cundall (1976) applied finite difference method to slope stability analyses. In his study, Cundall (1976) found that the equations that resulted from using a particular finite difference scheme were

same as those that resulted from finite element schemes, if particular integration methods were employed. Duncan and Dunlop (1969) employed the finite element method and the simulation of sequential slope excavation to study the effect of coefficient of lateral earth pressure on stability. Subsequently, Dunlop and Duncan (1970) expanded their method using a bilinear stress-strain relationship to study the development of failure around excavated slopes. More recently, Donald and Giam (1988) used nodal displacements obtained from the finite element analysis to determine the stability of slopes. Giam and Donald (1988) presented an approach that used an automatic search scheme to locate the critical slip surface on the basis of stress-strain calculations. Huang et al. (1989, 1992) described a theoretical approach that defined the failure surface in a slope by employing the concept of minimum factors of safety against local failures.

These numerical methods are able to model the stress-strain behavior of a soil and therefore should be capable of reproducing the actual slope behavior much more closely than the limit equilibrium methods (Huang et al., 1992). However, they are limited by the fact that they are generally difficult to use, and require significant data preparation time on the part of the user. Also, these methods require significant computing time. As a result, in practice, the quick and simple limit equilibrium methods have enjoyed widespread use, with numerical methods being employed for cases where it is necessary to know how a slope may behave due to excavation or loading or where advanced stress-strain models for the soil are needed (Duncan, 1996; Shioi and Sutoh, 1999).

2.2 Planar Failure Surface

A slope that is uniform and very long relative to the depth of the potentially unstable layer may often be analyzed as a planar-failure slope. The general model is shown in Figure 2–1.

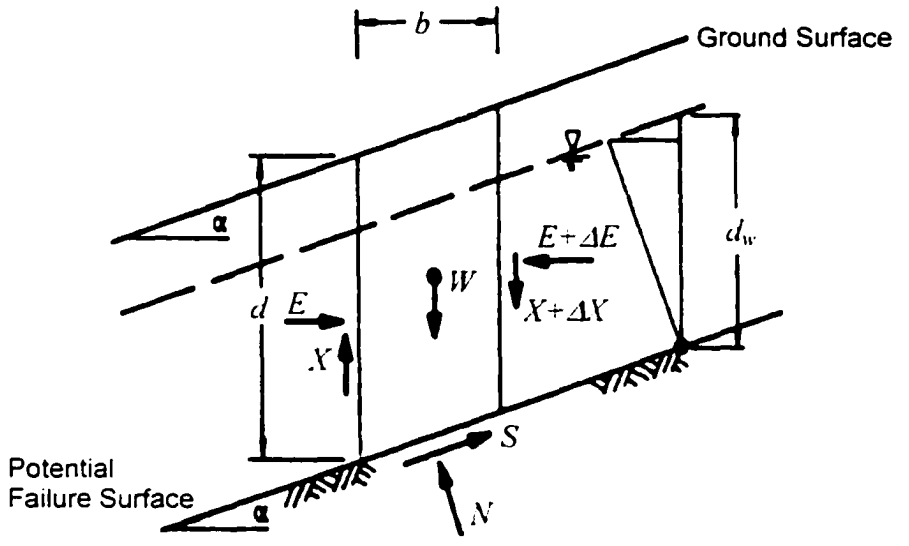

Figure 2–1 Forces Acting on a Vertical Slice (Mostyn and Small, 1987)

As can be seen, the failure plane is taken to be parallel to and at a depth, d, below the ground surface having an inclination α with the horizontal. The assumption that the slope is very long and uniform implies that any vertical slice is similar to all others. Thus, the side forces must be equal in magnitude, opposite in direction and co-linear. Groundwater flow is usually taken to be parallel to the ground surface with the phreatic surface at a distance, d_w, above the failure plane. For a material

with a Mohr-Coulomb failure criterion the factor of safety, F_s, of the slope is given by the following expression (Das, 1994):

$$F_s = \frac{c' + (\gamma d - \gamma_w d_w)\cos^2 \alpha \tan \phi'}{\gamma d \sin \alpha \cos \alpha} \qquad (2\text{–}1)$$

where c' is the effective cohesion of soil, γ is the unit weight of soil, γ_w is the unit weight of water and ϕ' is the effective angle of friction.

The derivation of the factor of safety for a slope with planar failure surface is presented in most textbooks on soil mechanics (e.g. Lambe & Whitman, 1979; Das, 1994) or slope stability (e.g. Bromhead, 1986). The effective cohesion is often ignored, or assumed to be zero, in which case Equation 2–1 simplifies to:

$$F_s = \left(1 - \frac{\gamma_w d_w}{\gamma d}\right) \frac{\tan \phi'}{\tan \alpha} \qquad (2\text{–}2)$$

If the water table is at or below the failure plane (i.e. a dry slope) then the slope is at limiting equilibrium (i.e. $F_s = 1$) when the slope angle equals the effective angle of friction. If the water table is at the surface (i.e. a saturated slope) then the slope angle at limiting equilibrium is near half the effective angle of friction (for typical friction angles and unit weights).

2.3 Circular Failure Surface

For many slope failures, the surfaces along which sliding took place were found to be non-planar or curved leading to the idea of using curved failure surfaces for the analysis of slope stability (Spencer, 1973; Chen and Shao, 1988). Although the actual failure surfaces in most cases are bowl shaped (if we consider three-

dimensional geometry), the representation of a failure surface as a single curve (in two dimension) greatly simplifies the analysis.

Early solutions for circular surfaces were obtained by Fellenius (1927) who used the method of slices, and by Taylor (1937, 1948) who used a friction circle method to produce charts of "Stability Numbers" to determine factors of safety against slope failure. Most modern circular slip circle methods make use of the method of slices, and the major differences between these methods involve the way in which the unknown quantities that arise in the analyses are dealt with. Some of the methods for analysis of circular failure surfaces using the method of slices are presented in the following section for completeness.

2.3.1 Fellenius Method

The simplest of all the methods which make use of vertically-sided slices is the Fellenius (1927) method. Figure 2–2 shows the region above the assumed circular failure surface divided into slices and a free body diagram of a single slice with all of the forces acting on it, and the unknown points of application of the forces. As there are too many unknowns to obtain a solution, some assumptions must be made about the forces and their locations. The interslice forces (X_n , X_{n+1}; E_n, E_{n+1}) are assumed to be equal and opposite to each slice and therefore they cancel each other. Taking moments about the center of the circle and assuming that everywhere along the failure surface the amount of shear stress mobilized τ_m is the same fraction of the total shear stress available (i.e. $\tau_m = (c' + \sigma' \tan\phi')/F$), we obtain:

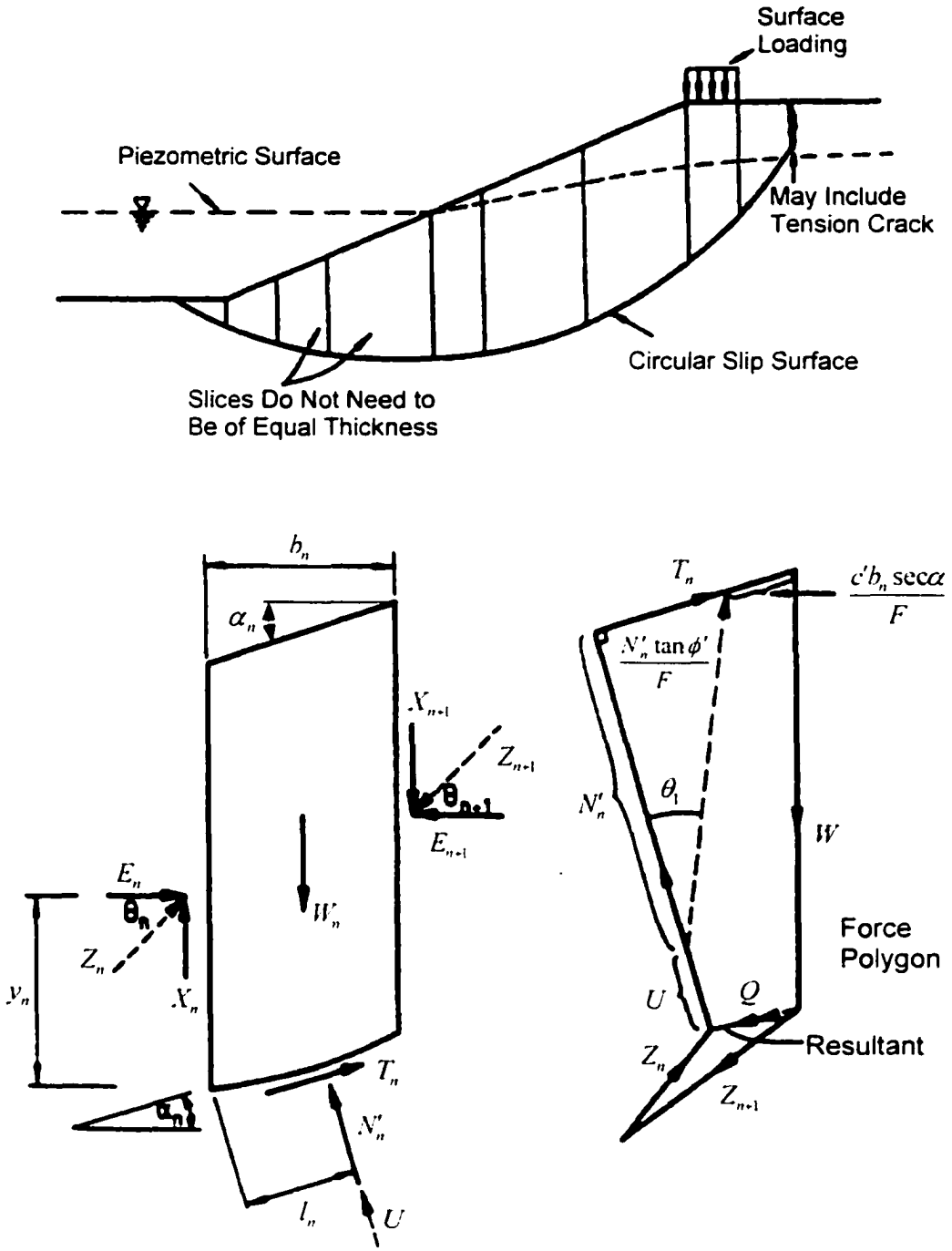

Figure 2–2 Circular Failure Surface and Forces Acting on a Single Slice

(Fellenius. 1927)

$$F_s = \frac{\sum[c'b\sec\alpha + (W\cos\alpha - ub\sec\alpha)\tan\phi')]}{\sum W\sin\alpha} \qquad (2\text{–}3)$$

where c' is the effective cohesion, b is the slice width, α is the angle of the base of the slice to the horizontal, W is the total weight of the slice, u is the water pressure acting on the base of the slice, ϕ' is the effective angle of friction, and the summation implies an addition over all slices.

2.3.2 Bishop Method

Bishop (1955) presented a method in which the interslice forces X and E were taken into account in the analysis. For a mathematically correct static solution, equilibrium of forces and moments must exist for each slice as well as for all of the slices. Bishop's rigorous formulation contains too many unknowns to enable a direct solution (Felio et al., 1984). Some assumptions must be made regarding the distribution of some of the unknown quantities, and for this method assumptions are made concerning the distribution of X force. The position of the line of thrust y_t (see Figure 2–3) of these X forces must be such that the moment equilibrium of each slice is maintained. As pointed out by Sarma (1979), Bishop did not consider the point of action of the normal force on the base of the slice, thereby eliminating another group of unknowns for the problem.

Using Bishop's original and now somewhat familiar notation, the expression for the factor of safety against a slip failure is expressed as:

$$F = \frac{\sum[c'b + (W - ub + \Delta X)\tan\phi')/m_\alpha]}{\sum W\sin\alpha} \qquad (2\text{–}4a)$$

where

$$\Delta X = X_n - X_{n+1} \tag{2–4b}$$

$$m_\alpha = \cos\alpha\left(1 + \frac{\tan\alpha \tan\phi'}{F}\right) \tag{2–4c}$$

b is the slice width, W is the total weight of the slice, c' is the effective cohesion, ϕ' is the effective angle of friction, u is the water pressure acting on the base of the slice, α is the angle of the base of the slice to the horizontal.

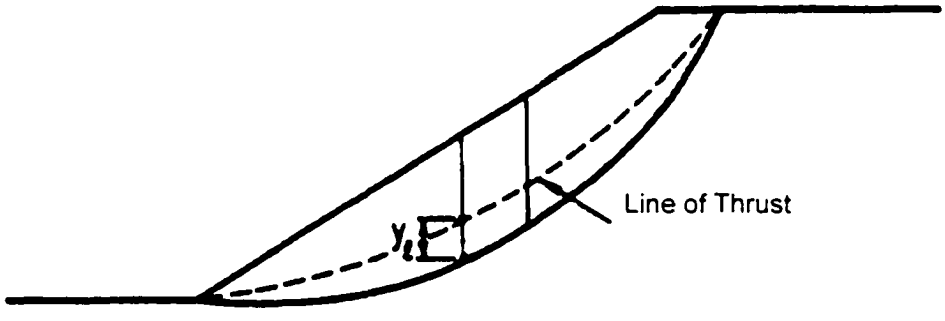

Figure 2–3 Position of Line of Thrust

It may be noted that assumptions about the X forces make the solution process more complex. Therefore, a simplified or modified-version of the Bishop's equation is used by many engineers. It is assumed that the difference in the X forces (i.e. ΔX) for any slice is zero. This type of analysis is adequate enough for most practical purposes (O'Conner and Mitchell, 1977; Hungr, 1987).

Equation 2–4a involves a factor of safety on both sides and so an iterative technique must be used in order to obtain a solution. In practice, this is often done

by computing the factor of safety using the Fellenius method which is then used as an initial value to estimate the quantity m_α which appears in the left hand side of Equation 2–4a. In most cases, if the Fellenius method is used for estimating the factor of safety initially, only 2 or 3 iterations are usually necessary to obtain a converged solution for the simplified Bishop method.

It is also of interest to know the magnitude of error introduced in the analysis by the method of calculating the area of each slice or in calculating the angle of the base inclination and to know the effect of the number of slices used in idealizing the slope to determine the factor of safety. All of these effects have been examined by Ting (1983) using the simplified Bishop method. According to Ting (1983), maximum error occurs when calculating the factor of safety for deep circles in cohesive slopes. With 45 slices, the error is about 10% depending on the method used in computing the area of slice. It is normal to specify between 50 and 100 slices within the region above the potential failure surface to limit errors introduced from such sources. Errors may also be introduced when a slice lies across the boundary between two different materials. Some computer codes adjust slice thicknesses to account for this, while others rely on the usage of a large number of slices of equal thickness so that the effect becomes small.

2.3.3 Spencer's Method

An alternative way of taking into account the interslice forces was proposed by Spencer (1967). It was noted that if resultants Z of the interslice forces were parallel

and all inclined at a constant angle, θ, then the resultant of the two interslice forces Q (see Figure 2–2) will also be inclined at an angle θ. To satisfy overall equilibrium, the following equations must be satisfied:

$$\sum(Q\cos\theta)=0 \tag{2–5a}$$

$$\sum(Q\sin\theta)=0 \tag{2–5b}$$

$$\sum(Q\cos(\alpha-\theta))=0 \tag{2–5c}$$

If the angle θ is chosen to be constant for all slices, then Equations 2–5a to 2–5c will reduce to:

$$\sum Q=0 \tag{2–5d}$$

The effect of assuming a constant angle for the interslice force resultants, when in reality it will vary from slice to slice, is claimed to be small by Spencer (1967). It may be shown that the force Q (for a particular slice) is given by the expression:

$$Q=\frac{\frac{c'b}{F_s}\sec\alpha+\frac{\tan\phi'}{F_s}(W\cos\alpha-u\sec\alpha)-W\sin\alpha}{\cos(\alpha-\theta)\left(1+\frac{\tan\phi'}{F_s}\tan(\alpha-\theta)\right)} \tag{2–5e}$$

For any particular value of the angle θ, a factor of safety can be found which satisfies force equilibrium F_f (equation 2–5b) and another factor of safety can be found which satisfies the moment equilibrium F_m (equation 2–5c). A plot of F_f and F_m against θ was presented by Spencer (1967) and is shown in Figure 2–4.

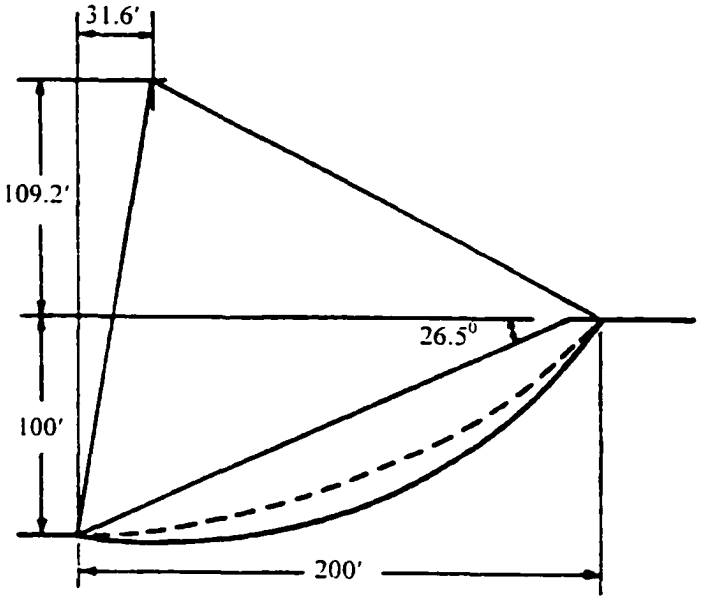

(a) Slope Data

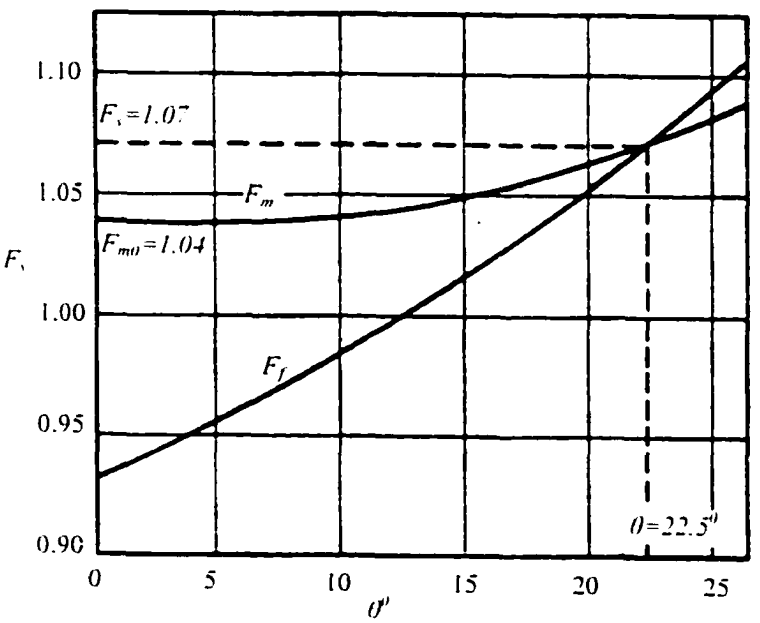

(b) F_s with θ

Figure 2–4 Variation of F_m and F_f with θ (Spencer, 1967)

The required (critical) factor of safety is obtained for the case $F_f = F_m = F_s$. This factor of safety $F_s = 1.07$ and the corresponding value of the interslice force angle $\theta = 22.5^0$ can be used to subsequently determine all the interslice forces and their line of thrust. The difference in the factor of safety obtained using the Spencer's method as compared to Bishop's simplified method is not large. It was noted by Spencer (1968) that the difference between the two methods exceeded 1% in only 7 of the 92 cases attempted.

Spencer (1968) also examined the effect of carrying out his analysis using effective interslice stresses instead of total stresses. It was found that the line of thrust as calculated from the effective stress analysis was often unacceptable. To remedy this, it was necessary to include tension cracks at the top of the slope and to allow for the water pressure in the cracks. The effect of this analysis was to slightly lower the factor of safety and Spencer concluded that the reduction in F_s was, however, very small and the effect of water pressure in a tension crack on the portion of the critical circle was also found to be relatively small.

2.3.4 Obtaining the Most Critical Circle

Whichever of the methods of obtaining the factor of safety is used, a number of trial circles must be taken and analyzed in order to obtain the one that gives the least factor of safety (Baker, 1980). As most analyses are done by computers, the process of analyzing a few hundred trial circles may be relatively quick and inexpensive in today's computing environment (Oboni and Bourdeau, 1983; Abramson, 1996).

Computer programs need some type of algorithm upon which the search for the slip surface with the minimum factor of safety is based. One of the most commonly used methods is to specify a grid on which the centers of trial slip circles lie (see Figure 2–5). Contours of the minimum factor of safety at each center on the grid can be plotted in order to determine where the critical center may lie.

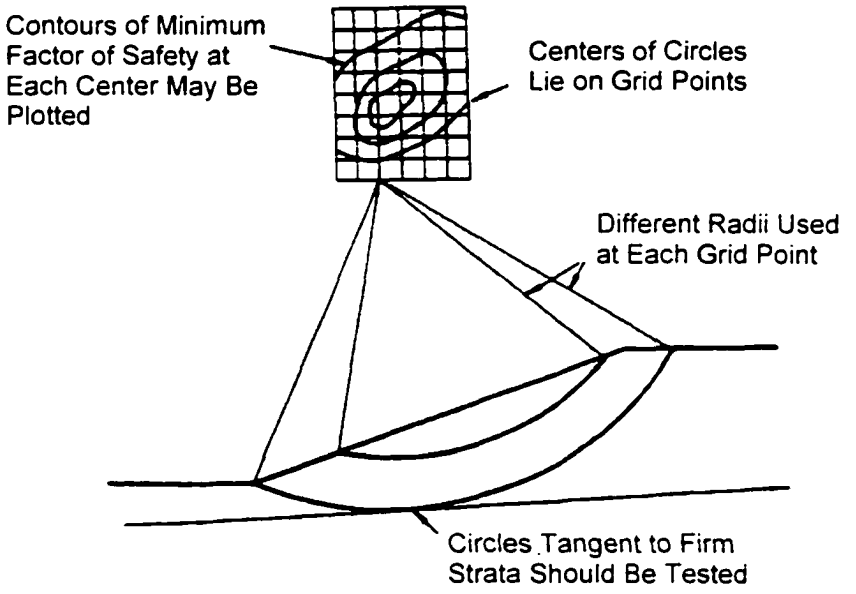

Figure 2–5 Grid Search Pattern (Mostyn and Small, 1987)

The amount of computation required to find the critical circle may be greatly reduced by using a technique by which one can automatically locate the center coordinates and radius of the circle yielding the minimum factor of safety. Such a technique has been described by Boutrup and Lovell (1980), who used the simplex reflection method. To explain how the method works, consider the problem of

finding the minimum factor of safety for a two-dimensional circular slip surface. The problem basically involves finding the coordinates a, b of the center and radius r of the circle which minimize the factor of safety F_s. This is done by evaluating F_s at the four corners of a tetrahedron defined in x, y, r space (i.e. the coordinates of the corners are defined by the values of x, y, r). The value of the factor of safety found at each corner may then be used to decide in which direction to move to obtain a lower factor of safety. Obviously this will be away from the vertex of the tetrahedron with the highest factor of safety. Depending on the coordinates and radii given to start the search, the minimum factor of safety can be found quite quickly.

2.4 Non-Circular Failure Surface

If the shear strength is non-uniform within a slope then the failure surface with the minimum factor of safety will not necessarily be a circle but the shape will depend on the distribution of shear strength (Baker and Garber, 1978; Charles, 1982). Sometimes the general shape of the critical failure surface will be highly constrained by the distribution of weak zones within the slope; other times it may require a lot of insight or work to find the critical surface or at least some surface with similar stability (Baker and Frydman, 1983).

Analysis of circular failure surfaces is easier than that of non-circular or generalized failure surfaces. This is because moments taken about the center of a circular failure surface result in a zero moment arm for the normal forces acting on the failure surface and a constant moment arm for the cohesive forces on the failure surface. Nevertheless the moments for the entire mass or each slice can be taken

about any point or points that are convenient, and failure surface of any shape can be adopted (Zhang and Chen, 1987). This approach is used in analyzing generalized failure surfaces.

As discussed in Section 2.3, the problem is indeterminate and some assumptions need to be made for evaluation of factor of safety. In the simplified method, Bishop (1955) assumed that the interslice shear forces on each side of any slice were equal. The shear forces on most downslope slices are almost always zero (unless there is an applied external shear) and thus Bishop's simplifying assumption is equivalent to setting all the shear forces to zero. The resultant interslice force is horizontal. This assumption renders the problem determinate.

The assumptions made to render the problem determinate are the main differences between the various methods of analysis for generalized failure surfaces (Graham, 1984). The methods generally make some assumption regarding either the location of the interslice resultant force (i.e. the line of thrust, as shown in Figure 2–3), or the magnitude of the interslice shear force (i.e. X_n and X_{n+1} in Figure 2–2). Some methods only satisfy the requirements of force equilibrium, while others satisfy both force and moment equilibria. These latter methods are generally referred to as rigorous methods (Madej, 1984).

It should be noted that the simplified Bishop and Fellenius methods of slices satisfy force equilibrium in one direction and the overall moment equilibrium. Also, the methods that satisfy moment equilibrium give a factor of safety that is relatively independent of the assumption regarding the interslice forces, while those that

satisfy only force equilibrium result in a factor of safety that is quite sensitive to the assumption regarding the interslice force (Fredlund et al., 1981). Some of the methods that are commonly used or have been recently developed to analyze generalized failure surfaces are briefly discussed below.

2.4.1 Janbu's Method

From the mid-50s to the early 70s, Janbu developed generalized and simplified methods which are best described in Janbu (1973). In the generalized method, a line of thrust is assumed and the equations of equilibrium solved. Sarma (1979) pointed out that this is not a rigorous solution because moment equilibrium of the last slice is not satisfied; this affects the line of thrust but does not greatly affect the factor of safety. Janbu (1973) noted that the factor of safety is relatively insensitive to the assumption regarding the location of the line of thrust as long as it is reasonable. According to Janbu (1973), the line of thrust should be near one third the height of the slice for cohesionless soils. It should be below this level in the active zone and above it in the passive zone for cohesive soils. This method sometimes gives answers that differ quite markedly from those obtained by other methods such as Bishop method (Maksimovic, 1979; Li and White, 1986).

Janbu's simplified method is based on satisfying only force equilibrium. It involves completing one iteration of the "rigorous" method to obtain first estimates of the normal stresses on the base of the slices and of the interslice forces (Mostyn and Small, 1987). The result derived from this first iteration is then multiplied by a correction factor that depends on the curvature of the failure surface and the

material parameters. These correction factors are based on limited comparisons of analyses of homogenous slopes with his "rigorous" method. Lumsdaine and Tang (1982) reported that, for more complex problems, there is very little correlation between the correction factors given by Janbu and "true" correction factors derived by using Janbu's rigorous method to solve the same problem. Janbu (1973) recommended that his simplified method should only be used when computers were not available and an estimate of the factor of safety was to be obtained by hand calculations. Thus, although there are many computer implementations of this method, it is hard to envisage an occasion where it would now be appropriate to use this method in lieu of other readily available computer-based methods.

2.4.2 Morgenstern-Price Method

This is perhaps the best known and most widely used method developed for analyzing generalized failure surfaces. The method was initially described by Morgenstern and Price (1965). It satisfies all static equilibrium requirements and is, therefore, a rigorous method, but the solution obtained must be checked for acceptability. The overall problem is made determinate by assuming a functional relationship between the interslice shear force and the interslice normal force. The function is referred to as $f(x)$ and most programs implementing the method provide a choice of such functions. Choosing such a function actually overdetermines the problem and thus part of the solution process is to determine a scaling factor, λ. The function $f(x)$ defines the relative inclination of the interslice forces, while λ

defines their absolute magnitude. Thus, the interslice forces on the left hand side of slice n in Figure 2–2 are related by the following equation:

$$X_n = \lambda * f(x) * E_n \qquad (2\text{–}6)$$

The solution procedure proposed by Morgenstern and Price (1965) differs from that adopted by most investigators in that the problem was formulated using differential equations that were integrated over each slice. The derivation of the governing equations, the equations themselves and the method of solving the equations are all quite complex (Fan et al., 1986).

The Morgenstern-Price method is generally implemented on computers; output should include adequate data to determine the admissibility of each solution. After reviewing numerous methods of analysis, Li and White (1987) recommended this method for general use. It should be noted that in certain occasions this method may have difficulty in analyzing problems where there are near vertical sections of either the failure or ground surface.

The Morgenstern and Price (1965) method does not make the assumption that the normal force on the base of each slice acts at the center of the slice. Thus, the accuracy of the other methods increases as the slices become thinner. A reasonable number of slices should be adopted in any analyses.

Fredlund and Krahn (1977) conducted a comparison of various methods by obtaining an equivalent λ for each. For the Morgenstern-Price method, the side force function, $f(x) = 1$, was adopted and λ determined. The simplified Bishop

method is equivalent to λ equal to zero, Spencer's method (1967) is equivalent to λ equal to $\tan\theta$, and an equivalent λ was determined for Janbu's method. From the comparison of results it was concluded that the factor of safety to satisfy moment equilibrium, F_m was relatively insensitive to the side force assumption. Thus, those methods that satisfy moment equilibrium give similar results provided that admissible side force functions are adopted.

Comparisons by Ching and Fredlund (1984) and Fredlund (1984) resulted in similar conclusions. The various methods considered by these researchers gave essentially the same answers for cohesionless soils; methods that satisfied moment equilibrium gave similar answers for frictionless soils. Methods that satisfied only force equilibrium resulted in factors of safety that were quite dependent on the side force assumption and the factor of safety varied by up to 20% for cohesive (c, φ) soils (Charles and Soares, 1984).

The Morgenstern-Price method as well as some more recent methods such as Bromhead (1986), Li and White (1987) and Fredlund and Krahn (1977) is fairly widely used and accepted for general analysis of non-circular failure surfaces and its results have been verified in several comparative studies; but acceptability of solutions should always be checked (Costa and Thomas, 1984; Abramson, 1996).

2.4.3 Location of Critical Failure Surface

Initially, methods of analysis were based on circular surfaces. However, development of methods for non-circular surfaces followed soon. For the most part,

non-circular methods may also be used for the analysis of circular failure surfaces, since a circle is merely a special type of curved failure surface. Many computer programs have been developed with procedures that determine the center and radius of the circular failure surface that give a minimum factor of safety. These programs do not always find the absolute minimum; instead sometimes they only locate a local minimum factor of safety. The equivalent problem of determining the generalized failure surface having minimum factor of safety is considerably more complex and routine procedures are uncommon (Chen and Morgenstern, 1983).

Often automatic search procedures are not required as the distribution of weak material within a particular slope is such that the critical failure surface can be determined by analyzing only a few cases. In addition, most non-circular analyses are computer-based and often the programs do not include any algorithm to assist in the location of the critical failure surface. Thus, it is often necessary to locate the critical failure surface by an intelligent selection of potential failure surfaces and manual iteration until the critical surface has been established. This may often be the most efficient means of locating the critical surface.

2.5 Computer Codes Based on Traditional Methods

Numerous commercial computer programs based on the traditional limit equilibrium methods have been developed for analysis of slope stability problems. Some of the available programs are DOS-based while the others are Windows-based that can make the solution process analogous to a graphical procedure. Table 2–2 presents a list of typical computer codes currently available.

Table 2-2 Features of Computer Codes Based on Traditional Methods

Code	Features
Galena Windows (Clover, Australia)	Based on Bishop, Spencer and Sarma methods. Single or multiple analyses for all methods. Back analysis features 'what strength is required' for past failures, User-defined restraints, external forces, distributed loads, and earthquake effects. Pore pressure defined by r_u or phreatic surface, piezometric surface. Automatic generation of tension cracks for multiple analysis.
GEOSLOPE DOS (Geocomp, USA)	Based on Bishop's simplified and Janbu's simplified methods. Automatic search slip surface with minimum F_s. Allows different soil types; several ways to describe strength and its variation, pore pressures, and surface loading. Single or multiple surface analysis.
GSlope Windows (Mitre, Canada)	Based on Bishop's simplified and Janbu's simplified methods. Pore pressure taken into account by r_u or piezometric surface. Pseudo-static analysis. Soil layers, piezometric surfaces, external forces, and search grids drawn by mouse. F_s updated automatically with slip surface change. Allow materials excavated or filled.
MStab Windows (GeoDelft, Netherlands)	Based on Fellenius, Bishop and Spencer methods. Automatic critical slip circle search; user-defined circle zones; output F_s contours and stress components along slip surface. Non-circular slip surface by user-defined coordinates. Interactive input of geometry with arbitrary shaped layers. Pore pressures defined by piezometric level or degree of consolidation. Point or distributed loads. Pseudo-static analysis; Drawdown and excess r_u.
SB-SLOPE DOS (Geosystem, USA)	Based on simplified Bishop and Spencer methods. Simultaneous analysis of upstream and downstream dam slopes. Interactive graphics to select circular/non-circular failure surface. Pore pressure taken into account by phreatic surface or r_u. Psuedo-static analysis. Distributed loads and tension crack. Rapid drawdown.
Slide Windows (Rocscience, Canada)	Based on Fellenius, simplified Bishop, Janbu, Spencer, Morgenstern-Price methods with integrated FEM groundwater analysis (unsaturated steady-state). Anisotropic strength. Pore pressure by phreatic/piezometric surface, r_u or grid. Automatic mesh generation. Line, uniform/triangular distributed loads, horizontal/vertical seismic loads. Circular grid/slope/auto-refinement search, non-circular block/path search; User-defined slip surface, slope limits, search focus, tension cracks, and water levels.
Slope DOS (Geoslove, UK)	Based on Fellenius, Bishop, Spencer and Janbu methods. Automatic search critical slip surface. Up to 9 soil strata. Multiple water tables or piezometric surfaces. Pore pressures from water table or flow line. Perched water and artesian pressures by piezometric surfaces. External forces, quasi-static forces. Menu driven data entry.
Slope DOS, Windows (Oasys, UK)	Based on Fellenius, Bishop, and Janbu methods. Pore pressure by phreatic surface, piezometric or r_u values; drained or undrained shear strength; A range of circle centers with variable radius or with all circles passing through a fixed point, or tangent to a surface; option to extend the grid to find minimum F_s; surface loads with horizontal ground acceleration.

Table 2-2 Continued

Code	Features
Slope2000 DOS, Windows, UNIX (HK Poly Univ., HK)	3-D analysis based on Bishop, Janbu, and Spencer methods. 2-D analysis based on Bishop, Janbu, Spencer, and Morgenstern-Price methods. Locates critical slip surface under general conditions. User-defined convergence criterion, soil layers, surcharge, perched water and earthquake.
Slope-W Windows (Geo-Slope, Canada)	Based on Fellenius, simplified Bishop, simplified Janbu, Spencer, Morgenstern-Price, and FEM analysis; variable or discontinuous soil strata, impenetrable layers, dry and water filled tension cracks. Pore pressure by r_u or grid, piezometric line. Total or effective stress, user defined failure envelope, surcharge and seismic loads.
Stabl for Windows (Purdue Univ., USA)	Based on simplified Bishop, simplified Janbu, and Spencer methods. Random generation of slip surface with minimum F_s. Specific trial failure surface and analysis allowed. Heterogeneous soils, anisotropic soil strengths, excess pore pressure, hydrostatic and surface water, pseudo-static loading and surcharge.
STABLE DOS, Windows (M Z Assoc., UK)	Based on Bishop, Morgenstern-Price and Sarma methods. Links to CAD for input and editing of geometric data. In-built graphics window. All geometry displayed as input for data validation. Pore pressures by piezometric surface, r_u values. Point loads, tension cracks.
TSLOPE Web/Java (TAGAsoft, USA)	Based on Spencer and Morgenstern-Price methods. Graphical interface to create surfaces, line loads or boundary pressures. Intelligent search for critical slip surface. Pseudo-static analyses. Automatically computes pressures on submerged slope, in tension cracks, and from phreatic surface or r_u. Variation of undrained shear strengths. Two-stage rapid drawdown analysis.
XSLOPE for Windows (Univ. of Sydney, Australia)	Based on Bishop simplified and Morgenstern-Price methods. Layered soils. Automatic search critical circle. Pore pressures by piezometric surface, r_u or grid. External normal/shear tractions on slope surface. Horizontal/vertical earthquake forces. Slip surfaces modified by mouse. F_s automatically updated with slip surface change.

Note: The computer codes presented can be found in the Geotechnical & Geoenvironmental Software Directory via the Internet (http://www.ggsd.com).

These computer codes inherit the strengths and weaknesses of the traditional limit equilibrium methods that they are based on. Most of the programs can handle both circular and non-circular failure surfaces. Some codes (Slide, Slope-W) even have the option to integrate finite element analysis, as discussed in the following section.

2.6 Numerical Methods for Slope Stability Analysis

With the rapid development of computational technologies, alternative numerical approaches have been sought for developing new modeling techniques. Among them, finite difference method and finite element method are being widely used by consulting firms as computing facilities become cheaper and more readily available. Although they are more complex to use than the conventional limit equilibrium methods, they nevertheless can provide a detailed insight into the way how a slope will deform and fail, and therefore provide a valuable addition to methods of analyzing slope behavior.

2.6.1 Finite Difference Method

Finite difference method widely used to obtain approximate solutions of many boundary value problems whose exact solutions are mathematically complex and in some cases impossible (Zaman, 1995). Response of a structural system is often represented by the governing differential equations. These equations involve derivatives of functions. Using finite difference approach these derivatives can be easily evaluated at discrete points. The partial differential equations (PDEs) can then be solved in the domain with respect to some given boundary conditions. Cundall (1976) gave an example of how finite difference methods might be applied to the problems of slope stability.

Finite difference method is an approximate method for determining derivatives of a function. Depending upon circumstances, the finite difference method may give exact results. However, frequently it yields only approximate

results. The magnitude or extent of error in using finite difference method in finding derivatives of a function depends on various including order of derivative (2^{nd} order, 3^{rd} order, etc.), type of function (polynomial, trigonometric, etc.), type of finite difference mesh (fine, coarse, etc.), and other factors (calculation accuracy, etc) (Zaman et al., 2000).

Nonetheless, some commercially available computer programs (FLAC/Slope, CHASM etc.) have been developed based on the finite difference method to solve slope stability problems. FLAC/Slope features a graphical interface, automatic factor-of-safety calculation, arbitrary slope geometries, multiple layers, pore pressure conditions, heterogeneous soil properties, and surface loading, etc. This method has the following advantages over the traditional methods: 1) failure mode develops naturally, no need to specify trial surfaces; 2) no parameters (e.g. functions for inter-slice angles) need to be given as input; 3) multiple failure surfaces (or complex internal yielding) evolve naturally.

2.6.2 Finite Element Method

The finite element method (FEM) represents a powerful alternative approach for slope stability analysis. This method is accurate, versatile, and requires fewer a priori assumptions, especially regarding the failure mechanism. The FEM is very powerful in solving problems with irregular boundaries and complex variation of potential and flow lines (Zaman et al., 2000). The region to be analyzed is divided into elements which are joined at nodes. The unknown displacements at each node

may be computed and from these the strain and stress fields within the body may be found.

Using such a numerical technique it is possible to model each soil type according to some constitutive law that describes the stress-strain behavior. Such a law may be a simple one such as the Mohr-Coulomb failure criterion in which the soil is assumed to be elastic until the stress state reaches a failure condition after which it is treated as being perfectly plastic. Huang and Yamasaki (1993) and others used the Drucker-Prager yield function in their local minimum factor-of-safety approach. The Drucker-Prager yield function describes the elasto-plastic stress-strain behavior of the soil (Desai and Siriwardare, 1984).

Application of finite element analysis to slope stability problems has been demonstrated by several authors. Wright et al. (1973) carried out analyses of slopes using both linear elastic and nonlinear behavior of soil. It was found that the normal stress distributions around a circular arc, as determined by the Bishop method, are very close to those found from a finite element analysis provided that the slope was not steep and the value of λ (i.e. $\gamma H \tan(\phi / c)$, where H is the slope height, γ is the unit weight of the soil, and c and ϕ are the shear strength parameters) is large. They also obtained local factors of safety around the circumference of the assumed slip surface by computing the ratio of the shear stresses (as found from the finite element analysis) to the shear strength of the soil. Although the local factor of safety varied widely around the circular slip surface, they noted that the average value of the

factor of safety as determined by the Bishop method was much the same as that found from the finite element analysis.

Zienkiewicz et al. (1975) applied elasto-plastic finite element analysis to problems involving embankments and cuttings. For stability analysis of embankments, they applied an initial state of stress that would result from gravity acting on the completed section, and then gradually reduced the cohesion of the material (keeping ϕ constant) until failure occurred. For the excavation problem, they set up an initial stress state that would result after removal of the soil, and once again reduced the cohesion until failure occurred. Zienkiewicz et al. (1975) also indicated that a conventional factor of safety could be obtained by simultaneously reducing c and $\tan\phi$ until collapse occurred, and then the ratio of the actual strength parameters to the parameters at plastic collapse would yield the factor of safety.

2.7 Slope Stability Analysis Conditions

Consideration of the conditions that will control drainage in the field are important to include in analysis of slopes. Drained conditions are analyzed in terms of effective stresses, using values determined from drained tests, or from undrained tests with pore water pressure (PWP) measurement. Undrained conditions are analyzed in terms of total stress in order to avoid having to rely on estimated values of PWP, which are difficult to predict accurately. Undrained shear strengths for total stress analyses can be evaluated using in-situ tests, unconsolidated undrained (UU) or consolidated undrained (CU) tests.

For total stress analysis, the PWP used as input for that soil should be specified as zero. This results in correct evaluation of the total stress when total unit weights and external water pressures are used. For effective stress analyses, internal PWPs are determined by seepage analyses for long-term steady-state conditions, or by hydrostatic pressure distributions if there is no flow.

External water pressures are included in both total stress and effective stress analyses, because forces due to external water pressures are components that must be included in the overall force and moment equilibrium of the slope. External water pressures can be included in analyses by representing the water outside the slope as a "soil" with c=0, ϕ=0, and unit weight = 9.81 kN/m^3.

For embankments and multi-stage loading conditions where the loading results in increased stresses in the soil, the short-term condition is critical. This is because these types of loads result in positive changes in PWPs, and, as these positive excess PWP dissipate over time, the effective stresses and the strength of the soil increase.

The reverse is true of excavations. An excavation results in negative changes in PWPs. When these PWP dissipate, the effective stresses and the strength of the soil decrease, and the slope becomes less stable. In cases where it is not clear whether the short-term or the long-term condition will be more critical, both should be analyzed.

For natural slopes, the most severe conditions are often associated with high PWPs and water pressures in cracks, during wet periods. These are drained

conditions, and are analyzed using effective stresses, with water pressures determined from seepage analyses (Duncan, 1996).

When carrying out an effective stress analysis, the pore water pressures need to be calculated at the base of each slice as the water force is involved in computing the factor of safety. One of the common ways to compute pore pressure is to use r_u, where r_u is defined as the ratio of the water pressure u to the overburden pressure γh, at a given point (i.e. $r_u = u / \gamma h$). This implies that the pore water pressure is related to the overburden pressure or that the water force U at the base of each slice is proportional to the total weight W of the slice (i.e. $U = r_u W$) (Mostyn and Small, 1987).

Another common way is to use a piezometric surface. A surface may be used in conjunction with a slip circle program such that the water pressure, u, at the base of each slice is computed as $\gamma_w h_w$, where h_w is the vertical distance between the piezometric surface and the base of the slice. The use of a piezometric surface for a slope in which seepage is taking place will lead to errors in estimating pore pressures, since pore pressures should be determined from a flow net and cannot be tied to a single piezometric surface (Zaman et al., 2000).

The use of a pore pressure grid can overcome the above problem. Pore pressure values may be specified at points on a regular grid and the values at the base of each slice found from interpolation of values at the nearest grid points. This is particularly useful with seepage problems where finite difference or finite element

solutions may be obtained and used to set up a grid of pore pressures (Mostyn and Small, 1987).

Most of the methods mentioned in the previous sections employ the definition of the factor of safety, F_s = shear strength of soil over shear stress required for equilibrium. As Lowe (1967) pointed out, defining the factor of safety as a factor on shear strength is logical because shear strength is usually the quantity that involves the greatest degree of uncertainty. The limitation results from the fact that these methods provide no information regarding the magnitudes of the strains within the slope, or any indication about how they may vary along the slip surface (Feld, 1965; Cavounidis, 1987; Chen and Liu, 1990). It is worth noting that the average value of F_s is the same for all practical purposes, even if the factor of safety is assumed to vary from place to place along the slip surface (Duncan and Wright, 1980; Chugh, 1986; Chen, 1999).

CHAPTER 3

PROPOSED SEMI-ANALYTICAL METHOD FOR SLOPE STABILITY ANALYSIS

3.1 Introduction

This chapter presents a semi-analytical method, developed in this study, for analysis of slope stability involving cohesive and non-cohesive soils. Two types of failure surfaces are considered: a planar failure surface and a circular failure surface. The circular slip surface is employed for analysis of clayey slopes, whereas the planar slip surface is employed for analysis of sandy slopes. Semi-analytical solutions for the factors of safety of these two types of slopes are developed. Sandy slope is a simple case for semi-analytical method, which is done for completeness. The method presented below is a simple process to locate both the smallest factor of safety and the slip surface of a slope.

Unless there are geological controls that constrain the slip surface to a noncircular shape, it can be assumed with a reasonable certainty that the slip surface would be circular (Duncan, 1996). Celestino and Duncan (1981) and Spencer (1973) found that, in analyses where the slip surface was allowed to take any shape, the critical slip surface was essentially circular.

Locating the slip surface having the lowest factor of safety is an important part of analyzing a slope stability problem. A number of computer techniques have been developed to automate as much of this process as possible (Chen and Shao,

1988). Most computer programs use systematic changes in the position of the center of the circle and the length of the radius to find the critical circle, which is rather time-consuming (Duncan, 1996).

The proposed semi-analytical method can be viewed as an extension of the method of slices, but it provides a more accurate treatment of the forces because they are represented in an integral form. The proposed solutions developed for circular failure surfaces allow the applications of an optimization technique to locate the centers of the circular slip surface. Therefore, the factor of safety can be obtained by using a minimization method rather than by a trial and error approach used commonly. A computer program is developed based on the proposed analytical solutions which makes it easy and less time-consuming to determine the most critical slip surface and the minimum factor of safety for a given slope.

3.2 Pseudo-Static Analysis

Stability of a slope can be significantly affected by the shaking caused by seismic forces such as earthquakes. The effect of an earthquake may be twofold; firstly, accelerations caused by the ground movement will induce an inertial force into the slope that will provide an extra overturning moment, and secondly, the vibration may cause pore pressure build up in the slope thus causing loss of frictional strength or even liquefaction of the soil. Both effects would reduce the factor of safety of slope and may lead to failure if the slope is subject to ground movement of sufficient magnitude and duration (Seed, 1968; A-Griva and Asaoka, 1982).

Analytical or closed-form solutions concerned with the stability of slopes subjected to earthquake loading has primarily been carried out for earth and rockfill dams as these have the greatest potential for damage and loss of life, if failure occurs (Clough and Chopra, 1966; Seed and De Alba, 1986). Much of the work that has been done for dams is applicable to natural slopes.

The type of material the slope is composed of is most important in assessing the potential of a slope to withstand earthquake accelerations (Newmark, 1965). Slopes that are composed of or underlain by loose sandy soils are most susceptible to failure due to liquefaction of sand when subjected to cyclic loading. Seed (1979) quotes the examples of the lower and upper San Fernando Dams which appeared to be safe when a seismic coefficient of 0.15 was used in a pseudo-static analysis. However, both these dams failed in the 1971 San Fernando earthquake due to the sand fill contained that liquefied when subjected to vibration.

On the other hand, Seed and De Alba (1986) quotes the San Francisco earthquake of 1906 that subjected some 48 dams in the region to accelerations of between 0.25g and 0.6g without any damage. All of these dams were built of clayey soils on rock or clayey foundations. Two of the dams consisted of sands but the sand was not saturated.

Some engineers believe that the pseudo-static method should not be used under any circumstances as it cannot take into account the cyclic nature of forces applied to the slope. In conjunction with the stability of the embankment of the dam,

however, Seed (1980) stated that in cases where the crest acceleration does not exceed about 0.75*g*, deformations of such embankments will usually be acceptably small, if the embankment can be shown to have a factor of safety of about 1.15 in a pseudo-static analysis performed using a seismic coefficient of 0.15.

Although the experience gained with embankment dams cannot by applied directly to natural slopes (because of geometrical differences), the seismic coefficient method may be suitable for stability analysis of slopes in the types of soils mentioned above, i.e. clayey soils, dry or moist cohesionless soils or extremely dense cohesionless soils (Chugh, 1982; Daddazio et al., 1987).

One of the simple ways of taking seismic effects into account is to carry out a limit equilibrium analysis where the forces induced by the earthquake accelerations are treated as a horizontal force (Cao and Zaman, 1999). In reality vertical forces may also be caused by an earthquake, however, these were not considered in above-mentioned limit equilibrium analyses (Ishihara, 1985).

The earliest mention of pseudo static analysis, as reported by Seed (1979), appears to be made by Terzaghi (1950) who applied a horizontal force to the soil above the slip circle. The magnitude of the horizontal force is taken as being equal to the weight of the soil W multiplied by a seismic coefficient k (i.e. $kW = kmg$). As can be seen, the acceleration acting on the mass m of the soil is kg. So, the seismic coefficient k is really a measure of the acceleration of the earthquake in terms of the acceleration due to gravity g.

The method of slices may be used to assess the stability of a slope subjected to earthquake loading. Sarma (1973, 1979) presented a method where earthquake-induced forces were accounted for by applying a horizontal force kW_i to the slice where W_i is the weight of a typical slice i. The critical horizontal acceleration (or value of k) required to bring the soil above the slip surface into a state of limiting equilibrium is computed and this critical acceleration may then be used as an index of stability.

Analysis of slopes that are composed of purely cohesive soils (i.e. $\phi = 0$) whose cohesion varies linearly with depth was carried out by Koppula (1984a, 1984b) using the seismic coefficient approach. Hadj-Hamou and Kavazanjian (1985) obtained an expression for the factor of safety of a gentle infinite slope where the failure plane and the acceleration due to the earthquake were assumed parallel to the slope surface.

The seismic coefficient is an empirical value that depends upon the accelerations caused by the earthquake. Terzaghi (1950) suggested that the values of k should vary from 0.1 for severe earthquakes to 0.5 for catastrophic earthquakes. The usual range of values for k that are employed in the United States is from 0.05 to 0.15, and in Japan characteristically less than 0.2 (Brunsden and Prior, 1984; Huang and Yamasaki, 1993). However, as Seed (1966) pointed out, these values seemed to be chosen empirically and still in use as many dams designed in this way have withstood earthquakes.

3.3 Planar Failure Surface

Failure surfaces in homogeneous or layered non-homogeneous sandy slopes are essentially planar (Skempton, 1964). Planar slides may happen in slopes with permeable soils such as sandy soil and gravel or some permeable soils, with limited cohesion, whose shear strength is principally provided by friction. For cohesionless sandy soils, the planar failure surface may happen in slopes where strong planar discontinuities develop, for example in the soil beneath the ground surface in natural hillsides or in man-made cuttings (Liu, 1990).

3.3.1 Proposed Semi-Analytical Solution for Sandy Slope

A planar-failure slope is shown in Figure 3-1. As can be seen, the failure plane is taken below the ground surface that is inclined at an angle α to the horizontal.

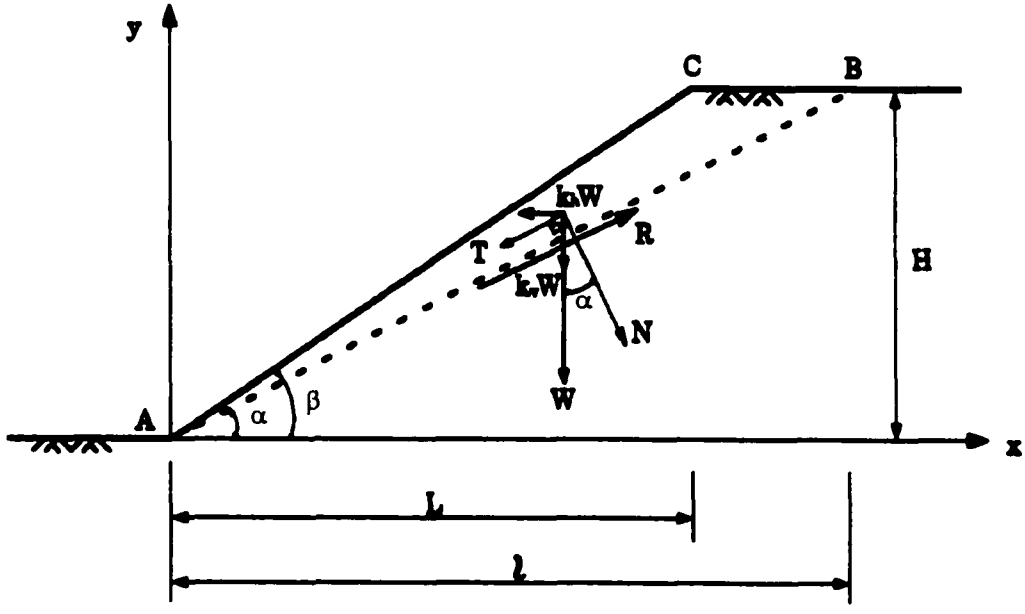

Figure 3-1 Typical Section for Planar Failure Surface (Cao and Zaman, 1999)

Earthquake effects are approximated by including a horizontal acceleration $k_h g$ which produces a horizontal force $k_h W$ and a vertical acceleration $k_v g$ which produces a vertical force $k_v W$ acting through the centroid of the slide body. From an equilibrium consideration of the slide body ABC by a vertical resolution of forces, the vertical force across the base of the slide body must equal the weight W. For a slice of unit thickness, the resolved forces of normal and tangential components N and T can be written as:

$$N = W[(1 + k_v)\cos\alpha - k_h \sin\alpha] \tag{3-1}$$

$$T = W[(1 + k_v)\sin\alpha - k_h \cos\alpha] \tag{3-2}$$

where α is the inclination of the failure surface and W is given by:

$$W = \frac{\gamma H^2}{2}(\cot\alpha - \cot\beta) \tag{3-3}$$

where γ is the unit weight of soil, H the height of the slope, $L = H\cot\beta$, $l = H\cot\alpha$, and β the inclination of the slope.

Since the length of the slip surface AB is $H/\sin\alpha$, the resisting force produced by cohesion is $cH/\sin\alpha$. The friction force produced by N is $W[(1 + k_v)\cos\alpha - k_h \sin\alpha]\tan\phi$. The total resisting or anti-sliding force is thus given by:

$$R = W[(1 + k_v)\cos\alpha - k_h \sin\alpha]\tan\phi + \frac{cH}{\sin\alpha} \tag{3-4}$$

For stability, the downslope slide force T must not exceed the resisting force R of the body. The factor of safety, F_s, of the slope can be defined in terms of effective force by ratio R/T, that is:

$$F_s = \frac{R}{T} = \frac{1 - k_h \tan\alpha}{k_h + (1 + k_v)\tan\alpha}\tan\phi + \frac{2c}{\gamma H[(1 + k_v)\sin\alpha + k_h \cos\alpha]\sin(\beta - \alpha)} \tag{3-5}$$

It can be observed from Equation (3-5) that F_s is a function of α. To find the minimum value of F_s, we need to satisfy:

$$\frac{dF_s}{d\alpha} = 0 \tag{3-6}$$

which leads to:

$$\frac{k_h \cos(\beta - 2\alpha) - \sin(\beta - 2\alpha)}{\sin^2(\beta - \alpha)}\tan^2\alpha + \frac{\gamma H}{2c}(1 + k_h)\tan\phi = 0 \tag{3-7}$$

3.3.2 Minimization of F_s

By trial and error, we can get from Equation (3-7) the value of α by which the minimum F_s can then be determined. However, the minimum value obtained by trial and error needs some *a priori* knowledge. Also, it is not as accurate as the value obtained by the optimization technique. The minimum value of F_s can be found directly from Equation (3-5) using Powell's minimization technique (Liu et al., 1988). Das (1994) reported a similar expression for F_s, developed by assuming that

$F_s = \tau_f / \tau_d$, where τ_f is the average shear strength of the soil, and τ_d the average shear stress developed along the potential failure surface.

For cohesionless soils, the effective cohesion is often ignored, or assumed to be zero ($c = 0$), in which case Equation (3–5) simplifies to:

$$F_s = \frac{1 - k_h \tan\alpha}{k_h + (1 + k_v)\tan\alpha} \tan\phi \qquad (3\text{–}8)$$

As can be observed from Equation (3–8), the minimum value of F_s occurs when $\alpha = \beta$, and the failure becomes independent of slope height. For such cases (i.e., $c = 0$), the factors of safety obtained from the proposed method and from Das (1994) are identical without seismic effects ($k_h = 0, k_v = 0$).

3.4 Circular Failure Surface

For many slope failures, the observation that the surfaces along which sliding took place were not planar but curved (Skempton and Golder, 1948; Brunsden and Prior, 1984; Liu, 1990), led to the idea of using curved failure surfaces for the analysis of slope stability. Although the actual surface of rupture is in most cases bowl shaped (if we consider three dimensions), the representation of the failure surface as a single curve (in two dimensions) greatly simplifies the analysis.

Slides in medium-stiff clays are often deep-seated, and failure takes place along curved surfaces that can be closely approximated in two dimensions by circular surfaces (Skempton and Golder, 1948; Brunsden and Prior, 1984; Liu, 1990). Early solutions for circular surfaces were obtained by Fellenius (1927) who

used a method of slices, and Taylor (1937, 1948) who used a friction circle method to produce charts of "Stability Numbers" to determine factors of safety against slope failure.

Most modern circular slip circle methods make use of the method of slices, and the major differences between these methods involve the way in which the unknown quantities in the analysis are dealt with. In the Fellenius method (Fellenius, 1927), it is assumed that the interslice forces are equal and opposite for each slice and so they cancel out. Bishop (1955) presented a method in which the interslice forces were taken into account in the analysis. For a mathematically consistent static solution, equilibrium of forces and moments must exist for each slice as well as for all of the slices together.

Bishop's rigorous formulation contains too many unknowns. Hence it is difficult to find a direct solution. Having to make assumptions about the interslice forces, makes the solution process more complex. Therefore, the Bishop's equation, which is used by many engineers, is the simplified version for which it is assumed that the difference in the interslice forces for any slice is zero. This type of analysis is accurate for most practical purposes and widely used for slope stability analysis.

It should be noted that the simplified Bishop and Fellenius methods of slices satisfy force equilibrium in one direction and overall moment equilibrium. Also, note that the methods that satisfy moment equilibrium give a factor of safety that is relatively independent of the assumption regarding the interslice forces.

3.4.1 Proposed Semi-analytical Solutions for Clayey Slope

Figure 3–2 shows a potential circular slip surface AB with center O and radius r. When the soil above AB is just on the point of sliding, the average shearing resistance which is required along AB for limiting equilibrium is given by $\tau_f = c' + \sigma' \tan\phi'$. The sliding mass is divided into vertical slices, and a typical slice $DEFG$ is shown. The self-weight of the slice is $dW = \gamma h dx$.

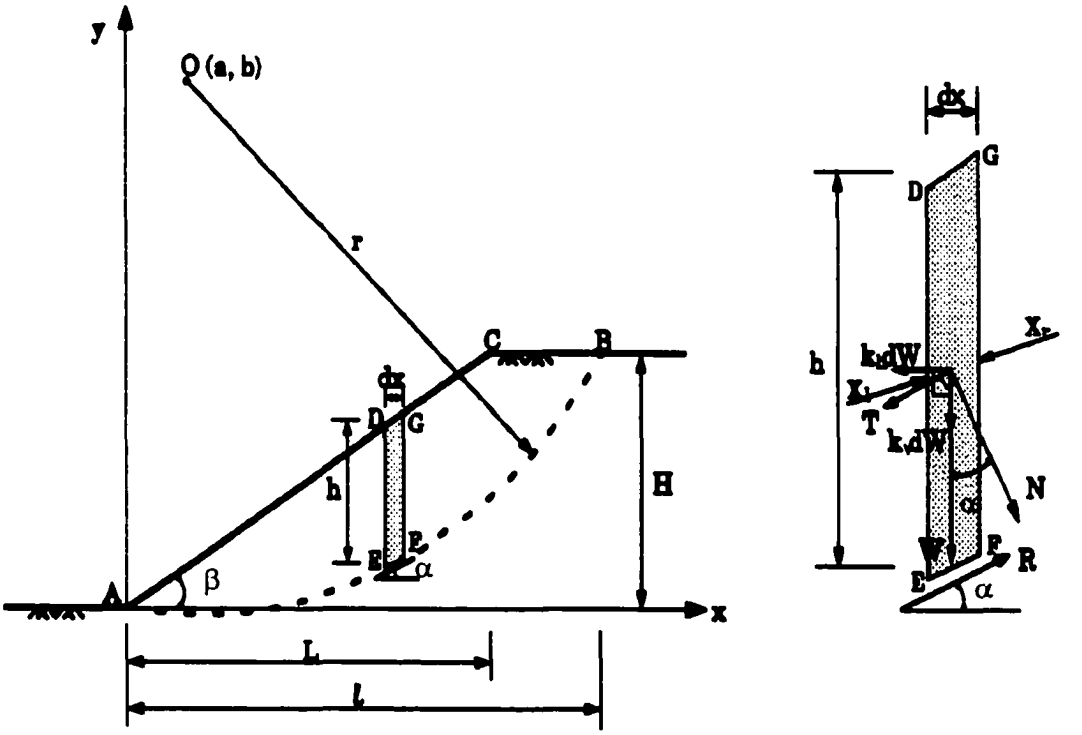

Figure 3–2 Typical Section for Toe Failure Slope (Cao and Zaman, 1999)

The first step in the analysis is to evaluate the sliding or disturbing moment M_s about the center of the circle O. It is assumed that the resultant forces X_l and X_r

on *DE* and *FG*, respectively, are equal and opposite, and parallel to the base of the slice *EF*. Earthquake effects are approximated by including a horizontal acceleration $k_h g$ that produces a horizontal force $k_h W$ and a vertical acceleration $k_v g$ that produces a vertical force $k_v W$ acting through the centroid of the body. It is realized that these assumptions are necessary to keep the analytical solution of the slope stability problem addressed in this study achievable. However, analytical solutions have a special usefulness in engineering practice, particularly in terms of obtaining approximate solutions. More rigorous methods, e.g., finite element technique, can then be used to pursue a detail solution.

Since X_l and X_r are internal forces, $\Sigma(X_l - X_r)$ must be zero for the whole section. Resolving forces perpendicular and parallel to *EF*, we get:

$$T = \gamma h dx(1 + k_v)\sin\alpha + k_h \gamma h dx \cos\alpha \tag{3-9}$$

$$N = \gamma h dx(1 + k_v)\cos\alpha - k_h \gamma h dx \sin\alpha \tag{3-10}$$

where,

$$\alpha = \arcsin\frac{(x-a)}{r} \tag{3-11}$$

$$r = \sqrt{a^2 + b^2} \tag{3-12}$$

The force N produces a maximum shearing resistance when failure occurs according to Mohr-Coulomb failure criterion, which can be expressed in the following form:

$$R = c dx \sec\alpha + \gamma h dx\left[(1 + k_v)\cos\alpha - k_h \sin\alpha\right]\tan\phi \tag{3-13}$$

The slip body, ABC, is defined by lines AC, CB, and AB. The equations of lines AC, CB, and AB are given by y_1, y_2, and y_3, respectively, that is:

$$y_1 = x\tan\beta \tag{3-14}$$

$$y_2 = h \tag{3-15}$$

$$y_3 = b - \sqrt{r^2 - (x-a)^2} \tag{3-16}$$

The sums of the disturbing and resisting moments for all slices about the center of the circle $O(a, b)$ can be written in an integral form as follows:

$$\begin{aligned} M_s &= \int_0^l r\gamma h\left[(1+k_v)\sin\alpha - k_h\cos\alpha\right]dx \\ &= \int_0^L r\gamma(y_1 - y_2)\left[(1+k_v)\sin\alpha - k_h\cos\alpha\right]dx \\ &+ \int_L^l r\gamma(y_2 - y_3)\left[(1+k_v)\sin\alpha - k_h\cos\alpha\right]dx \\ &= r\gamma\left[(1+k_v)I_s - k_h I_c\right] \end{aligned} \tag{3-17}$$

Likewise, the sums of the resisting moments for all slices about the center of the slip circle can be written as in the form below:

$$\begin{aligned} M_r &= \int_0^l r\{c\sec\alpha + \gamma h\left[(1+k_v)\cos\alpha - k_h\sin\alpha\right]\tan\phi\}dx \\ &= r\int_0^l c\sec\alpha dx + \int_0^L r\gamma(y_1 - y_3)\left[(1+k_v)\cos\alpha - k_h\sin\alpha\right]\tan\phi dx \\ &+ \int_L^l r\gamma(y_2 - y_3)\left[(1+k_v)\cos\alpha - k_h\sin\alpha\right]\tan\phi dx \\ &= r^2 c\psi + \left[(1+k_v)I_c - k_h I_s\right]r\gamma\tan\phi \end{aligned} \tag{3-18}$$

where,

$$L = H\cot\beta \tag{3-19}$$

$$l = a + \sqrt{r^2 - (b-H)^2} \tag{3-20}$$

$$\psi = \arcsin\frac{(l-a)}{r} + \arcsin\frac{a}{r} \tag{3-21}$$

$$\begin{aligned} I_c &= \int_0^L (y_1 - y_3)\cos\alpha dx + \int_L^l (y_2 - y_3)\cos\alpha dx \\ &= -\frac{\tan\beta}{6r}\left[2r^2 + (L-a)^2\right]\sqrt{r^2-(L-a)^2} + \frac{b\tan\beta}{r}\left(\frac{a^2}{2} + \frac{b^2}{3}\right) \\ &+ \frac{r}{2}(a\tan\beta - H)\arcsin\left(\frac{L-a}{r}\right) + \frac{r}{2}(a\tan\beta - b)\arcsin\left(\frac{a}{r}\right) \\ &- \frac{r}{2}(b-H)\arcsin\left(\frac{l-a}{r}\right) + \frac{1}{6r}\left[4r^2 l - ab^2 + (l-a)(H-a)^2\right] \end{aligned} \tag{3-22}$$

$$\begin{aligned} I_s &= \int_0^L (y_1 - y_3)\sin\alpha dx + \int_L^l (y_2 - y_3)\sin\alpha dx \\ &= \frac{H^2}{2r}\left[(a\cot\beta + b) - \frac{1}{3}H\sec^2\beta\right] \end{aligned} \tag{3-23}$$

To satisfy the moment equilibrium and the slope stability, the available resisting moment must be larger than or equal to the disturbing moment. Thus, the factor of safety for the case of Toe Failure is expressed as the ratio of the maximum available resisting moment to the disturbing moment, that is:

$$F_s = \frac{M_r}{M_s} = \frac{c\psi r + \gamma\tan\phi\left[(1+k_v)I_c - k_h I_s\right]}{\gamma\left[(1+k_v)I_s + k_h I_c\right]} \tag{3-24}$$

From Equations (3-9) through (3-23), it can be observed that the factor of safety F_s is a function of two unknown variables, a and b, which is also the center of

the circular slip surface. The minimum value of F_s can be found by solving the following equations:

$$\begin{cases} \dfrac{\partial F_s}{\partial a} = 0 \\ \dfrac{\partial F_s}{\partial b} = 0 \end{cases} \tag{3-25}$$

which is part of the minimization techniques to be discussed in the following section (3.4.2).

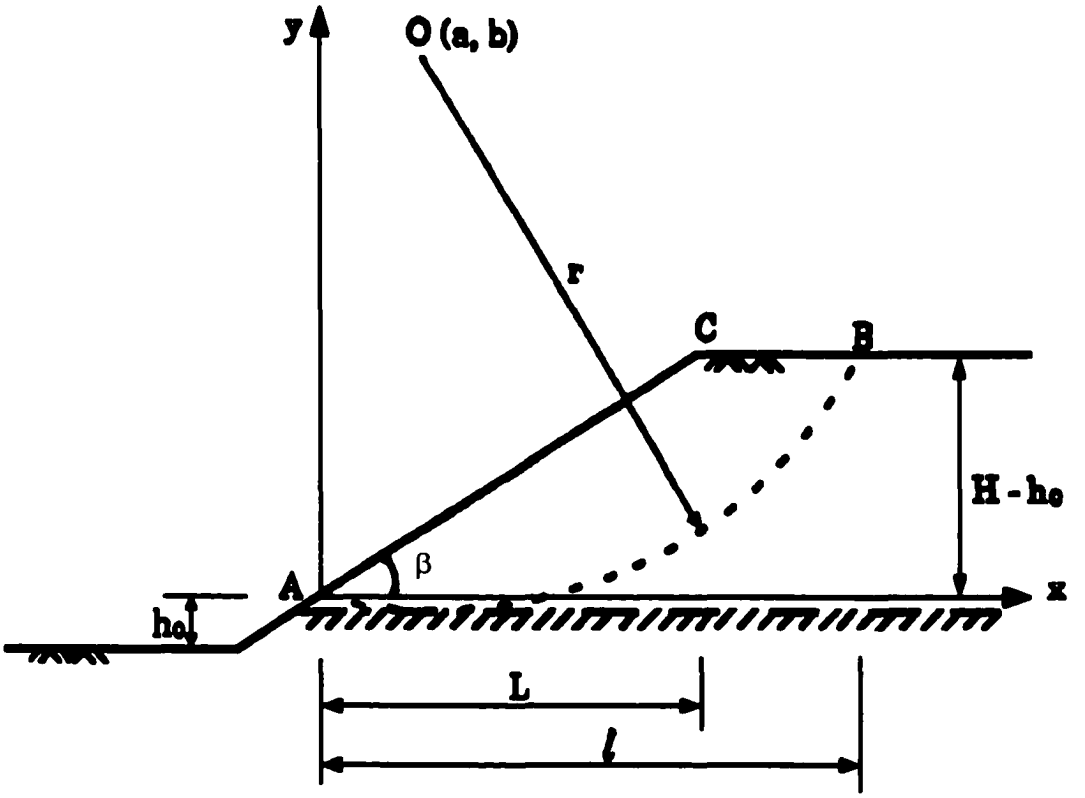

Figure 3-3 Typical Section for Face Failure Slope (Cao and Zaman, 1999)

When the slope inclination exceeds 54^0, all failures emerge at the toe of the slope (Brunsden and Prior, 1984; Liu, 1990), and therefore it is called Toe Failure (Figure 3-2). However, when the slope height H is relatively large compared with the undrained shear strength or when a hard stratum is under the top of a clayey slope with $\phi < 30^0$, the slide often emerges from the face of the slope (Brunsden and Prior, 1984), and hence it is called Face Failure, as shown in Figure 3-3. For Face Failure, the factor of safety F_s is the same as that of Toe Failure using $(H\text{-}h_0)$ instead of H.

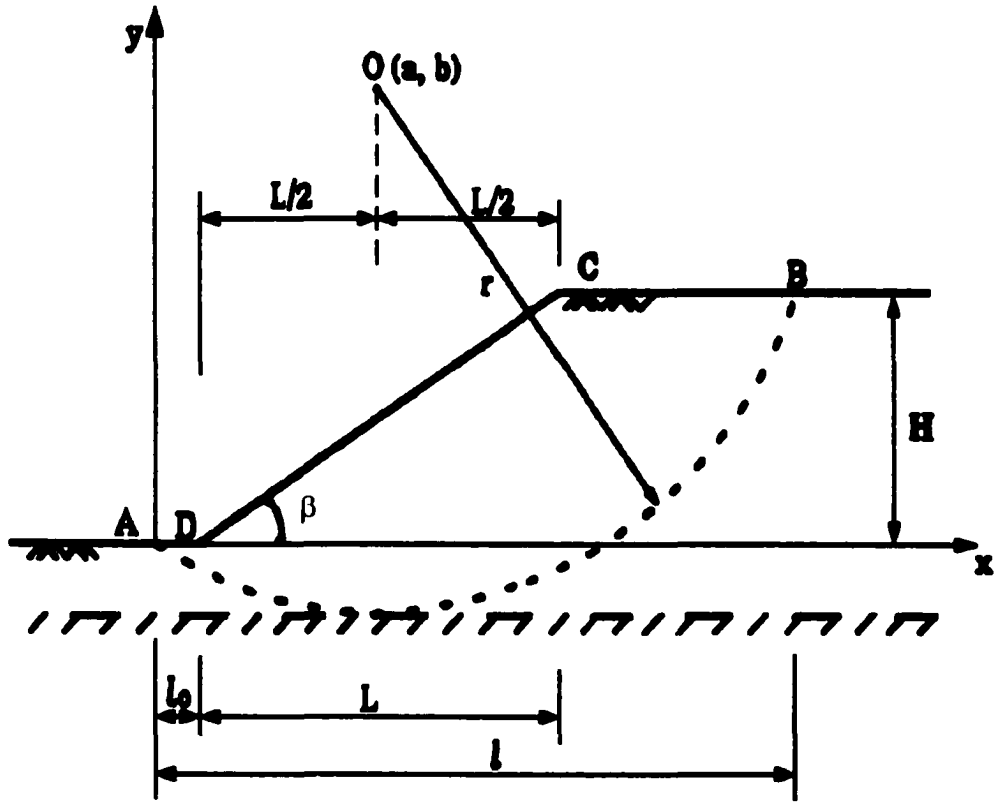

Figure 3-4 Typical Section for Base Failure Slope (Cao and Zaman, 1999)

For flatter slopes, failure is deep-seated and extends to the hard stratum forming the base of the clay layer, which is called Base Failure, as shown in Figure 3-4. By following the same procedure as that for Toe Failure, the factor of safety for Base Failure can be obtained from the following equation:

$$F_s = \frac{c\psi r + \gamma \tan\phi[(1+k_v)I_c' - k_h I_s']}{\gamma[(1+k_v)I_s' + k_h I_c']} \tag{3-26}$$

where ψ is given by Equation (3-21), and I_s' and I_c' are given by:

$$\begin{aligned} I_s' &= \int_0^{l_0}(y_0 - y_3)\sin\alpha dx + \int_{l_0}^{l_1}(y_1 - y_3)\sin\alpha dx + \int_{l_1}^{l}(y_2 - y_3)\sin\alpha dx \\ &= \frac{H^3}{12r}\cot^2\beta + \frac{H}{2r}(l-l_0)(l-l_1) - \frac{bl}{2r}(l-2a) + \frac{H}{3}(3b^2 - 3bH + H^2) \end{aligned} \tag{3-27}$$

$$\begin{aligned} I_c' &= \int_0^{l_0}(y_0 - y_3)\cos\alpha dx + \int_{l_0}^{l_1}(y_1 - y_3)\cos\alpha dx + \int_{l_1}^{l}(y_2 - y_3)\cos\alpha dx \\ &= -\frac{Hl_0}{2r}\sqrt{r^2 - \frac{1}{4}H^2\cot^2\beta} + \frac{r}{2}(b-H)\arcsin\left(\frac{l-a}{r}\right) \\ &+ r\left(a\tan\beta - \frac{H}{2}\right)\arcsin\left(\frac{H\cot\beta}{2r}\right) - \frac{rb}{2}\arcsin\left(\frac{a}{r}\right) \\ &+ \frac{1}{6r}\left[4r^2 l - ab^2 + (l-a)(H-a)^2\right] \end{aligned} \tag{3-28}$$

where,

$$y_0 = 0 \tag{3-29}$$

$$y_1 = x\tan\beta \tag{3-30}$$

$$y_2 = H \tag{3-31}$$

$$y_3 = b - \sqrt{r^2 - (x-a)^2} \tag{3-32}$$

$$l_0 = a - \frac{1}{2} H \cot \beta \tag{3-33}$$

$$l_1 = a + \frac{1}{2} H \cot \beta \tag{3-34}$$

$$l = a + \sqrt{r^2 - (b - H)^2} \tag{3-35}$$

It can be observed from Equations (3-26) through (3-35) that the factor of safety F_s for a given slope is a function of the unknown variables a and b. Thus, the minimum value of F_s can be found using the Powell's minimization technique (Liu et al., 1988; Press et al., 1995), as discussed below.

3.4.2 Minimization of F_s

For a given single function f which depends on two independent variables, such as the problem under consideration here, minimization techniques are needed to find the value of these variables where f takes on a minimum value, and then to calculate the corresponding value of f. If one starts at a point $\boldsymbol{P}$ in an n-dimensional space, and proceed from there in some vector direction $\boldsymbol{n}$, then any function of N variables $f(\boldsymbol{P})$ can be minimized along the line $\boldsymbol{n}$ by one-dimensional methods. Different methods will differ only by how, at each stage, they choose the next direction $\boldsymbol{n}$. Powell first defined a direction set method that produces N mutually conjugate directions (Press et al., 1995). Unfortunately, a problem of linear dependence was observed in Powell's algorithm. The modified Powell's method avoids a buildup of linear dependence (Press et al., 1995).

The closed-form slope stability Equation (3-26) allows the application of an optimization technique to locate the center of the sliding circle (a, b). The minimum factor of safety F_s is then obtained by substituting the values of these parameters into Equations (3-27) through (3-35) and the results into Equation (3-26), for a Base Failure problem (Figure 3-4). While using the modified Powell's method, the key is to specify some initial values of a and b. Well-assumed initial values of a and b can result in a rapid convergence. If the values of a and b are given inappropriately, it may result in a delayed convergence or may not produce a convergent solution. Generally, a should be assumed within $\pm L$, while b should be equal to or greater than H (Figure 3-4). Similarly, Equation (3-24) could be used to compute the minimum F_s for Toe Failure (Figure 3-2) and Face Failure (Figure 3-3), except (H-h_0) is used instead of H in the case of Face Failure.

In addition to the modified Powell's method, other available minimization methods were also tried in this study such as downhill simplex method, conjugate gradient methods, and variable metric methods (Liu et al., 1988; Press et al., 1995). These methods need more rigorous or closer initial values of a and b to the target values than the modified Powell's method.

A computer program has been developed using the modified Powell's method to locate the center of the sliding circle (a, b) and to find the minimum value of F_s based on the proposed solution for each case (Toe Failure, Face Failure, Base Failure). There are no clear boundaries among the three types of failures, which

represent three possibilities. For a particular case, all the three failure types might be checked to see which type of failure yields the lowest F_s. The program helps make the semi-analytical approach straightforward and simple for slope stability analysis. The reason the proposed approach is called as semi-analytical method is due to the minimization technique involved in the process of finding the minimum value of F_s, although a closed-form solution of the factor of safety has been developed.

3.5 Results and Comments

The validity of the proposed semi-analytical method was evaluated using two well-established methods of slope stability analysis: the finite element method (FEM) (Huang and Yamasaki, 1993) and the Bishop (1952) method. The cases were chosen from homogeneous dry soil slopes, without seismic effects initially and then with seismic effects. The slopes are about *8 m* high with unit weight of soils about *18.5* kN/m^3. The slope configurations range from 26.7^0 to 45^0. Cohesions of soils range from *5 kPa* to *30 kPa* and friction angles range from 10^0 to 20^0. The results obtained by the proposed semi-analytical method are found to be in good agreement, as shown in Table 3–1, with those determined by the FEM model (Huang and Yamasaki, 1993) as well as by the Bishop method.

For the 23 slopes analyzed (Table 3–1), statistical analyses show that the factors of safety obtained from the proposed semi-analytical method are closer to the values obtained from the FEM models (Huang and Yamasaki, 1993) than those by the Bishop method. The average differences between the FEM and the proposed

semi-analytical method are small (5% with a standard deviation of 4%). The average difference between the proposed method and the Bishop method is 6% with a standard deviation of 3%. The proposed semi-analytical method yields 2 larger and 6 smaller factors of safety than both the FEM models and the Bishop method, while 15 out of 23 (about 65%) results from the proposed method are between the results obtained from the FEM model and the Bishop method. Basically, the Bishop method yields the lower bound (i.e., smaller stability values) among the three methods.

Table 3–1 Comparison of F_s by Different Methods (without Seismic Effects)

No.	β (deg.)	c (kPa)	ϕ (deg.)	FEM (1993)	Bishop (1952)	Semi-analy. (proposed)
1 (119)	45	25.00	20.00	1.87	1.74	1.81
2 (37)	45	20.00	20.00	1.68	1.50	1.60
3 (23)	45	15.00	20.00	1.46	1.29	1.39
4	45	10.00	20.00	1.00	1.05	1.17
5 (109)	45	30.00	15.00	1.85	1.75	1.81
6 (86)	45	25.00	15.00	1.65	1.53	1.60
7 (36)	45	20.00	15.00	1.45	1.32	1.40
8	45	15.00	15.00	1.24	1.11	1.19
9	45	10.00	15.00	1.00	0.89	0.98
10 (44)	45	25.00	10.00	1.42	1.35	1.40
11 (46)	45	20.00	10.00	1.23	1.15	1.20
12	45	15.00	10.00	1.00	0.97	1.00
13 (18)	26.7	20.00	20.00	2.05	2.09	2.01
14 (55)	26.7	15.00	20.00	1.85	1.82	1.76
15 (120)	26.7	10.00	20.00	1.60	1.54	1.51
16 (54)	26.7	5.00	20.00	1.23	1.21	1.24
17 (110)	26.7	25.00	15.00	1.87	2.05	1.98
18 (63)	26.7	20.00	15.00	1.72	1.78	1.74
19 (87)	26.7	15.00	15.00	1.54	1.53	1.49
20 (94)	26.7	10.00	15.00	1.29	1.29	1.25
21	26.7	5.00	15.00	1.00	0.99	0.99
22	26.7	15.00	10.00	1.19	1.27	1.23
23	26.7	10.00	10.00	1.00	1.03	0.99

Note: The numbers in parentheses indicate the slopes that are also included in ANN modeling.

The proposed semi-analytical method was evaluated further by considering seismic effects and the results compared with the FEM-based software GFA2D (He, 1996) and the traditional methods-based software Slope2000 (Cheng, 2002), including data preparation time, computing time, and interpretation of results. The GFA2D is a FEM-based global failure analysis program for 2-D slope stability problems using the Mohr-Coulomb failure criterion and four-noded quadrilateral elements. The Slope2000, as mentioned in Table 2-2, is used here for 2-D analysis by the Bishop method. The slopes are chosen from case studies with the heights ranging from *10 m* to *20 m*. The unit weights of soils range from *17.3* to *20 kN/m*^{3}. The inclinations vary from 22^0 to 45^0, while cohesions range from *0* to *20 kPa* and friction angles range from 7^0 to 30^0. The results are summarized in Table 3-2.

Table 3-2 Comparison of F_s by Different Methods (with Seismic Effects)

No.	H	β	γ	c	ϕ	k_h	k_v	GFA2D	Slope2000	Semi-Analy.
	(m)	(deg.)	(kN/m^3)	(kPa)	(deg.)			(FEM)	(Bishop)	(Proposed)
1 (124)	10.0	45.00	19.60	11.80	30.00	0.20	0.00	1.22	1.00	1.32
2 (21)	11.5	27.60	17.71	9.09	20.35	0.20	0.00	1.09	1.10	1.05
3 (22)	11.5	27.60	17.71	9.09	20.35	0.10	0.00	1.15	1.20	1.14
4 (121)	11.5	27.60	17.71	9.09	20.35	0.05	0.00	1.21	1.25	1.23
5 (122)	11.5	27.60	17.71	9.09	20.35	0.00	0.10	1.16	1.00	1.10
6 (123)	11.5	27.60	17.71	9.09	20.35	0.00	0.20	0.90	0.87	0.96
7	13.5	26.57	17.30	57.50	7.00	0.10	0.00	1.49	1.37	1.55
8	13.5	26.57	17.30	57.50	7.00	0.15	0.00	1.33	1.20	1.37
9	13.5	26.57	17.30	57.50	7.00	0.20	0.05	1.19	1.10	1.21
10 (68)	13.7	26.57	18.71	0.00	14.00	0.05	0.00	1.30	1.28	1.23
11 (64)	20.0	26.57	18.71	0.00	23.50	0.51	0.10	0.95	1.03	1.00
12 (117)	20.0	22.00	20.00	20.00	20.00	0.04	0.25	1.02	1.12	1.06
13 (118)	20.0	22.00	20.00	20.00	20.00	0.10	0.05	0.94	0.96	1.00
14 (19)	20.0	22.00	20.00	0.00	20.00	0.04	0.00	1.05	1.00	0.98

Note: The numbers in parentheses indicate the slopes that are included in ANN modeling.

The factors of safety obtained by the proposed semi-analytical method are found to be in general agreement, as shown in Table 3–2, with the values determined by the FEM model (GFA2D) and the Bishop method (Slope2000). It can be observed from Table 3–2 that the results obtained from the proposed semi-analytical method are closer to that by the FEM (with a difference of 5% on an average and a standard deviation of 2%) than the results obtained from the Bishop method (with an average difference of 9% and a standard deviation of 8%). The proposed semi-analytical method generally yields reasonable results (in comparison with the FEM models), while the Bishop method yields relatively conservative low values.

For Slopes 7, 8 and 9 in Table 3-2, the minimum factor of safety $F_{s\,min}$ is obtained as 2.08 for $k_v = 0$ and $k_h = 0$ using the proposed semi-analytical method. When $k_v = 0$ and $k_h = 0.1$ or 0.15, $F_{s\,min}$ becomes 1.55 and 1.37; these values are 25% and 34% lower, respectively, than $F_{s\,min} = 2.08$. When $k_v = 0.05$ and $k_h = 0.2$, we get $F_{s\,min} = 1.21$, which is 42% lower than $F_{s\,min} = 2.08$. These results show the earthquake effect on the slope stability to be significant.

The GFA2D, as a general-purpose finite element method, can model complex conditions with a high degree of realism, including in the analyses such things as nonlinear stress-stain behavior and non-homogeneous conditions. This generality and flexibility, however, does not come without its price. Each analysis takes a considerable amount of time to obtain material property values, to perform

the computer analyses, and to evaluate and interpret the results. Although availability of powerful new microcomputers greatly reduce the computing time, the time spent on data preparation and interpretation of results is still very significant. In the above 14 cases (Table 3–2), the GFA2D needed about 20 times the effort, on an average, as compared with the proposed semi-analytical method.

The Slope2000 software greatly simplifies the analysis process of a slope by the Bishop method, especially in locating the critical slip surface. The graphical user interfaces for construction of slope geometry and for display of results also make it easy to evaluate the results. However, the Slope2000 software still needed about 5 times the effort, on an average, than the proposed semi-analytical method to reach the solution for each case analyzed, as presented in Table 3–2, due to the trial and error approach used in selecting different number of slices and different locations of slip surfaces.

3.6 Concluding Remarks

In this chapter, a semi-analytical method is presented for analysis of slope stability involving cohesive and non-cohesive soils. Two types of failure surfaces are considered: a planar failure surface, and a circular failure surface. Earthquake effects are considered in an approximate manner in terms of seismic coefficient-dependent forces. For circular failure surfaces, three failure conditions are considered, namely Toe Failure, Face Failure and Base Failure for clayey slopes resting on a hard stratum. The proposed method can be viewed as an extension of the method of

slices, but it provides a more accurate treatment of the forces because they are represented in an integral form. Also, the factor of safety is obtained by using the Powell's minimization technique rather than by a trial and error approach used commonly.

The factors of safety obtained from the proposed method are in good agreement with those determined by the finite element method-based approach and the Bishop method. The solution processes show that the proposed semi-analytical method is as effective as the Bishop method but more straightforward and simpler. Also, the semi-analytical method yields results that are very similar to the results obtained from the FEM technique, but needs much less effort to obtain the solution for a given slope. The limitation of the proposed method is that it works only for circular failure surfaces and cannot be used to analyze problems involving layered soils and pore water pressures. These aspects are further discussed in Chapter 4.

CHAPTER 4

PROPOSED NEURAL NETWORK MODEL FOR SLOPE STABILITY ANALYSIS

4.1 Introduction

In this chapter, an artificial neural network approach is outlined to predict the factors of safety of slopes. The solution is attempted by employing a recurrent neural network and predicting the results using the data collected from literature as well as some limited data from field case studies.

An artificial neural network can acquire, store, and utilize experiential knowledge like a physical cellular system, to some extent. Neural networks are composed of many simple elements usually operating in parallel (McCullock and Pitts, 1943). The network computation is performed by a dense mesh of computing nodes and connections. They operate collectively and simultaneously on most or all data and inputs (Minsky, 1954, Minsky and Papert, 1969). The network function is determined largely by the connections between elements. We can train a neural network to perform a particular function by adjusting the values of the connections between elements.

The basic processing elements of neural networks are called artificial neurons, or simply neurons (McCullock and Pitts, 1943; Rosenblatt, 1958). Often we simply call them nodes. Neurons can be perceived as summing and non-linear mapping functions. In some cases they can be considered as threshold units that get activated when their total input exceeds certain bias levels (Rosenblatt, 1958;

Widrow and Hoff, 1960). Neurons operate in parallel and are configured in regular architectures. They are often organized in layers, and feedforward and/or feedback connections both within the layer and toward adjacent layers are allowed (Kohonen, 1977, 1982; Hopfield, 1984). The strength of each connection is expressed by a numerical value called weight, which can be modified.

The most basic characteristic of a neural network is its architecture. Design of network architecture includes selecting the number of layers and the number of nodes in each layer and the interconnection schemes between layers. A variety of functions can be used as the interconnection function between inputs and hidden layer or between hidden layer and output layer (Kohonen, 1977, 1984; McClelland and Rumelhart, 1986). Neural networks differ from each other in their learning modes (Widrow and Hoff, 1960). There are a variety of learning rules that establish when and how the connecting weights change. Networks exhibit different speeds and efficiency of learning, thus they also differ in their ability to accurately respond to the values presented at the input (Amari, 1977, 1990; Anderson et al., 1977; Kohonen, 1982, 1988).

A neural network's ability to perform computations is based on the premise that we can reproduce some of the flexibility and power of a human brain by artificial means (Von Neumann, 1958; Arbib, 1987). Advances have been made in applying such systems for problems found intractable or difficult for traditional computation approaches (Kohonen, 1984; Hopfield, 1984; Zurada, 1992). Neural network users do not specify an algorithm to be executed by each computing node

(neuron). Instead, they select what in their view is the best architecture, specify the characteristics of the neurons and initial weights, and choose a training mode for the network (Rumelhart et al., 1986; Hertz et al., 1991; Demuth and Beale, 1995, 2000). Appropriate inputs are then applied to the network so that it can acquire knowledge from the environment. As a result of such exposure, the network assimilates information that can be later recalled by the user (Kohonen, 1988).

The field of neural networks has a history of some six decades but has found meaningful applications only in the past twenty years. The field is still developing rapidly. Today neural networks can be trained to solve problems that are difficult for conventional computational, physics-based methods (Demuth and Beale, 1995, 2000). Neural networks are becoming a useful tool for industry, education and research, a tool that helps users find what works and what does not, and a tool that helps develop and extend the field of neural networks (Zurada, 1992). However, the neural network modeling is limited to the fact that it is based on the data available and extrapolation might not be reliable.

Application of artificial neural network to slope stability analysis is a relatively new topic. It has been well known that neural network can be used to solve both linear and especially non-linear problems. For the case of slope stability, the problem is known to be highly non-linear and a non-linear model may be warranted. The non-linear model attempted in this study is a recurrent neural network (RNN) model. A brief introduction to concepts of artificial neural systems

such as artificial neuron model and network architectures would be helpful before discussing the recurrent network model developed in this study.

4.2 Artificial Neuron Model and Network Architecture

The neuron model and the architecture of a neural network describe how a network transforms its input into an output. This transformation can be viewed as a computation. The model and the architecture each place limitations on what a particular neural network can compute (Hertz et al., 1991). The way a network computes its output must be understood before training methods for the network can be explained.

4.2.1 Artificial Neuron Model

A single artificial neuron with R inputs is shown in Figure 4–1. Here the input vector p is represented by the solid dark vertical bar at the left. The dimensions of p are shown below the symbol p in the figure as $Rx1$. Thus, p is a column vector of R input values. These inputs go to the row vector w, which is of size R.

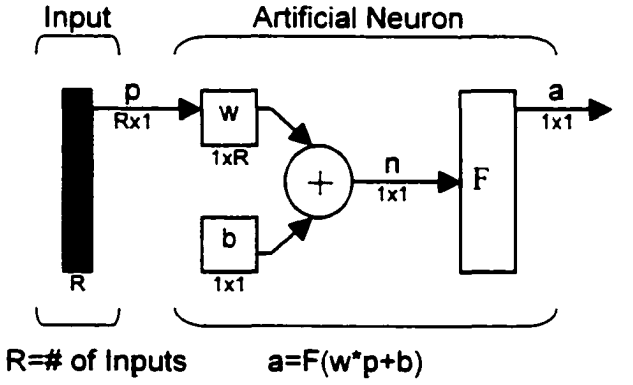

Figure 4–1 Artificial Neuron Model (McCullock and Pitts, 1943)

As shown in Figure 4–1, the net input to the transfer function F is n, the sum of the bias b and the product wxp. This sum is passed to the transfer function F to get the neuron's output a, which in this case is a scalar. If we have more than one neuron, the network output will be a vector. The row vector w and the column vector p are shown below.

$$w = [w(1,1)w(1,2)...w(1,R)] \tag{4–1}$$

$$p = [p(1)p(2)...p(R)]^T \tag{4–2}$$

A layer of a network is defined in the figure shown above. A layer includes the combination of the weights, the multiplication and summing operation, the bias b, and the transfer function F. The input vector, p, will not be called a layer.

The transfer function F can take different shapes depending on different problems. Two of the most commonly used functions are shown below. The linear transfer function, as shown in Figure 4–2, can be used as a linear approximator (Widrow and Hoff, 1960; Hertz et al., 1991).

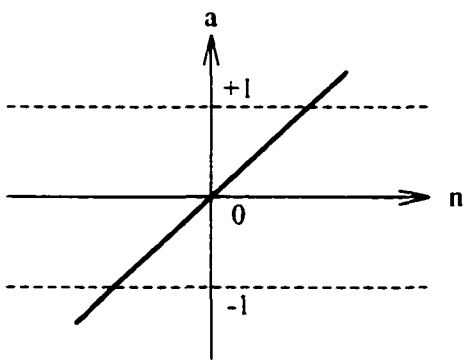

Figure 4–2 Linear Transfer Function (Widrow and Hoff, 1960)

The sigmoid transfer function, as shown in Figure 4–3, takes the input and transforms the output into the range -1 to +1. This transfer function is commonly used in multiple-layer networks, in part because it is differentiable (McClelland and Rumelhart, 1986; Demuth and Beale, 1995).

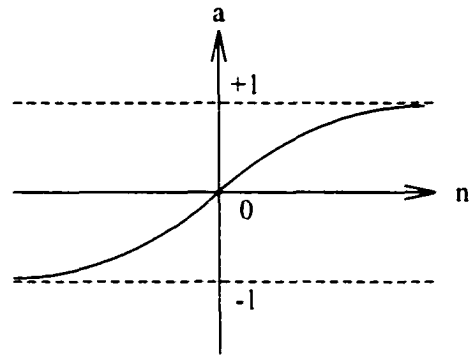

Figure 4–3 Sigmoid Transfer Function (McClelland and Rumelhart, 1986)

4.2.2 Neural Network Architecture

Two or more of the neurons shown in Figure 4–1 may be combined into a layer, and a particular network might contain one or more such layers.

Single-layer Network

A single-layer network with R inputs and S neurons is shown below. Here p is an input vector of length R, w is a matrix (SxR) as shown below, and a and b are vectors of length S. As defined previously, the neuron layer includes the weight matrix, the multiplication operations, the bias vector b, the sum, and the transfer function boxes.

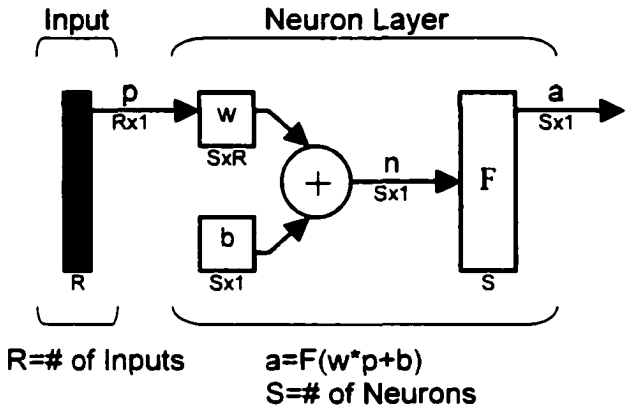

Figure 4–4 Single-layer Neural Network (Rosenblatt, 1958)

$$w^{SXR} = \begin{bmatrix} w(1.1)w(1.2)...w(1,R) \\ w(2.1)w(2.2)...w(2,R) \\ ..... \\ ..... \\ ..... \\ w(S.1)w(S.2)...w(S,R) \end{bmatrix} \qquad (4\text{–}3)$$

In this network, as shown in Figure 4–4, each element of the input vector p is connected to each neuron input through the weight matrix w (Equation 4–3). The ith neuron has a summing that gathers its weighted inputs and bias to form its own scalar output $n(i)$. The various $n(i)$ taken together form an S-element vector n. The neuron layer outputs form a column vector a. A single-layer network is generally used for simple problems, while a multiple-layer network can be used to solve complex problems.

Multiple-layer Feedforward Network

A network can have several layers. Each layer has a weight matrix w, a bias vector b. and an output vector a. The network shown below (Figure 4–5) has R inputs. $S1$ neurons in the first layer, $S2$ neurons in the second layer, etc. It is common for different layers to have different number of neurons.

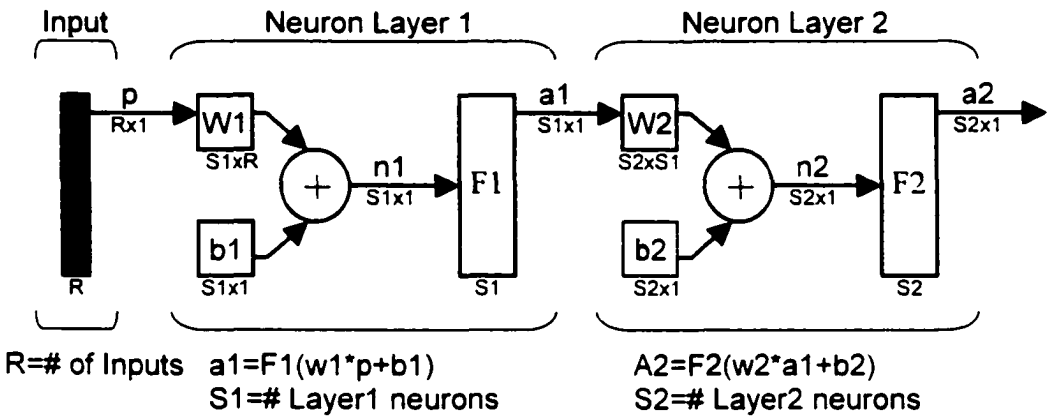

Figure 4–5 Multiple-Layer Feedforward Network (Rosenbaltt, 1958)

Note that the outputs of the intermediate layer are the inputs to the following layer. Thus, layer 2 can be analyzed as a single layer network with $R = S1$ inputs, $S = S2$ neurons, and a $S1$x$S2$ weight matrix $w = w2$. The input to layer 2 is $p = a1$, the output is $a = a2$. Now that all the vectors and matrices of layer 2 are identified, it can then be treated as a single layer network on its own. This approach can be taken with any layer of the network.

The layers of a multiple-layer network play different roles. A layer that produces the network output is called an output layer. All other layers are called hidden layers. The two layer networks shown above has one output layer and one

hidden layer. Multiple-layer networks are much more powerful than single layer networks since multiple-layer networks are able to use the combination of sigmoid and/or linear transfer functions. If the last layer of a multiple-layer network has sigmoid neurons then the outputs of the network are limited to a small range. If linear output neurons are used, the network outputs can take on any values (Rumelhart, 1990).

Multiple-layer feedforward networks use the back-propagation algorithm to evaluate the contribution of each particular weight to the output error. It might appear that the back-propagation algorithm has made a breakthrough in the learning of layered networks. In practice, however, implementation of the algorithm may encounter different difficulties (Zurada, 1992; Demuth and Beale, 1995). One of the problems is that the error minimization procedure may produce only a local minimum of the error function. The learning procedure would stop prematurely if it starts at wrong point; thus the trained network would be unable to produce the desired performance in terms of its acceptable terminal error. Also, the initialization of the network strongly affects the ultimate solution. If all weights start out with equal weight values, and if the solution requires that unequal weights be developed, the network may not train properly. Unless the network is disturbed by random factors or the random character of input patterns during training, the internal representation may continuously result in symmetric weights (Zurada, 1992). These problems can be overcome by the dynamic learning of the recurrent network to be introduced later in this section.

Feedback Network

A feedback network is different from the networks described above in that its outputs are connected to its inputs. A S neuron feedback network is shown below in Figure 4–6. The feedback network is the most general available in that it has all possible connections between neurons. Some of the weights can be constrained to zero to create layers within the feedback network, if desired. By doing so, a multiple-layer network of the kind described previously can be created.

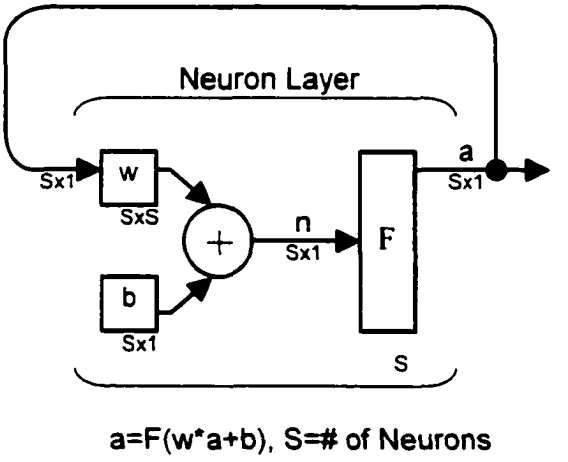

Figure 4–6 Feedback Network (Hopfield, 1984)

Feedback networks are quite powerful because they are sequential rather than combinational like the networks discussed previously. The feedback connection from output to input makes a multiple-layer network able to learn dynamically. The feedback network is commonly supplied with an initial input vector. After that start, the network outputs are used as inputs for each succeeding cycle (Hopfield, 1984).

In multiple-layer feedback networks, it is important to be able to calculate the derivatives of any transfer functions used. Each of the transfer functions mentioned above, namely sigmoid and linear, has a corresponding derivative function. These transfer functions are also monotonically increasing functions. That is, the output of each function increases as its input increases. Thus, the transfer functions have no minima, which would tend to cause error minima that could trap the network as it learned. These three transfer functions are the most commonly used transfer functions for multiple-layer networks, but other differentiable transfer functions can be created and used with multiple-layer networks, if desired (Carpenter, 1989; Dreyfus, 1990).

Recurrent Network

Recurrent networks are based on multiple-layer feedback networks. A recurrent network can be created by generalizing the Widrow-Hoff learning rule (Widrow and Hoff, 1960) to multiple-layer networks and non-linear differentiable transfer functions, with the addition of a feedback connection from the output of the hidden layer to its input (Parlos et al., 1994).

Figure 4–7 shows a two-layer recurrent network. The feedback connection in the first layer of the recurrent network makes it different from multiple-layer feedforward networks. The delay in this connection stores values from the previous time step, which can be used in the current time step. Thus, even if two recurrent networks, with the same weights and biases, are given identical inputs at a given time step, their outputs can be different due to different feedback states.

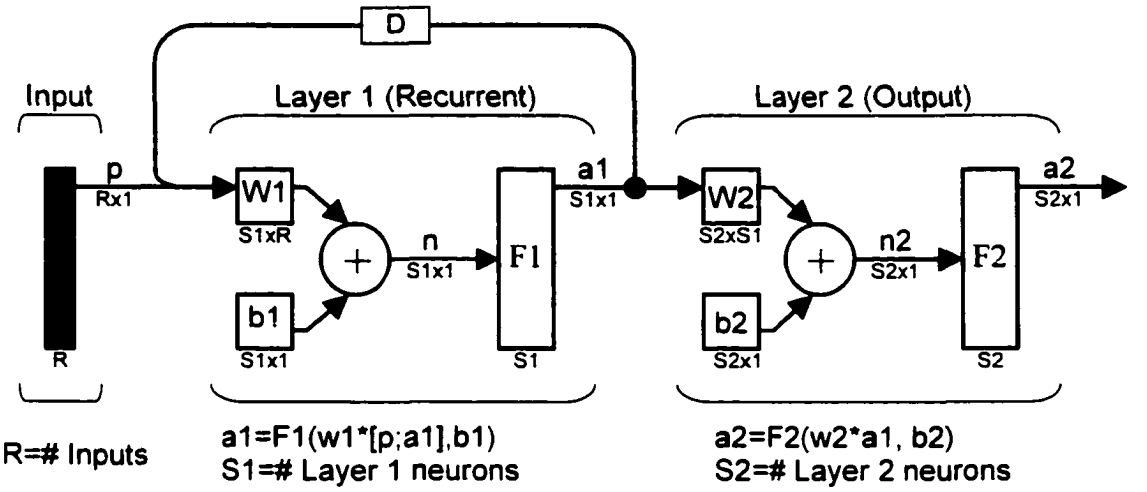

Figure 4–7 Two-Layer Recurrent Network (Demuth and Beale, 1995)

Multiple layers of neurons with non-linear transfer functions allow the network to learn non-linear and linear relationships between input and output vectors (Bernasconi, 1988; Faustt, 1994). If it is desirable to constrain the outputs of a network, such as between -1 and +1, then the output layer should use a sigmoid transfer function (Demuth and Beale, 1995). The linear output layer lets the network produce values outside the range -1 to +1. Therefore, the combination of sigmoid hidden layer(s) and a linear output layer can approximate any function with a finite number of discontinuities with arbitrary accuracy (Mitchison, 1989; Poggio and Girosi, 1990; Connor et al., 1994). The only requirement is that the hidden layer must have enough neurons (Hopfield, 1982; Dayhoff, 1990). More hidden neurons are needed, as the function being fit increases in complexity (Zurada, 1992; Demuth and Beale, 1995).

4.3 Modeling Slope Stability with Neural Network

A two-layer feedforward network model was initially developed in this study for slope stability analysis. Unfortunately, the predicted results by this model were rather irrational perhaps because a feedforward-type training could be easily trapped in local minimum in this situation (Rumelhart, 1990; Demuth and Beale, 1995). The recurrent neural network (RNN) was then adopted since its dynamic training can overcome the local minimum difficulties and reach global minimum. The proposed slope stability analysis model is based on the two-layer recurrent network, as discussed in the following.

4.3.1 Proposed RNN Model

The proposed RNN model is a black box model rather than the semi-analytical model, as developed in Chapter 3. The architecture of the proposed RNN model is shown diagrammatically in Figure 4–8.

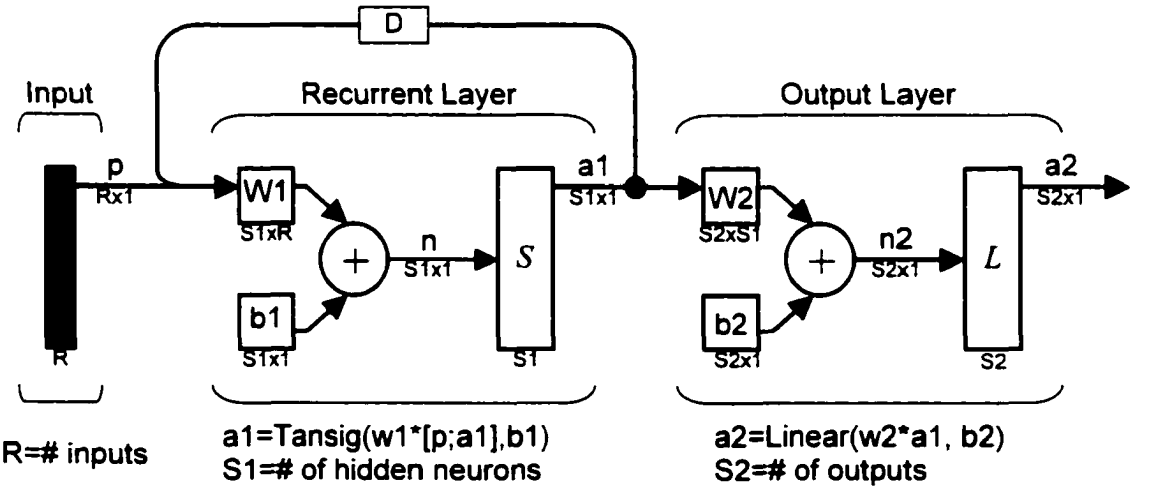

Figure 4–8 Proposed RNN Model for Slope Stability Analysis

The number of input is specific for the proposed model and can be identified based on the data collected from slope stability analyses, whereas the number of neurons in the hidden layer can be determined in the process of initializing the network. The number of neurons in the output layer depends on whether the factor of safety or the slip surface is chosen as the target.

In the proposed two-layer recurrent network model (Figure 4–8), the tan-sigmoid transfer function is used in the hidden layer. A single neuron is used in the output layer to predict the factor of safety, F_s, since it is usually the only target for most of the slope stability analyses available. And three neurons are used in the output layer to predict the slip surface including the coordinates of slip center (a, b) and the radius (r). Because the factors of safety of slopes are usually in the range of say less than one to 2 or 3 (they are not negative for sure), the linear transfer function is used in the output layer.

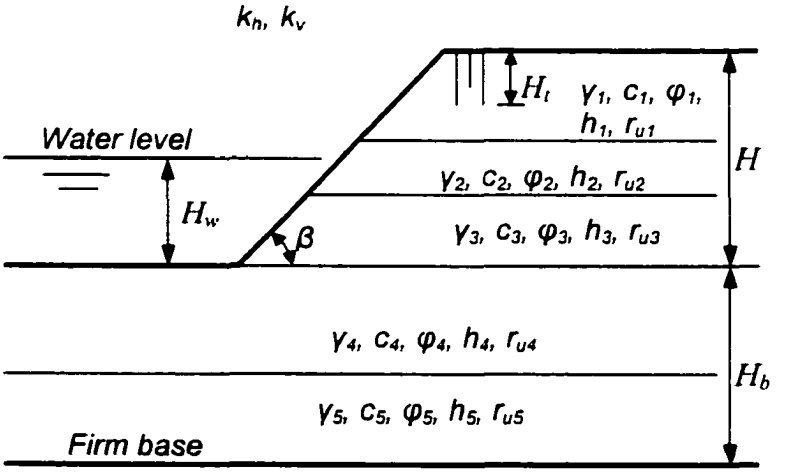

Figure 4–9 A Typical Slope for the Proposed RNN Model

Determination of the input parameters (32) for the proposed recurrent network model is a difficult task, and is also limited to the data that are collected in this study primarily from the slope stability literature. Only a limited number of field case studies could be identified in the literature, having relevance to the proposed RNN model. The rule of thumb is to choose all the parameters that could possibly contribute to the failure of a slope. The parameters selected, as shown in Figure 4–10, include the height of slope (H), the inclination of slope (β), the height of water level (H_w), the height of tension cracks at crest of slope (H_t), the depth of firm base (H_b), horizontal and vertical seismic coefficients (k_h, k_v), the unit weight of soil (γ_i, $i=1$ *to* 5), the cohesion of soil (c_i, $i=1$ *to* 5), the friction angle of soil (ϕ_i, $i=1$ *to* 5), the thickness of each layer (h_i, $i=1$ *to* 5), and the pore pressure ratio (r_{ui}, $i=1$ *to* 5) where r_u is defined as the ratio of the pore pressure u to the overburden pressure γh, for a given layer (i.e., $r_u = u / \gamma h$). For simplicity, five soil layers ($i=1$ *to* 5) are assumed, as shown in Figure 4–9, for a typical layered slope. Thus, for a homogeneous slope, the soil properties (γ_i, c_i, ϕ_i) would be the same for each layer. Totally, 32 input parameters are used for the proposed RNN model. With the wide range of factors, the training data are well represented for the proposed model.

After determining the architecture of the proposed model, we can then train it using the data collected. Since the proposed recurrent network slope model is solely based on the slope data, a brief review of the slope data is given before initializing the network.

4.3.2 Slope Data for Constructing the Model

As noted previously, the data used for constructing the model are from the slope stability literature, with some data from field case studies where failure records of slopes and/or laboratory test results are available. Data for a total of 124 slopes were collected, as shown in Table 4–1, with the principal parameters of each slope listed. While some slopes are homogeneous (Slopes 1, 2, etc.), others are layered (Slopes 8, 24, 25, 43, 62, 83, 84, 93, 107, 113). The soil properties (γ, c, ϕ) listed in Table 4–1 are the weighted average values for layered slopes. The properties of each layer are presented in Appendix. The layers of the slopes range from 1 to 5.

The slopes typically composed of sandy and clayey soils, including clayey sand, sandy clay, silty clay and clayey silt. The slope heights range from 4 to 67.8 m. The inclinations range from 11° to 71.6°. The unit weights of soils range from 9 to 22.8 kN/m^3, cohesions from 0 to 67 kPa and friction angles from 0° to 37.5°. Approximately, the pore pressure ratio (r_u listed in Table 4–1) representing steady-state scenario is calculated at the center of each layer where it is applicable. The values of r_u range from 0 to 1. The factors of safety available from FEM analyses are listed in Table 4–1. It is known that FEM models can adequately represent field conditions in most cases. Also, the factors of safety available from the Bishop method are listed since the Bishop method can give fairly accurate results for most cases where this method is applicable. These analysis results are needed to train and evaluate the proposed RNN model.

Table 4–1 Slopes for Developing the Proposed RNN Model

Slope (#)	Height (m)	Layers (#)	Inclination (deg)	Unit Wt (kN/m^3)	Cohesion (kPa)	Friction (deg)	r_u (ratio)	k_h	k_v	FEM	Bishop (1952)
1	10.00	1	33.69	20.00	10.00	20.00	0	0	0	1.14	1.32
2	15.20	1	71.60	18.00	20.00	20.00	0	0	0	1.00	0.94
3	50.00	1	21.80	11.00	15.00	21.00	0	0	0	1.13	0.97
4	10.00	1	26.57	19.61	31.70	13.00	0.9	0	0	1.44	1.61
5	10.50	1	26.57	20.27	31.70	13.00	0	0	0	1.82	1.64
6	5.00	1	20.00	20.00	40.00	30.00	0	0	0	1.56	1.35
7*	8.05	1	26.57	18.50	15.00	10.00	0	0	0	1.19	1.27
8	23.75	2	29.20	17.15	0.00	35.00	0	0	0	0.92	1.06
9	10.00	1	30.00	18.00	25.00	10.00	0	0	0	1.54	1.55
10	6.00	1	33.69	19.80	4.00	32.00	0	0	0		1.40
11	44.20	1	19.98	22.76	16.76	37.50	0	0	0		1.18
12	20.00	1	33.69	19.65	4.31	32.00	0	0	0	1.00	1.31
13	6.20	1	16.72	18.80	0.00	20.00	0.3	0	0		0.75
14	7.20	1	19.98	18.80	1.00	20.00	0.24	0	0		0.80
15	7.00	1	18.43	18.80	1.00	20.00	0.28	0	0		0.77
16*	7.80	1	44.50	18.60	10.20	20.00	0	0	0	1.00	1.05
17	12.20	1	17.10	18.80	1.50	20.00	0.32	0	0		0.98
18	8.00	1	26.57	18.50	20.00	20.00	0	0	0	2.05	2.09
19	20.00	1	22.00	20.00	0.00	20.00	0	0.035	0		1.00
20	20.00	1	22.00	20.00	0.00	20.00	0.5	0.035	0		0.90
21	11.50	1	27.60	17.71	9.09	20.35	0	0.2	0	1.09	1.10
22	11.50	1	27.60	17.71	9.09	20.35	0	0.1	0	1.15	1.20
23	8.00	1	45.00	18.50	15.00	20.00	0	0	0	1.46	1.29
24*	8.00	2	45.00	18.45	15.06	10.10	0.14	0	0	1.00	0.97
25*	7.62	5	26.57	17.61	7.66	26.00	0.2	0	0	1.16	1.13
26	32.80	1	18.16	17.00	12.00	16.30	1	0	0	0.94	0.86
27	20.40	1	22.00	20.00	20.00	20.00	1	0.035	0		1.12
28	20.40	1	22.00	20.00	20.00	20.00	1	0.1	0		0.96
29	44.20	1	19.98	22.80	16.80	37.50	0.6	0	0		1.00
30	44.20	1	19.98	22.80	16.80	37.50	0.55	0	0		1.12
31	4.90	1	18.43	18.80	1.20	20.00	0.27	0	0		1.10
32	20.00	1	33.69	18.80	41.70	15.00	0	0	0		1.68
33	15.20	1	63.40	18.00	20.00	20.00	0	0	0	1.00	
34	46.00	1	41.01	9.00	25.00	20.00	0	0	0	1.03	0.99
35*	45.50	1	41.01	12.00	23.00	25.00	0	0	0	1.08	1.03
36	8.00	1	45.00	18.50	20.00	15.00	0	0	0	1.45	1.32
37	8.00	1	45.00	18.50	20.00	20.00	0	0	0	1.68	1.50
38*	30.00	1	20.56	19.61	14.71	20.00	0	0	0	1.75	1.52
39*	32.80	1	18.16	17.00	12.00	16.30	0	0	0	1.08	1.11
40	17.00	1	33.69	18.80	1.00	20.00	0.43	0	0		0.97
41	6.10	1	33.69	19.62	4.31	32.00	0	0	0	1.54	1.47
42	10.00	1	26.57	16.00	10.00	15.00	0	0	0		0.93
43*	9.10	3	26.60	18.31	5.16	15.12	0.1	0	0	1.00	0.99
44	8.00	1	45.00	18.50	25.00	10.00	0	0	0	1.42	1.35
45	17.68	1	26.57	19.65	10.06	27.00	0	0	0	0.86	0.79

Table 4–1 Continued

Slope (#)	Height (m)	Layers (#)	Inclination (deg)	Unit Wt (kN/m^3)	Cohesion (kPa)	Friction (deg)	r_u (ratio)	k_h	k_v	FEM	Bishop (1952)
46*	8.56	1	44.50	18.50	20.00	10.00	0	0	0	1.23	1.15
47	44.00	1	19.98	22.80	16.80	37.50	0.4	0	0		1.50
48	13.50	1	26.57	17.30	57.50	7.00	0	0	0	2.11	2.08
49	6.10	1	33.69	19.65	4.31	32.00	0	0	0	1.11	1.19
50	6.00	1	23.96	18.80	1.00	20.00	0	0	0		0.93
51	7.00	1	26.57	18.80	1.00	20.00	0.1	0	0		0.81
52	10.00	1	26.57	18.93	11.97	32.00	0	0	0	1.22	1.05
53*	10.00	1	33.69	17.66	7.85	25.00	0.25	0	0	1.05	1.07
54	8.00	1	26.57	18.50	5.00	20.00	0	0	0	1.23	1.21
55	8.00	1	26.57	18.50	15.00	20.00	0	0	0	1.85	1.82
56	10.40	1	15.24	18.80	0.00	20.00	0.33	0	0		0.97
57	5.10	1	25.25	18.05	5.75	18.00	0.64	0	0		0.62
58	4.00	1	20.00	17.95	5.00	15.00	0	0	0	0.89	0.78
59	20.00	1	20.00	19.72	30.00	30.00	0.5	0	0	1.25	1.54
60	4.50	1	20.00	15.92	2.16	17.33	0	0	0	0.88	0.93
61	12.19	1	33.69	19.24	22.80	35.00	0	0	0	1.78	1.62
62*	9.50	2	25.50	18.61	10.42	10.14	0.31	0	0	1.00	1.03
63	8.00	1	26.57	18.50	20.00	15.00	0	0	0	1.72	1.78
64	20.00	1	26.57	18.71	0.00	23.50	0	0.51	0.1		1.03
65	21.50	1	24.13	17.40	5.00	10.00	0	0	0		1.23
66	44.20	1	20.00	22.00	16.80	37.50	0.5	0	0		1.25
67	44.20	1	20.00	22.00	16.80	37.50	0.45	0	0		1.37
68	13.70	1	26.57	18.71	0.00	14.00	0	0.05	0		1.28
69*	8.20	1	45.00	18.50	15.00	15.00	0	0	0	1.24	1.11
70	44.10	1	19.98	22.80	16.50	37.50	0.3	0	0	0.68	
71	44.10	1	19.98	22.80	16.50	37.50	0.2	0	0	0.70	
72	12.19	1	27.15	18.87	0.00	33.00	0	0	0		1.20
73	12.19	1	27.15	18.87	67.00	0.00	0	0	0	2.13	2.15
74	12.19	1	27.15	18.87	28.70	20.00	0	0	0	1.76	1.35
75*	8.45	1	45.00	18.50	10.00	15.00	0	0	0	1.00	0.89
76	21.50	1	24.13	17.40	0.00	14.00	0	0	0		0.92
77	21.50	1	24.13	17.40	0.00	17.20	0	0	0	1.06	0.64
78*	46.00	1	38.66	14.00	20.00	26.30	0	0	0	1.19	1.14
79	22.70	1	16.27	18.20	0.00	14.10	0	0	0		1.19
80	22.70	1	16.27	18.20	0.00	17.20	0	0	0	1.00	0.87
81	15.50	1	15.01	18.00	5.00	10.00	0	0	0	1.05	
82	15.50	1	15.01	18.00	0.00	14.00	0	0	0	1.11	1.17
83	15.00	3	12.99	20.00	45.00	0.00	0	0	0	1.39	1.31
84	15.00	3	12.99	20.00	21.00	17.00	1	0	0		1.05
85	25.00	1	22.00	18.80	30.00	20.00	0.25	0	0		1.36
86	8.00	1	45.00	18.50	25.00	15.00	0	0	0	1.65	1.53
87*	8.00	1	26.50	18.50	15.00	15.00	0	0	0	1.54	1.53
88	10.06	1	21.80	18.44	0.96	24.50	0	0	0	1.06	1.00
89	10.06	1	21.80	18.44	0.72	25.60	0	0	0	1.00	0.83
90	6.00	1	33.69	19.65	1.50	30.00	0	0	0		0.79

Table 4–1 Continued

Slope (#)	Height (m)	Layers (#)	Inclination (deg)	Unit Wt (kN/m^3)	Cohesion (kPa)	Friction (deg)	r_u (ratio)	k_h	k_v	FEM	Bishop (1952)
91	12.80	1	27.76	21.85	8.62	32.00	0	0	0		1.03
92*	27.43	1	26.40	17.29	44.54	12.00	0	0	0	1.52	1.45
93	14.33	3	36.53	20.47	51.39	0.00	0	0	0	1.65	1.64
94	8.00	1	26.57	18.50	10.00	15.00	0	0	0	1.29	1.29
95	10.00	1	39.81	20.36	0.98	32.50	0.7	0	0	1.11	1.01
96	18.00	1	26.57	19.50	9.81	27.00	0	0	0	1.02	1.07
97	12.80	1	28.50	21.55	8.62	30.00	0	0	0	0.92	1.05
98	10.06	1	21.80	18.01	15.33	20.00	0	0	0		0.73
99	10.06	1	21.80	18.84	0.00	20.00	0	0	0	1.43	
100	7.01	1	18.43	21.29	0.00	20.00	0	0	0	1.05	
101	7.01	1	18.43	19.79	0.96	13.00	0	0	0	1.03	1.00
102	18.29	1	11.00	22.32	15.33	21.00	0	0	0	1.00	1.28
103	12.10	1	24.38	16.10	25.00	20.00	0	0	0	1.18	1.00
104	30.00	1	30.00	21.00	22.11	18.29	0	0	0	1.22	0.86
105	5.00	1	33.69	19.60	2.56	27.60	0	0	0	1.06	0.98
106	67.80	1	29.05	19.00	33.00	29.50	0	0	0	1.01	1.21
107	67.80	2	29.05	19.00	25.00	24.00	0	0	0		1.31
108*	14.30	1	27.00	19.60	9.60	25.00	0.32	0	0	1.00	0.97
109	8.00	1	45.00	18.50	30.00	15.00	0	0	0	1.85	1.75
110	8.00	1	26.57	18.50	25.00	15.00	0	0	0	1.87	2.05
111	11.50	1	27.60	17.71	9.09	20.35	0	0	0	0.99	0.82
112	5.00	1	26.57	17.64	4.90	10.00	0	0	0		1.00
113	12.80	4	28.00	21.80	8.60	32.00	0	0	0	1.19	0.98
114	10.00	1	14.04	20.00	10.00	25.00	0	0	0		0.67
115	6.00	1	45.00	18.00	10.00	37.00	0	0	0	1.15	1.76
116	6.00	1	33.69	18.00	10.00	37.00	0	0	0	1.19	1.20
117	20.15	1	22.00	20.00	20.00	20.00	0.5	0.035	0.25		1.12
118	20.15	1	22.00	20.00	20.00	20.00	0.4	0.1	0.05		0.96
119	8.00	1	45.00	18.50	25.00	20.00	0	0	0	1.87	1.74
120*	8.30	1	26.57	18.50	10.00	20.00	0	0	0	1.60	1.54
121	11.50	1	27.60	17.71	9.09	20.35	0	0.05	0	1.21	1.25
122*	11.50	1	27.60	17.71	9.09	20.35	0	0	1	1.16	1.00
123	11.50	1	27.60	17.71	9.09	20.35	0	0	2	0.90	0.87
124*	10.20	1	45.00	19.60	11.80	30.00	0	0.2	0	1.23	1.00

Note: * indicates that the slope is used for validation.

Among the 124 slopes, 20 slopes are chosen for prediction and evaluation of the strengths/weaknesses of the developed RNN model including 10 representative slopes selected and 10 randomly chosen from the 114 slopes. The remaining 104 slopes are used for training the proposed model.

The slopes analyzed by finite element methods are typically clayey slopes. Most (85) of the finite element analyses collected from the literature used two-dimensional (2-D) analyses (Slopes #7, #16, etc.), while some (17) used three-dimensional (3-D) analyses (Slopes #53, #124, etc.) (Appendix). The soil constitutive models used in the finite element analyses include the Mohr-Coulomb failure criterion and the Drucker-Prager failure criterion (Drucker and Prager, 1952). The finite element meshes used in the finite element analyses usually consisted of three-noded triangular or four-noded quadrilateral elements for 2-D analyses and eight-noded brick-type elements for 3-D analyses. Table 4-2 presents the FEM results for the 20 slopes to be used for prediction/evaluation.

While all the methods employ the same definition of factor of safety as the ratio of shear strength available to shear stress required for equilibrium, some finite element analyses used the summed values of shear strength/stress called the overall factor of safety (Zienkiewicz et al., 1975; Zhou, 1993; Yang et al., 1994; Fredlund and Scoular, 1999; Cai and Ugai, 1999; Cheng et al., 2000) and some used the local values of shear strength/stress called the local factor of safety (Hunt, 1986; Huang and Yamasaki, 1993; Press et al., 1995, Wakai and Ugai, 1999).

By considering pore pressure as a nodal variable, it is realized that the pore pressures could be better treated by finite element solutions. This is one of the limitations of the proposed neural network model in that it does not comprehensively treat the effect of pore pressure. The Young's modulus and Poisson's ratio were included in the finite element analyses. Initially they were also

included as inputs in the proposed RNN model. These two parameters are related to the movement of a slope. Therefore, it was considered inappropriate to include them in the proposed RNN model that is developed to predict the failure of a slope. Consequently, Young's modulus and Poisson's ratio were not included in the final RNN model.

Table 4–2 Slopes with Finite Element Analysis

Slope #	FEM Dim.	Element Node	Soil Constitutive Model	Young's Mod. (MPa)	Poisson's Ratio	F.S.
7	2-D	4	Drucker-Prager	5.0	0.30	1.19
16	2-D	4	Drucker-Prager	5.0	0.30	1.00
24	2-D	4	Drucker-Prager	5.0	0.30	1.00
25	2-D	4	Mohr-Coulomb	40.0	0.40	1.16
35	2-D	4	Mohr-Coulomb	20.0	0.33	1.08
38	2-D	4	Mohr-Coulomb	20.0	0.33	1.75
39	2-D	3	Mohr-Coulomb	50.0	0.35	1.08
43	2-D	4	Drucker-Prager	5.0	0.33	1.00
46	2-D	4	Drucker-Prager	5.0	0.30	1.23
53	3-D	8	Mohr-Coulomb	98.1	0.30	1.05
62	2-D	4	Drucker-Prager	10.0	0.30	1.00
69	2-D	4	Drucker-Prager	5.0	0.30	1.24
75	2-D	4	Drucker-Prager	5.0	0.30	1.00
78	2-D	4	Mohr-Coulomb	20.0	0.33	1.19
87	2-D	4	Drucker-Prager	5.0	0.30	1.45
92	2-D	4	Mohr-Coulomb	20.0	0.33	1.52
108	2-D	4	Drucker-Prager	20.0	0.33	1.00
120	2-D	4	Drucker-Prager	5.0	0.30	1.60
122	2-D	4	Mohr-Coulomb	20.0	0.33	1.16
124	3-D	8	Mohr-Coulomb	98.1	0.30	1.23

4.3.3 Initializing the Proposed Model

A computer code has been developed for use with Matlab based on the proposed RNN model utilizing the Neural Network Toolbox - a commercially available software. In developing this program, the Widrow-Hoff learning rule (Widrow and

Hoff, 1960), also called backpropagation, is used to adjust the weights and biases of the network in order to minimize the sum-squared error of the network. This is done by continually changing the values of the network weights and biases in the direction of the steepest descent with respect to error. Derivatives of error called delta vectors are calculated for the network's output layer, and then backpropagated through the network. Calculating a layer's delta vector from the following layer's delta vector is referred to as the backpropagation of deltas (Widrow, 1962; Vogl et al. 1988).

Initialization creates initial weights and biases for the proposed recurrent network model. It takes as arguments a matrix of input vectors, the number of recurrent neurons, the number of output neurons, and the transfer functions of each layer. With the input matrix and the output target vector set up from the 104 randomly selected slopes, it is found that 45 recurrent neurons is a proper number for the hidden layer after other numbers has been tried according to the Widrow-Hoff learning rule.

4.3.4 Training the Proposed Model

Training the proposed model generates new weights and biases of network when it is presented with the given sequence of input and target vectors and the initial weights and biases. The training parameters (tp) specified during the training process include the number of epochs between displaying progresses, the maximum number of epochs to train, the sum-squared error goal, and the learning rate. The learning rate specifies the size of changes that are made in the weights and biases at

each epoch. Small learning rates result in long training time but can prevent the network's values from jumping over valleys in the error surface that lead to lower errors (Demuth and Beale, 1995). Training continues until either the error goal is met, or the maximum number of epochs has occurred.

The recurrent training may lead to a local rather than a global error minimum. The local error minimum obtained may be satisfactory, but if it is not, a network with more neurons may do a better job. However, the number of neurons or layers to add may not be obvious. Alternatively, several different sets of initial conditions may be used to run the problem to see if they led to the same or different solutions (Parlos et al., 1994).

During training, the network error and the current training status can be displayed at intervals defined by the training parameter. These displays show how the network is doing. Training process returns, in addition to the new weights and bias, the number of epochs of training that actually occurred, and a row vector that records errors throughout training.

The interpretation of training often depends on the point of view that one takes on the recurrent network (Luk, 1999). The view we take here is simply that the network is a function approximator of the model. The input data point is taken as the training set to determine the set of weights of the network $\{w_{ij}\}$ by solving the non-linear least-squares problem of minimizing $(y-\hat{y})^2$ where $\hat{y} \equiv \hat{f}(w_{ij})$ is the function of weights of the network.

Figure 4–10 shows an example of training curve from the proposed RNN model - the normalized sum of squared error (SSE) versus the number of iterations. As specified, the training is stopped when the normalized SSE is less than 0.001 or when the number of iterations reaches 1000 whichever occurs first.

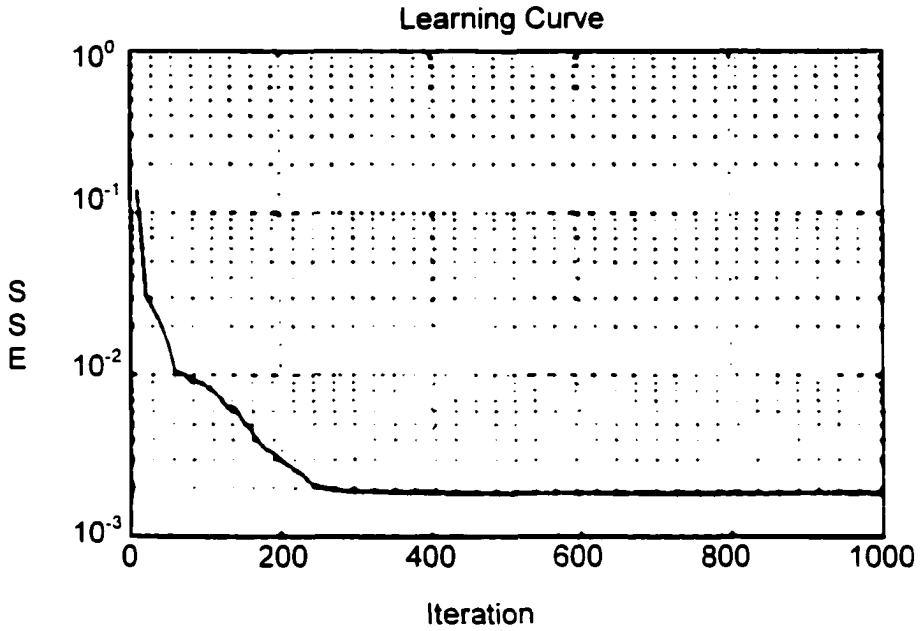

Figure 4–10 Normalized SSE vs. Number of Iterations

After finalizing the weights and bias for the proposed RNN model, we then can use the RNN model to predict the factors of safety for the slopes selected.

4.3.5 Prediction with the Proposed Model

Prediction was processed with a new matrix of input vectors from the 20 slopes selected as well as the weights and bias obtained from the training process. Prediction returns a matrix of output vectors – the factors of safety of the slopes. The results of the predicted factors of safety are presented in Table 4–3.

Table 4–3 RNN Model Prediction Results

Slope #	Height (m)	Inclinatior (deg)	Unit Wt. (kN/m^3)	Cohesion (kPa)	Friction (deg)	r_u (ratio)	FEM	Bishop (1952)	Semi-analy. (proposed)	RNN (proposed)
7	8.05	26.57	18.50	15.00	10.00	0.00	1.19	1.27	1.23	1.34
16	7.80	44.50	18.60	10.20	20.00	0.00	1.00	1.05	1.06	1.10
24	8.00	45.00	18.45	15.06	10.10	0.14	1.00	0.97	1.15	0.95
25	7.62	26.57	17.61	7.66	26.00	0.20	1.16	1.13	1.21	1.02
35	45.50	41.01	12.00	23.00	25.00	0.00	1.08	1.03	1.01	1.09
38	30.00	20.56	19.61	14.71	20.00	0.00	1.75	1.52	1.50	1.63
39	32.80	18.16	17.00	12.00	16.30	0.00	1.08	1.11	1.16	1.18
43	9.10	26.60	18.31	5.16	15.12	0.10	1.00	0.99	1.06	0.87
46	8.56	44.50	18.50	20.00	10.00	0.00	1.23	1.15	1.20	1.19
53	10.00	33.69	17.66	7.85	25.00	0.25	1.05	1.07	1.10	1.11
62	9.50	25.50	18.61	10.42	10.14	0.31	1.00	1.03	1.14	0.93
69	8.20	45.00	18.50	15.00	15.00	0.00	1.24	1.11	1.19	1.27
75	8.45	45.00	18.50	10.00	15.00	0.00	1.00	0.89	0.98	1.16
78	46.00	38.66	14.00	20.00	26.00	0.00	1.19	1.14	1.13	1.20
87	8.18	26.50	18.50	15.00	15.00	0.00	1.45	1.35	1.49	1.69
92	27.43	26.40	17.29	44.54	12.00	0.00	1.52	1.45	1.38	1.43
108	14.30	27.00	19.60	9.60	25.00	0.32	1.00	0.97	1.08	0.98
120	8.30	26.57	18.50	10.00	20.00	0.00	1.60	1.54	1.51	1.59
122	11.50	27.60	17.71	9.09	20.35	0.00	1.16	1.00	0.99	1.16
124	10.20	45.00	19.60	11.80	30.00	0.00	1.23	1.00	1.32	1.20

For the 20 slopes selected for prediction, cohesions of soils range from 5 kPa to 44.54 kPa and friction angles range from 10° to 30°. The heights of the slopes range from 7.62 meters to 46 meters. Slope angles range from 18.16° to 45°. The pore pressure ratios, r_u, are within the range of 0 to 0.32. The unit weights of soils are within the range of 12 to 19.61 kN/m^3. Also, listed in the table are the results from the finite element analyses, the Bishop method and the semi-analytical method developed in the previous chapter for the purpose of comparison. The multiple layers are used in the finite element analyses, the Bishop method and the proposed RNN model, while single layer is used in the semi-analytical method.

It can be observed from Table 4–3 that the factors of safety obtained by the proposed RNN model are in general agreement with the results from the finite element analyses, the Bishop method, and the semi-analytical method. Statistical analyses show that the results from the proposed RNN model are closer to the finite element method than to the Bishop method and the semi-analytical method. The difference between the proposed RNN model and the FEM averages 8% with a standard deviation of 6%. The difference between the proposed RNN model and the Bishop method is about 10% with a standard deviation of 8.5%. In two cases (Slopes #75, #87), the factors of safety are over-predicted with the differences between the proposed RNN model and the FEM being 16%, and 17%, respectively. And in one case (Slope #25), it is under-predicted with the difference between the proposed RNN model and the FEM being 14%. The over or under-predictions might be caused by one or more parameters that are over or under-valued.

The difference between the semi-analytical method and the finite element method averages 9% with a standard deviation of 6% for the 20 slopes. The proposed semi-analytical method is closer to the Bishop method with a difference of 8% on an average and a standard deviation of 7%. The difference between the proposed RNN model and the proposed semi-analytical method averages 11% with a standard deviation of 6%. There are six cases (Slopes #24, #25, #43, #53, #62, #108) in which the pore pressures are involved in the prediction of the proposed RNN model. Since the semi-analytical method does not include pore pressure in its

formulation, it generally sets the upper bounds of the factors of safety for the six slopes as shown in Table 4–3.

4.3.6 Predicting Slip Surface by the RNN Model

The slip surfaces are determined, based on the results (slip center and radius) obtained from the semi-analytical method, by retraining the RNN model discussed above. However, for this case, the output layer has three neurons or target values, a, b, and r that represent the coordinates of the center and the radius of a circular slip surface. The input parameters are same as those used for predicting F_s. 20 slopes are used for the prediction of slip surfaces, as listed in Table 4–4.

Table 4–4 RNN-Based Results of Circular Slip Surface

Slope	Height	Inclination	Unit Wt.	Cohesion	Friction	Semi-Analytical			RNN		
#	(m)	(deg)	(kN/m^3)	(kPa)	(deg)	x (m)	y (m)	r (m)	x (m)	y (m)	r (m)
7	8.05	26.57	18.50	15.00	10.00	6.36	11.65	13.27	6.15	11.56	13.09
16	7.80	44.50	18.60	10.20	20.00	1.90	8.96	9.16	2.36	9.47	9.76
24	8.00	45.00	18.45	15.06	10.10	2.35	9.67	9.95	2.51	9.83	10.15
25	7.62	26.57	17.61	7.66	26.00	4.78	9.32	10.47	4.89	9.20	10.42
35	45.50	41.01	12.00	23.00	25.00	3.24	58.45	58.54	3.67	52.49	52.62
38	30.00	20.56	19.61	14.71	20.00	6.50	38.04	38.59	6.16	34.64	35.18
39	32.80	18.16	17.00	12.00	16.30	7.17	41.26	41.88	6.85	38.08	38.69
43	9.10	26.60	18.31	5.16	15.12	5.23	11.52	12.65	5.12	11.03	12.16
46	8.56	44.50	18.50	20.00	10.00	2.51	9.96	10.27	2.65	10.62	10.95
53	10.00	33.69	17.66	7.85	25.00	3.82	13.05	13.60	3.37	12.54	12.98
62	9.50	25.50	18.61	10.42	10.14	6.14	11.33	12.97	5.79	11.88	13.22
69	8.20	45.00	18.50	15.00	15.00	2.27	9.28	9.55	2.08	9.74	9.96
75	8.45	45.00	18.50	10.00	15.00	2.10	9.89	10.11	2.34	9.87	10.14
78	46.00	38.66	14.00	20.00	26.00	3.29	56.85	56.95	3.79	53.20	53.33
87	8.18	26.50	18.50	15.00	15.00	6.18	11.07	12.68	5.71	12.09	13.37
92	27.43	26.40	17.29	44.54	12.00	4.86	33.84	34.19	4.75	32.55	32.89
108	14.30	27.00	19.60	9.60	25.00	1.33	26.35	26.38	3.37	21.97	22.23
120	8.30	26.57	18.50	10.00	20.00	5.57	11.20	12.51	5.48	11.52	12.76
122	11.50	27.60	17.71	9.09	20.35	4.60	14.39	15.11	4.56	13.46	14.21
124	10.20	45.00	19.60	11.80	30.00	2.85	12.67	12.99	2.84	12.79	13.10

4.4 Results and Discussions

To evaluate the proposed RNN model, the five slopes (#16, #24, #43, #62, #108) from Table 4–4 with circular slip surfaces predicted by the proposed RNN model were further analyzed to compare the factors of safety with respect to the slip surfaces determined by the Bishop method, the finite element method and the semi-analytical method, as shown in the following figures (4–11 through 4–15).

Slope #16 is a homogenous dry soil slope, as shown in Figure 4–11. The unit weight of soil is 18.6 KN/m^3. The height of slope is 7.8 m and the depth to an underlying rigid layer boundary is 3.2 m from the bottom of the slope excavation. The slope angle is 44.5°. The cohesion and friction angle are 10.2 kPa and 20°, respectively. The factors of safety and slip surfaces for this slope determined by the above-mentioned four different methods are also presented in Figure 4–11.

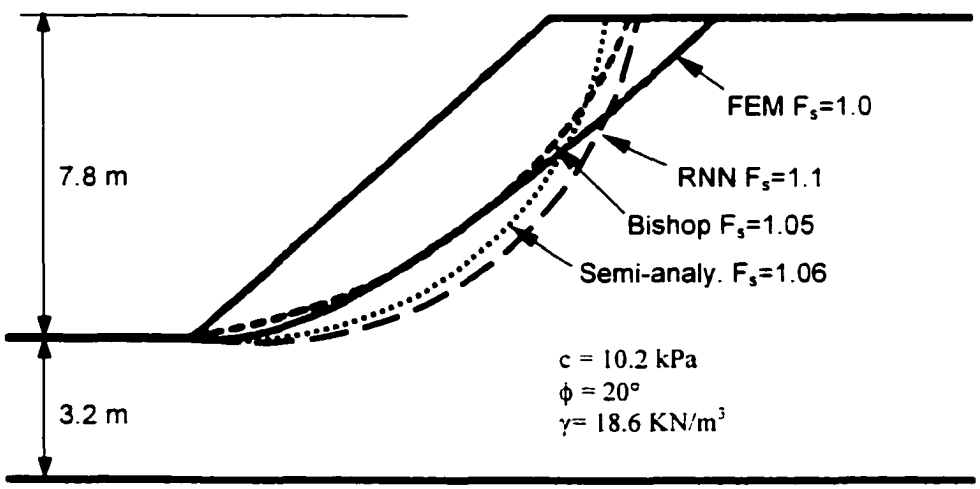

Figure 4–11 Slip Surfaces for Slope #16

The factors of safety for Slope #16, as shown in Figure 4–11, are in good agreement for this simple slope with 1.0 by the FEM model (Zhou, 1993) to 1.1 predicted by the proposed RNN model to 1.05 by the Bishop method and 1.06 by the semi-analytical method, which is between the two methods.

The location of the slip surface for Slope #16 (Figure 4–11) obtained from the RNN model is slightly lower than that defined by the semi-analytical method developed in this study but much lower than that defined by the Bishop method and the FEM model (Zhou, 1993) in the lower portion of the slope. The RNN model yielded a slip surface extending from a point of the upper slope that is further away from the slope face than that predicted by the semi-analytical method but closer than that predicted by the FEM model and not far away from the Bishop method. The lower portions of the failure surfaces determined by the four approaches, however, are in good agreement with each other, and they all pass through the toe of the slope. The RNN model predicted the mixed solution - higher in the upper portion and lower in lower portion than that by the FEM model.

Slope #24, as shown in Figure 4–12, is a layered slope with the unit weight of soil 18.45 KN/m^3 and the cohesion and friction angle of 15.06 kPa and 10.1°, respectively, in an weighted average sense. The height of slope is 8 m and the depth to an underlying rigid layer boundary is 5.6 m. The slope angle is 45°. The water level is 5.6 m above the firm base. The factors of safety and slip surfaces for this slope determined by the above-mentioned four different methods are also presented in Figure 4–12.

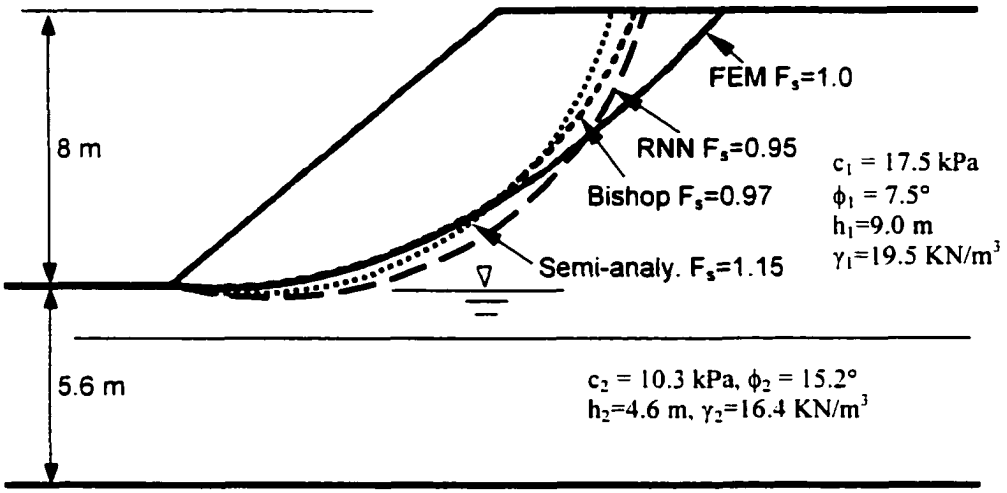

Figure 4–12 Slip Surfaces for Slope #24

The factors of safety of Slope #24, as shown in Figure 4–12, varied slightly from one method to another. The RNN model yields the lowest value of 0.95 which is very close to the value 0.97 predicted by the Bishop method. The FEM model (Zhou, 1993), however, predicts a value of 1.0. The semi-analytical method gives the highest value of 1.15, which might be due to its inability to include layered soils and the effect of pore pressure in its formulation.

It can be observed that the relative locations of the slip surfaces among different methods in Slope #24 show a similar pattern to that of Slope #16, with the slip surfaces by the RNN model and the semi-analytical method becoming closer to that by the Bishop method and the FEM model (Zhou, 1993). Also, as expected, the lower portions of the slip surfaces determined by these four approaches all pass through the toe of the slope.

Slope #43, as shown in Figure 4–13, is a three-layered slope. The unit weights of soils range from 16.5 to 19.2 KN/m^3 with the weighted-average of 18.31 KN/m^3. The height of the slope is 9.1 m and the second layer has the maximum height of 7.2 m. The depth to an underlying rigid layer boundary is 5 m from the bottom of the slope excavation. The slope angle is 26.6°. The cohesion and friction angle are 5.16 kPa and 15.12°, respectively, in a weighted average sense. The water level is 4 m above the firm base. The factors of safety and slip surfaces for this slope defined by the four different methods are presented in Figure 4–13.

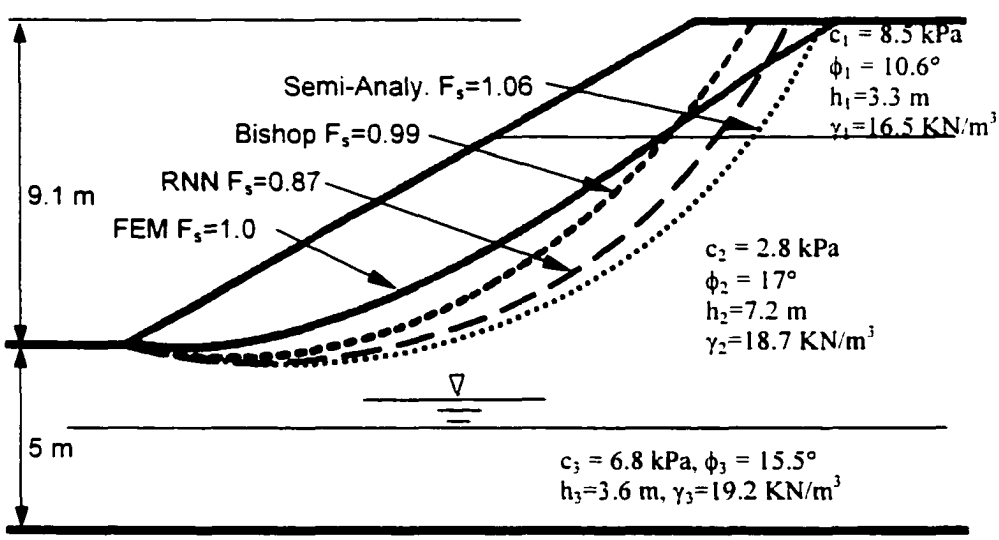

Figure 4–13 Slip Surfaces for Slope #43

As shown in Figure 4–13, the factors of safety of Slope #43 are quite close between the FEM model (Song and Chang, 1995) and the Bishop method with values of 1.0 and 0.99, respectively. The semi-analytical method gives a higher

value of 1.06. However, the RNN model predicts a much lower value of 0.87 than other methods.

The slip surface of Slope #43, defined by the RNN model, lie (Figure 4–13) slightly above that defined by the semi-analytical method and somewhat lower than that by the Bishop method but much lower than that defined by the FEM model (Song and Chang, 1995). The RNN model exhibited a slip surface extending from a point of the upper slope that is further away from the slope face than that predicted by the Bishop method but closer than that predicted by the FEM model and the semi-analytical method. The lower portions of the slip surfaces determined by these four approaches, however, all pass through the toe of the slope, as expected. However, in the middle portions of the slip surfaces, the semi-analytical method and the RNN model deviate from the FEM model. The reason might be that the semi-analytical method fails to treat the slope as a layered soil while the RNN model used the semi-analytical solutions in its training.

Slope #62 is a two-layered slope with the weighted-average unit weight of soil 18.61 kN/m^3 and cohesion and friction angle 10.42 kPa and 10.14°, respectively, as shown in Figure 4–14. The height of slope is 9.5 m and the depth to an underlying rigid layer boundary is 6 m. The slope angle is 25.5°. The water level is 4 m below the top of slope. The phreatic surface is shown in the figure. As reported by Yang et al. (1994), the pore pressure played a key role in the failure of this slope and the location of the actual failure surface is close to the finite element model they developed.

The factors of safety for Slope #62 from the FEM model (Yang et al., 1994) and the Bishop method are quite close to each other with values of 1.0 and 1.03, respectively. The RNN model gives the lowest value of 0.93, while the semi-analytical method yields the highest value of 1.14. The high value from the semi-analytical method might be due to no pore pressure involved in its formulation. The low value by the RNN model might be caused by the approximation of pore pressure and by the limited cases with pore pressures involved in its training.

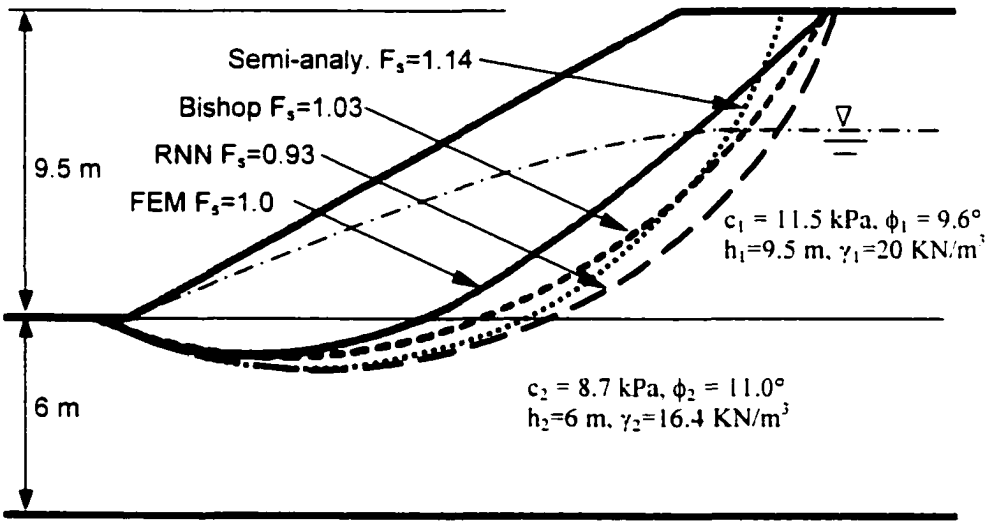

Figure 4–14 Slip Surfaces for Slope #62

The slip surfaces of Slope #62 defined from the four methods deviate from each other (Figure 4–14) in the middle portions of the slope. The slip surface by the Bishop method exhibits a small amount of shift from the FEM model, while the semi-analytical method shift further and the RNN model sets the lower bound in general. It is worth noticing that the lower portions of the slip surfaces determined

by these four approaches somewhat go beyond the toe of the slope but still not far away from each other, which might be caused by the pore water pressure.

Slope #108 is the failure of the Springfield Dam in Kentucky (Huang, 1983). as shown in Figures 4–15. The slope is about 14.3 m high in front and 10 m high in the back of the dam. The slope angle is about 27^0. The water level is about 9 m from the bottom of the dam or 1 m from the top. The circular failure surface determined by Huang (1983) using the Bishop method had a factor of safety of 0.97 with the assumed soil properties of c =9.6 kPa, ϕ = 25°, and γ = 19.6 kN/m^3. Huang (1983) indicated that the actual location of the failure surface is very close to the theoretical circle determined by the Bishop method shown in Figure 4–15.

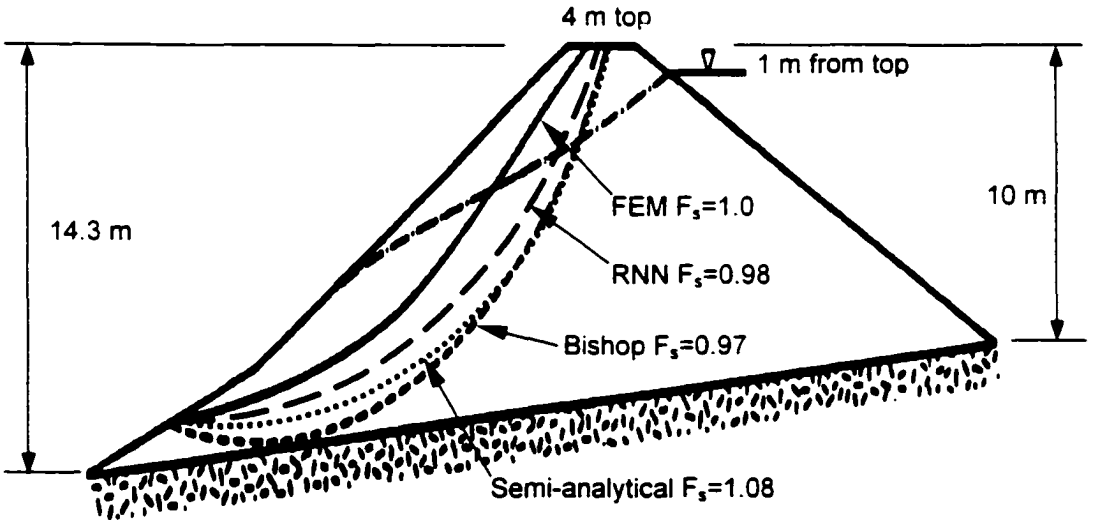

Figure 4–15 Stability Analysis of Springfield Dam

Since the dam had been built long before the failure occurred, it is therefore assumed that no excess pore-water pressure existed in the soils at the time of failure.

Thus, the buoyant weight of the soils below the phreatic surface is used in the analysis. Analysis of the dam failure using the FEM model with soil properties of c = 9.6 kPa, $\phi = 25°$, and $\gamma = 19.6$ kN/m^3 does not indicate a stability problem (Huang and Yamasaki, 1993). One of the strength parameters of the soils below the phreatic surface is then reduced. The cohesion of the soils in a saturated state was taken as one-third of the cohesion of the same soils above the phreatic surface, and the angle of friction was kept the same, since it does not vary much with the degree of saturation. With these changes, the FEM model (Huang and Yamasaki, 1993) gives a factor of safety of 1.0.

Using the same soil properties as used in the Bishop method, the RNN model predicts a factor of safety of 0.98, which is fairly consistent with that from the Bishop method. However, the slip surface determined by the RNN model is much shallower than the circular failure surfaces obtained from the Bishop method and the semi-analytical method but deeper than that from the FEM model (Huang and Yamasaki, 1993), as presented in Figure 4–15. The emerging points of the slip surfaces near the toe of the dam agree well. The projected locations of the three slip surfaces are different at the crown of the dam with the Bishop method predicting a failure surface further away from the slope face, the FEM model (Huang and Yamasaki, 1993) predicting a failure surface closest to the slope face and the RNN model predicting a failure surface between them.

These examples illustrate the use of the proposed RNN model as an alternative approach to slope stability analyses. The predicted results shows that the

104 cases are sufficient for training the proposed RNN model for the factor of safety and the failure surfaces. For the five slopes examined, the factors of safety from the semi-analytical method generally set the upper bound in the cases where pore water pressures are involved, which is one of its limitations. The locations of the slip surfaces defined by the four methods also deviate somewhat from each other. One possible explanation is the concept of constancy of the factor of safety along the failure surface that the limit equilibrium analysis (the Bishop method and the semi-analytical method) is based on. Soil properties (Young's modulus and Poisson's ratio) and the constitutive laws (Mohr-Coulomb failure criterion, Drucker-Prager failure criterion) used in the finite element analyses might contribute to this difference. Additionally, minor errors also could be introduced to the results from the mesh design on which the finite element analysis is based. The results from the proposed RNN model might be affected by the limited number of slopes available for training the model. The lower bounds set by the RNN model in some cases might be caused by its failure to comprehensively treat the effect of pore pressure and also by the limited cases with pore water pressures involved in its training. It might be possible that the proposed RNN model does not have enough training.

4.5 Concluding remarks

In this chapter, an artificial neural network model is presented for slope stability analysis. The proposed model is a two-layer recurrent network with a sigmoid hidden layer and a linear output layer – a powerful combination to perform non-linear modeling. Five layers are assumed for a typical layered slope. The model is

developed based on the data from 124 slopes collected in this study, including 32 input parameters that could possibly contribute to the failure of each slope. The training data are well represented for the proposed model with wide range of factors. 45 recurrent neurons are used in the hidden layer. Training is performed on the 104 slope data selected from the 124 slopes, and prediction or evaluation is based on the remaining 20 slopes. The predicted results by the proposed RNN model are in general agreement with that obtained by the finite element method and the Bishop method as well as the proposed semi-analytical method. The circular slip surfaces are determined by retraining the proposed RNN model with the output targets (slip center and radius) obtained from the semi-analytical method. The output layer has three neurons, namely the coordinates of the center and the radius of the circular slip surface.

In comparison with the proposed semi-analytical method, the proposed RNN model can do better in representing the layered soils or relatively complex cases with pore pressures involved, while the semi-analytical method would be as good as any other methods for simple slopes. The study also shows that the solutions from the Bishop method are quite accurate for most cases.

CHAPTER 5

SUMMARY, CONCLUSIONS AND RECOMMENDATIONS

5.1 Summary

In this study, the slope stability problems (Chapter 1) were introduced and followed by a detailed literature review of the slope stability analysis methods (Chapter 2). A semi-analytical method (Chapter 3) was presented for calculating the factor of safety in which an integral approach is used to accurately represent the forces in various slices and an optimization technique is used to obtain the critical slip surface. As an alternative to numerical approach, an artificial neural network model was developed for estimating slope stability (Chapter 4).

The semi-analytical method presented in Chapter 3 is developed for analysis of slope stability involving cohesive and non-cohesive soils. For sandy slopes, a planar slip surface is employed, while for clayey slopes, circular slip surfaces are employed including Toe Failure, Face Failure and Base Failure resulting from different locations of a hard stratum. Earthquake effects are considered in an approximate manner in terms of seismic coefficient-dependent forces.

The proposed method can be viewed as an extension of the method of slices, but it provides a more accurate treatment of the forces because they are represented in an integral form. Also, the minimum factor of safety is obtained by using the Powell's optimization technique rather than by a trial and error approach used commonly. The results (factor of safety) from the proposed semi-analytical method are compared with the solutions by the Bishop method (1952) and the finite element

method, and satisfactory agreements are obtained. The proposed method appears to be simpler and more straightforward than the Bishop method and the finite element method.

In Chapter 4, an artificial neural network model is introduced, as an alternate approach, for modeling slope stability. The proposed neural network model is a two-layer recurrent neural network (RNN) with a sigmoid hidden layer and a linear output layer. The model is developed by using data from 124 slopes collected for this study, including a limited number of slopes for which field data are available. The input variables include the parameters that contribute to the failure of a slope and include the height of slope, the inclination of slope, the height of water level, the height of tension cracks at crest of slope, the depth of firm base, horizontal and vertical seismic coefficients, the unit weight of soil, the cohesion of soil, the friction angle of soil, the thickness of each layer, and the pore pressure ratio which is defined as the ratio of the pore pressure to the overburden pressure for a given layer. The output layer is a single neuron – the factor of safety of slope. Training is performed using data from 104 slopes selected from the 124 slopes. Prediction or evaluation of the proposed model is based on the remaining 20 slopes.

Statistical analyses performed show that the results from the proposed RNN model are closer to the finite element method than to the Bishop method and the proposed semi-analytical method. A separate RNN model is developed to determine circular slip surfaces by retraining the proposed neural network model with three neurons in the output layer, namely the coordinates of the center and the radius of

the circular slip surface. In comparison with the proposed semi-analytical method, the proposed RNN model is found to be more effective in representing relatively complex slopes with layered soils and/or pore water pressures. The proposed semi-analytical method is found to be as good as or better than traditional slope stability analysis methods.

5.2 Conclusions

Base on the results presented in the preceding chapters, the following conclusions can be made:

1. The proposed semi-analytical method provides an accurate treatment of the inter-slice forces in an integral form. The closed-form analytical solutions presented allow the application of Powell's optimization technique to determine the most critical slip surface and the minimum factor of safety for a given slope. In comparison with the Bishop method and the finite element method, the proposed semi-analytical approach is accurate, more straightforward, simpler and less time-consuming.
2. For the 23 slopes analyzed without seismic effects, the factors of safety obtained from the proposed semi-analytical method are closer to the values obtained from the FEM models (with a difference of 5% on an average and a standard deviation of 4%) than those by the Bishop method (with an average difference of 6% and a standard deviation of 3%). About 65% results from the proposed method are between those obtained from the FEM model and

the Bishop method. The Bishop method yields the lower bound (i.e., smaller stability values) among the three methods.

3. Among the 14 cases analyzed with seismic effects, the factors of safety obtained by the proposed semi-analytical method are found to be closer to that by the FEM (with a difference of 5% on an average and a standard deviation of 2%) than the results obtained from the Bishop method (with an average difference of 9% and a standard deviation of 8%).
4. The GFA2D, a general-purpose FEM, needed about 20 times the effort, on an average, as compared with the proposed semi-analytical method. The Slope2000, a computer code to simplify the analysis process of a slope by the Bishop method, still needed about 5 times the effort, on an average, than the proposed semi-analytical method.
5. The study shows that the solutions from the Bishop method are accurate for most cases.
6. The proposed two-layer RNN model with a sigmoid hidden layer (45 neurons) and a linear output layer is demonstrated to be a powerful tool for analysis of layered slopes including pore pressure effects.
7. The database developed in this study, having data for 124 slopes including some field data, is found to be adequate for training the proposed RNN model. Additional field data would enrich the database further.
8. The factors of safety obtained by the proposed RNN model are in general agreement with the results from the FEM analyses, the Bishop method, and

the semi-analytical method. The difference between the proposed RNN model and the FEM averages 8%. The difference between the proposed RNN model and the Bishop method is about 10%.

9. This study illustrates that the proposed semi-analytical method and RNN model are useful alternatives for slope stability analyses. Other techniques such as finite element method can be used for a more detailed analysis when needed.
10. Artificial neural network is still very much a developing field. It is, therefore, necessary for the potential users of this new tool (i.e. neural network technique) to be well aware of the assumptions underlying the technique as well as of its limitations. One must, therefore, be wary of attaching overwhelming importance to the absolute values of calculated factors of safety. It is the comparison of calculated factors of safety using different alternatives that is really important. These thoughts should be kept well in mind when adopting any analyses of slope stability.

5.3 Recommendations

Based on the observations from this study, the following recommendations are made for future studies:

1) In view of the limitations of the proposed semi-analytical approach, future work should include layered soils and effect of pore water pressure in the formulation.

2) As to the neural network-based approach, further study should involve collecting more field data that can be used to enhance training and evaluation of the model. Also, future studies should account for the effect of pore water pressure in a more comprehensive manner including the time-dependent nature of pore pressure and slope failure.

3) The principal component analysis and ranking of input factors used in developing the neural network model are also considered important topics for future research.

4) Laboratory and field studies can be pursued to generate data that can be used for further development and validation of semi-analytical and neural network models.

REFERENCES

A-Grivas D. and Asaoka A. (1982), Slope safety prediction under static and seismic loads. ASCE, Journal of the Geotechnical Engineering Division, V108, GT5, Hay, pp. 713-729.

Abramson L. W. (1996), Slope Stability and Stabilization Methods. Wiley, New York.

Amari S. I. (1972), Learning Patterns and Pattern Sequences by Self-Organizing Nets of Threshold Elements. IEEE Trans. Computers C-21: 1197-1206.

Amari S. I. (1977), Neural Theory of Association and Concept Formation. Biol. Cybern. 26: 175-185.

Amari S. I. (1990), Mathematical Foundations of Neurocomputing. IEEE Proc. 78(9):1443-1463.

Anderson J. A., Silverstein J. W., Rite S. A. and Jones R. S. (1977), Distinctive Features, Categorical Perception, and Probability Learning: Some Applications of a Neural Model. Psych. Rev. 84: 413-451.

Anderson M. G. and Richards K. S. (1987), Slope Stability: geotechnical engineering and geomorphology. Wiley, New York.

Arai K. and Tagyo K. (1985), Determination of noncircular slip surface giving the minimum factor of safety in slope stability analysis. Soils and Foundations, V25, 1, pp. 43-51.

Arbib M. A. (1987), Brains, Machines, and Mathematics. 2nd ed. New York: Springer Verlag.

Atkinson J. H. (1993), An introduction to the mechanics of soils and foundations: through critical state soil mechanics. MdGraw-Hill International (UK) Limited.

Ayalew L. and Vernier A. (1999), Slope Stability Engineering, Yagi, Yamagami & Jiang, Balkema, Rotterdam, pp. 1181-1186.

Babu G. L. S. and Bijoy A. C. (1999), Appraisal of Bishop's method of slope stability analysis. Slope Stability Engineering, Yagi, Yamagami & Jiang, Balkema, Rotterdam, pp. 249-252.

Baker R. (1980), Determination of the critical slip surface in slope stability computations. International Journal for Numerical and Analytical Methods in Geomechanics, V4, pp. 333-359.

Baker R. and Frydman S. (1983), Upper bound limit analysis of soil with non-linear failure criterion. Soils and found., Tokyo, 23(4), 34-42.

Baker R. and Garber M. (1978), Theoretical analysis of the stability of slopes. Geotechnique, V28, 4, pp. 395-411.

Baker R. and Tanaka Y. (1999), A convenient alternative representation of Taylor's stability chart. Slope Stability Engineering, Yagi, Yamagami & Jiang, Balkema, Rotterdam, pp. 253-257.

Bernander S. and Gustass H. (1984), Consideration of in situ stresses in clay slopes with special reference to progressive failure analysis. International Symposium on Landslides, pp. 235-240.

Bernasconi J. (1988), Analysis and Comparison of Different Learning Algorithms for Pattern Association Problems. Neural Information Processing Systems, ed. D. Anderson. New York: American Institute of Physics.

Bishop A. V. (1955), The use of the slip circle in the stability analysis of slopes. Geotechnique, V5, 1, pp. 7-17.

Bishop A. V. (1971), The influence of progressive failure on the choice of the method of stability analysis. Geotechnique, V21, pp. 168-172.

Bishop A. V. and Morgenstern N. (1960), Stability coefficients for earth slopes. Geotechnique, V10, 4, pp. 129-150.

Bjerrum L. (1967), Progressive failure in slopes of overconsolidated plastic clay and clay shales. ASCE, Journal of the Soil Mechanics and Foundations Division, V93, SM5, pp. 3-49.

Booker J. R. and Davis E. H. (1972), A note on a plasticity solution to the stability of slopes in homogeneous clays. Geotechnique, V22, pp. 509-513.

Booker J. R. and Small J. C. (1981), Finite element analysis of problems with infinitely distant boundaries. International Journal for Numerical and Analytical Methods in Geomechanics, V5, pp. 345-368.

Boutrup E. and Lovell C. V. (1980), Searching techniques in slope stability analysis. Engineering Geology, V16, pp. 51-61.

Bromhead E. N. (1986), The stability of slopes. Surrey University Press (USA: Chapman and Hall),

Brunsden D. and Prior D. B. (1984), Slope Instability. John Wiley & Sons, New York.

Byrne R. J., Kendall J. and Brown S. (1992), Cause and mechanism of failure Kettleman Hills Landfill B-19, Phase IA. Stability and Performance of Slopes and Embankments II: Proceeding of a Specialty Conference Sponsored by ASCE, Geotechnical Special Publication No. 31, ASCE, Volume 2, pp. 1188-1215.

Cai F. and Ugai K. (1999a), Effects of horizontal drains on ground water level and slope stability. Slope Stability Engineering, Yagi, Yamagami & Jiang, Balkema, Rotterdam, pp. 551-556.

Cai F. and Ugai K. (1999b), Stability of slope reinforced with piles. Slope Stability Engineering, Yagi, Yamagami & Jiang, Balkema, Rotterdam, pp. 883-888.

Cao J. and Zaman M. M. (1999), Analytical method for analysis of slope stability. Int. J. Numer. Anal. Meth. Geomech., 23, 439-449.

Carpenter G. A. (1989), Neural Network Models for Pattern Recognition and Associative Memory. Neural Networks 2: 243-257.

Cavounidis S. (1987), The ratio of factors of safety in slope stability analyses. Geotechnique, V37, 2, pp. 207-210.

Celestino T. B. and Duncan J. M. (1981), Simplified search for non-circular slip surfaces. Proc. of the 10th International Conference on Soil Mechanics and Foundation Engineering, Stockholm, pp. 391-394.

Charles J. A. (1982), An appraisal of the influence of a curved failure envelope on slope stability. Geotechnique, V32, 4, pp. 389-392.

Charles J. A. and Soares M. M. (1984), The stability of slopes in soils with nonlinear failure envelopes. Canadian Geotechnical Journal, V21, pp. 397-406.

Chen R. H. and Chameau J. L. (1982), Three dimensional slope stability analysis. Proc. of the 4th International Conference on Numerical Methods in Geomechanics, Edmonton, pp. 671-677.

Chen W. F., and Liu X. L. (1990), Limit Analysis in Soil Mechanics. Elsevier Science Publishers B.V., New York.

Chen W. F. and Snitbahn N. (1976), Plasticity solutions for slopes. Proc. of the 2nd International Conference on Numerical Methods in Geomechanics, Blacksburg, VII, pp. 731-743.

Chen Z. and Morgenstern N. R. (1983), Extensions to the generalized method of slices for stability analysis. Can. Geotech. J., 20(1), 104-119.

Chen Z. and Shao C. (1988), Evaluation of minimum factor of safety in slope stability analysis. Can. Geotech. J., 20(1), 104-119.

Chen Z. Y. (1999), The limit analysis for slopes: Theory, methods and applications. Slope Stability Engineering, Yagi, Yamagami & Jiang, Balkema, Rotterdam, pp. 15-29.

Cheng Y. M. (2002), Slope 2000 version 1.6. Department of Civil and Structural Engineering Hong Kong Polytechnic University, Hong Kong.

Cheng Q. G., Hu H. T., Peng J. B. and Hu G. T. (2000), Visco-elastoplastic Finite Element Simulation of Progressive Failure of High-steep Slope. Journal of Engineering Geology, Vol. 8, No. 1, p. 25-30.

Ching R. K. H. and Fredlund D. G. (1983), Some difficulties associated with the limit equilibrium method of slices. Can. Geotech. J. 20(4), 661-672.

Ching R. K. H. and Fredlund D. G. (1984), Quantitative comparison of limit equilibrium methods of slices. International Symposium on Landslides, pp. 373-379.

Chirica A., Mlenajek R., Olteanu A. and Banciu C. (1998), Slope stability analysis in an open mining area. Geotchnical Hazards, Proc. of the 11th Danube-European Conference on Soil Mechanics and Geotechnical Engineering, Croatia.

Chowdhury R. N. (1985), Progressive reliability of a strain-softening slope. Transactions (Civil Engineering), Institution of Engineers, Australia, Vol. CE27, No. 1, 79-95.

Chugh A. K. (1982), Slope stability analysis for earthquakes. International Journal for Numerical and Analytical Methods in Geomechanics, V6, pp. 307-322.

Chugh A. K. (1986), Variable factor of safety in slope stability analysis. Geotechnique, London, 36(1), 57-64.

Clough R. Y. and Chopra A. K. (1966), Earthquake stress analysis in earth dams. ASCE, Journal of the Engineering Mechanics Division, V92, EM2, pp. 197-211.

Connor J. T., Martin R. D. and Atlas L. E. (1994), Recurrent Neural Networks and Robust Time Series Prediction. IEEE Transactions on Neural Network, Vol. 5(2), pp. 240-254.

Costa F. L. M. and Thomas J. E. S. (1984), Stability analysis of slopes in soils with non-linear strength envelopes using non-circular slip surfaces. International Symposium on Landslides, pp. 393-397.

Cousins B. F. (1978), Stability charts for simple earth slopes. ASCE, Journal of the Geotechnical Engineering Division, V104, GT2, pp. 267-279.

Cundall P. (1976), Explicit finite-difference methods in geomechanics. Proc. of the 2nd International Conference on Numerical Methods in Geomechanics, Blacksburg, VI, pp. 132-150.

Daddazio R. P., Ettouray M. M. and Sandler I. S. (1987), Nonlinear dynamic slope stability analysis. ASCE, Journal of the Geotechnical Engineering Division, V113, GT4, pp. 285-298.

Dai F. C., Chen S. Y. and Li Z. F. (2000), Analysis of landslide initiative mechanism based on stress-strain behavior of soil. Chinese Journal of Geotechnical Engineering, Vol. 22, No. 1, p. 127-130.

Das B. M. (1994), Principles of Geotechnical Engineering. PWS Publishing Company, Boston.

Davis E. H. (1968), Theories of plasticity and the failure of soil masses. Soil Mechanics Selected Topics (Ed. I.K. Lee), Butterworths, London, pp. 341-380.

Dayhoff J. (1990), Neural Network Architectures-An Introduction. New York: Van Nostrand Reinhold.

Demuth H. and Beale M. (1995), Neural Network Toolbox for Use with MATLAB. The Math Works Inc., Natick, Mass.

Demuth H. and Beale M. (2000), Neural Network Toolbox for Use with MATLAB. The Math Works Inc., Natick, Mass.

Desai C. S, and Watagala G. W. (1993), Constitutive model for cyclic behavior of clays. J. of Geotech. Eng. Div., ASCE, Vol. 119, No. 4, pp. 714-729.

Desai C. S, and Siriwardare H. J. (1994), Constitutive laws for engineering materials with emphasis on Geologic Materials. Prentice Hall, Englewood Cliffs, New Jersey.

Donald I. B. and Giam S. K. (1988), Application of the nodal displacement method to slope stability analysis. Proc. 5th Australia-New Zealand Conf. On Geomech., Sydney, Australia, 456-460.

Drucker D. C. and Prager W. (1952), Soil mechanics and plastic analysis or limit design. Q. Appl. Math., 10(2), 157-165.

Dreyfus S. E. (1990), Artificial Neural Networks. Back Propagation and the Kelly-Bryson Gradient Procedure. J. Guidance, Control Dynamics. 13(5): 926-928.

Duncan J. M. (1996), State of the art: limit equilibrium and finite-element analysis of slopes. J. Geotech. Engrg., ASCE, 122(7), 577-596.

Duncan J. M. and Dunlop P. (1969), Slopes in stiff-fissured clay and shales. J. Soil Mech. And Found. Div., ASCE, 95(2), 467-492.

Duncan J. M. and Stark T. D. (1992), Soil strengths from back analysis of slope failures. Stability and Performance of Slopes and Embankments II: Proceeding of a Specialty Conference Sponsored by ASCE, Geotechnical Special Publication No. 31, ASCE, Volume 2, pp. 890-904.

Duncan J. M. and Wright S. G., (1980), The accuracy of equilibrium methods of slope stability analysis. Engrg. Geol., 16(1), 5-17.

Dunlop P. and Duncan J. M. (1970), Development of failure around naturally excavated slopes. ASCE, Journal of the Soil Mechanics and Foundations Division, V96, SM2, pp. 471-493.

Fan K., Fredlund D. G. and Wilson G. Y. (1986), An interslice force function for limit equilibrium slope stability analysis. Canadian Geotechnical Journal, V23, pp. 287-296.

Faustt L. (1994), Fundamentals of Neural Networks: Architectures, Algorithms and Applications. Prentice Hall, Englewood Cliffs, New Jersey.

Feld J. (1965), The factor of safety in soil and rock mechanics. Proc. of the 6th International Conference on Soil Mechanics and Foundation Engineering, pp. 185-197.

Felio G. Y., Lytton R. L. and Briaud J-L. (1984), Statistical approach to Bishop's method of slices. International Symposium on Landslides, pp. 411-415.

Fellenius Y. (1927), Erdstatische berechnungen mit reibung und kohaesion. Ernst, Berlin.

Fredlund D. G. (1984), Analytical methods for slope analysis. International Symposium on Landslides, pp. 229-250.

Fredlund D. G. and Krahn J. (1977), Comparison of slope stability methods of analysis. Canadian Geotechnical Journal, V14, 3, pp. 429-439.

Fredlund D. G., Krahn J. and Pufahl D. E. (1981), The relationship between limit equilibrium slope stability methods. Proc. 10th Int. Conf. on Soil Mech. and Found. Engrg., A. A. Balkema, Rotterdam, The Netherlands, 3, 409-416.

Fredlund D. G. and Scoular R. E. G. (1999), Using limit equilibrium concepts in finite element slope stability analysis. Slope Stability Engineering, Yagi, Yamagami & Jiang, Balkema, Rotterdam, pp. 31-47.

Giam S. K. and Donald I. B. (1988), Determination of critical slip surfaces for slopes via stress-strain calculations. Proc. 5th Australia-New Zealand Conf. On Geomech., Sydney, Australia, 461-464.

Gottardi G., Marchi G. and Righi P. V. (1998), Learning from a large landslide in Northern Italy. Slope Stability Engineering, Yagi, Yamagami & Jiang, Balkema, Rotterdam, pp. 811-818.

Graham J. (1984), Methods of stability analysis in "Slope instability" (ed Brunsden D. and Prior D.B.), Wiley, pp. 171-215.

Hadj-Hamou T. and Kavasanjian E. (1985), Seismic stability of gentle infinite slopes. ASCE, Journal of the Geotechnical Engineering Division, VIII, GT6, pp. 681-697.

Hansbo S. (1994), Foundation Engineering. Elsevier, Amsterdam.

Hansbo P., Liberg N. E. and Runesson K. (1985), Stability and progressive failure of natural slopes. Proc. of the 5th International Conference on Numerical Methods in Geomechanics, Nagoya, pp. 973-979.

Hardin B. O. and Hardin K. O. (1984), A new statically consistent formulation for slope stability analysis. International Symposium on Landslides, pp. 429-434.

Haug M. D., Sauer E. K. and Fredlund D. G. (1976), Retrogressive slope failure near Saskatoon. Proc. of the 29th Canadian Geotechnical Conference, Vancouver, BC.

He S. Z. (1996), Analyzing two dimensional slope stability and foundation problems considering soil-structure interaction effects. ASCE Congress for Computing in Civil Engineering, June 20, 1996, Anaheim, California

Hertz J. A. and Palmer R. G. (1991), Introduction to the Theory of Neural Computation. Redwood City, Calif.: Addison-Wesley Publishing Co.

Hopfield J. J. (1982), Neural Networks and Physical Systems with Emergent Collective Computational Abilities. Proc. Natl. Acad. Sci. 79: 2554-58.

Hopfield J. J. (1984), Neurons with Graded Response Have Collective Computational Properties Like Those of Two State Neurons. Proc. Natl. Acad. Sci. 81: 3088-3092.

Hovland H. J. (1977), Three-dimensional slope stability analysis method. ASCE, Journal of the Geotechnical Engineering Division, V103, GT9, pp. 971-987.

Huang Y. H. (1983), Stability analysis of earth slope. Van Nostrand Reinhold, Inc., New York.

Huang S. L. and Yamasaki K. (1993), Slope Failure Analysis Using Local Minimum Factor-of-Safety Approach. J. Geotech. Engrg., ASCE, 119(12), 1974-1987.

Huang S. L., Speck, R. C. and Yamasaki K. (1989), Direct determination of failure

surface in earth slopes. Proc. 30th U.S. Symp. On Rock Mech., International Society for Rock Mechanics/U.S. National Committee for Rock Mechanics, 817-824.

Huang S. L., Speck, R. C. and Xu M. (1992), Evaluation of coal mine spoil pile instability in the interior Alaska. Bull. Assoc. Engrg. Geologists, 29(1), 1-9.

Hungr O. (1987), An extension of Bishop's simplified method of slope stability analysis to three dimensions. Geotechnique, V37, 1, pp. 113-117.

Hunt R. E. (1986), Geotechnical engineering analysis and evaluation. McGraw-Hill Book Co.

Hunter J. H. and Schuster R. L. (1968), Stability of simple cuttings in normally consolidated clays. Geotechnique, V18, pp. 327-378.

Ishihara K. (1985), Stability of natural deposits during earthquakes. Proc. of the 11th International Conference on Soil Mechanics and Foundation Engineering, San Francisco, V1, pp. 321-376.

Janbu N. (1968), Slope stability computations. Soil Mech. and Found. Engrg. Rep., The Technical University of Norway, Trondheim, Norway.

Janbu N. (1973), Slope stability computations in "Embankment dam engineering." Casagrande Volume (ed Hirschfeld R. C. and Poulos S. J.), Wiley, pp. 47-86.

Jiang J. C., Yamagami T. and Ueta Y. (1999), Back analysis of unsaturated shear strength from a circular slope failure. Slope Stability Engineering, Yagi, Yamagami & Jiang, Balkema, Rotterdam, pp. 305-310.

Jiao Y. Y., Ge X. R., Liu Q. S. and Feng S. R. (2000), Three-dimensional discrete element method and its application in landslide analysis. Chinese Journal of Geotechnical Engineering, Vol. 22, No. 1, p. 101-104.

Jurak V., Matkovic I., Miklin Z. and Cvijanovic D. (1998), Landslide hazard in the Medvednica sub-mountain area under dynamic conditions. Geotechnical Hazards, Proc. of the 11th Danube-European Conference on Soil Mechanics and Geotechnical Engineering, Croatia.

Koda E. (1999), Stability reinforcement of the old embankment sanitary landfills for remediation works. Slope Stability Engineering, Yagi, Yamagami & Jiang, Balkema, Rotterdam, pp. 305-310.

Kohgo Y. and Yamashita T. (1988), Finite element analysis of fill type dams - stability during construction by using the effective stress concept. Proc. Conf. Numer. Meth. in Geomech., ASCE, 98(7), 653-665.

Kohonen T. (1977), Associative Memory: A System-Theoretical Approach, Berlin: Springer-Verlag.

Kohonen T. (1982), A Simple Paradigm for the Self-Organized Formation of Structured Feature Maps. Competition and Cooperation in Neural Nets. ed. S. Amari, M. Arbib. vol. 45. Berlin: Springer-Verlag.

Kohonen T. (1984), Self-Organization and Associative Memory. Berlin: Springer-Verlag.

Kohonen T. (1988), The Neural' Phonetic Typewriter. IEEE Computer27(3): 11-22.

Koppula S. D. (1984a), Stability of slopes in clays with linearly increasing strength. Canadian Geotechnical Journal, V21, pp. 577-581.

Koppula S. D. (1984b), Simplified approach for computing stability of slopes. International Symposium on Landslides, pp. 445-450.

Lambe T. W. and Whitman R. V. (1979), Soil Mechanics. SI Edition. John Wiley and Sons, New York.

Lambe T. W. and Silva T. F. (1992), Stability analysis of an earth slope. Stability and Performance of Slopes and Embankments II: Proceeding of a Specialty Conference Sponsored by ASCE, Geotechnical Special Publication No. 31, ASCE, Volume 2, pp. 27-67.

Larsson R., Ottosson E. and Sallfors G. (1998), Major landslide triggered by local instability. Geotechnical Hazards, Proc. of the 11th Danube-European Conference on Soil Mechanics and Geotechnical Engineering, Croatia.

Law K. T. and Lumb P. (1978), A limit equilibrium analysis of progressive failure in the stability of slopes. Canadian Geotechnical Journal, V15, pp. 113-122.

Lee I. K. (1968), Soil Mechanics Selected Topics. American Elsevier Publishing Company, Inc., New York.

Lee I. K., White W. and Ingles O. G. (1983), Geotechnical Engineering. Pitman Publishing Inc., Marshfield, Massachusetts.

Lefevre G., Duncan J. M. and Wilson E. L. (1973), Three-dimensional finite element analysis of dams. J. Soil Mech. and Found., ASCE, 99(7), 495-507.

Leshchinsky D., Baker R. and Silver M. L. (1985), Three dimensional analysis of slope stability. International Journal for Numerical and Analytical Methods in Geomechanics, V9, pp. 199-223.

Leshchinsky D. and Huang C. (1992), Generalized three dimensional slope stability analysis. J. Geotch. Engrg., ASCE, 118(11), 1748-1764.

Li K. S. and White W. (1986), Rapid evaluation of the critical slip surface in slope stability problems. Research Studies from the Department of Civil Engineering, University College, Australian Defense Force Academy, UNSW, Report No.9.

Li K. S. and White W. (1987), A unified solution scheme for the generalized procedure of slices in slope stability problems. Research Studies from the Department of Civil Engineering, University College, Australian Defense Force Academy, UNSW, Report No.18.

Liu C. Y. (1990), Soil Mechanics, China Railway Press, Beijing, China.

Liu D. G., Fei J. G., Yu Y. J. and Li G. Y. (1988), FORTRAN Programming, National Defense Industry Press, Beijing, China.

Lovell C.W. (1984), Three-dimensional analysis of landslides. International Symposium on Landslides, pp. 451-455.

Lowe J. (1967), Stability analysis of embankments. J. Soil Mech. and Found. Div., ASCE, 93(4), 1-33.

Luk S. T. (1999), Predicting pore water pressures in slopes using artificial neural networks. Slope Stability Engineering, Yagi, Yamagami & Jiang, Balkema, Rotterdam, pp. 87-92.

Lumsdaine R. W. and Tang K. Y. (1982), A comparison of slope stability calculations. Proc. of the 7th South East Asian Geotechnical Conference, Hong Kong, pp. 31-38.

Madej J. S. (1984), The accurate solution of the limit equilibrium slope stability analysis. International Symposium on Landslides, pp. 457-462.

Maksimovic M. (1979), Limit equilibrium for nonlinear failure envelope and arbitrary slip surface. Proc. of the 3rd International Conference on Numerical Methods in Geomechanics, Aachen, pp. 769-777.

McClelland T. L., Rumelhart D. E., and the PDP Research Group (1986), Parallel Distributed Processing. Cambridge: The MIT Press.

McCullock W. S. and Pitts W. H. (1943), A Logical Calculus of the Ideas Imminent in Nervous Activity. Bull. Math. Biophy. 5:115-133.

Minsky M. (1954), Neural Nets and the Brain. Doctoral Dissertation, Princeton University, NJ.

Minsky M. and Papert S. (1969), Perceptrons. Cambridge, Mass.: MIT Press.

Mitchison G. (1989), Learning Algorithms and Networks of Neurons. Computing Neuron, ed. R. Durbin, C. Miall, G. Mitchison. Reading, Mass.: Addison-Wesley Publishing Co.

Mochizuki A., Xiong J. and Mikasa M. (1999), Influence of stress-strain curves on safety factors and inter-slice forces in FEM. Slope Stability Engineering, Yagi, Yamagami & Jiang, Balkema, Rotterdam, pp. 259-264.

Morgenstern N. (1963), Stability charts for earth slopes during rapid drawdown. Geotechnique, V13, pp. 121-131.

Morgenstern N. R. and Price V. E. (1965), The analysis of the stability of general slip surface. Geotechnique, London, 15(1), 79-93.

Morii T., Shimada K. and Hasegawa T. (1999), Stability of embankment dams based on minimum-experience of safety factor. Slope Stability Engineering, Yagi, Yamagami & Jiang, Balkema, Rotterdam, pp. 817-822.

Mostyn G. R. and Small J. C. (1987), Methods of stability analysis. Soil Slope Instability and Stabilization, Walker & Fell (eds), Balkema, Rotterdam.

National Research Council (1985), Liquefaction of soils during earthquakes. Committee on Earthquake Engineering, Commission on Engineering and Technical Systems, National Research Council, National Academic Press, Washington, D.C.

Newmark N. M. (1965), Effects of earthquakes on dams and embankments. Geotechnique, V15, 2, pp. 139-160.

O'Conner M. J. and Mitchell R. J. (1977), An extension of the Bishop and Morgenstern stability charts. Canadian Geotechnical Journal, V14, pp. 144-151.

Oboni F. and Bourdeau P. L. (1983), Determination of the critical slip surface in stability problems. Proc. of the 4th International Conference on the Application of Statistics and Probability to Soil and Structural Engineering, Florence, pp. 1413-1424.

Parlos A. G., Chong K. T. and Atiya A. F. (1994), Application of the Recurrent Multilayer Perceptron in Modeling Complex Process Dynamics. IEEE Transactions on Neural Network, Vol. 5, No. 2, pp. 255-285.

Pentz D. L. (1982), Slope stability analysis techniques incorporating uncertainty in critical parameters. Proc. of the 3rd International Conference on Stability in Surface Mining, pp. 197-228.

Petterson K. E. (1956), The early history of circular sliding surfaces. Geotechnique, 5, 275-296

Poggio T. and F. Girosi. (1990), Networks for Approximation and Learning. Proc. IEEE 78(9): 1481-1497.

Press W. H., Flannery B. P., Teukolsky S. A. and Vetterling W. T. (1995), Numerical Recipes: The Art of Scientific Computing. Cambridge University Press, Cambridge.

Rosenblatt F. (1958), The Perceptron: A Probabilistic Model for Information Storage and Organization in the Brain. Psych. Rev. 65: 386-408.

Rumelhart D. E. (1990), Brain Style Computation: Learning and Generalization. Introduction to Neural and Electronic Networks. New York: Academic Press.

Rumelhart D. E., Hinton G. E. and Williams R. J. (1986), Learning internal representations by error propagation. Parallel Data Processing, MIT Press, Cambridge, pp. 318-362.

Sanglerat G., Olivari G. and Cambou B. (1985), Practical Problems in Soil Mechanics and Foundation engineering, 2. Elsevier, Amsterdam.

Sarma S. K. (1973), Stability analysis of embankments and slopes. Geotechnique, V23, 4, pp. 423-433.

Sarma S. K. (1979), Stability analysis of embankments and slopes. J. Geotch. Engrg., ASCE, 105(12), 1511-1524.

Schuster R. L. (1978), Introduciton in Landslide, Analysis and Control. Transportation Research Board Special Report 176, National Academy of Sciences, Washington, DC, 1-10.

Seed H. B. (1966), A method for the earthquake resistant design of earth dams. ASCE, Journal of the Soil Mechanics and Foundations Division, V92, SM1, pp. 13-41.

Seed H. B. (1968), Landslides during earthquakes due to soil liquefaction. ASCE, Journal of the Soil Mechanics and Foundations Division, V94, SM5, pp. 1055-1122.

Seed H. B. (1979), Considerations in the earthquake-resistant design of earth and rockfill dams. Geotechnique, V29, 3, pp. 215-263.

Seed H. B. (1980), Earthquake-resistant design of earth dams. Symposium on problems and practice of dam engineering, Bangkok, A.A. Balkema.

Seed H. B. and De Alba P. (1986), Use of SPT and CPT tests for evaluating the liquefaction resistance of sands. Use of In Situ Tests in Geotechnical Engineering, Specialty Conference, ASCE, pp. 281-302.

Seed H. B., Tokimatsu K., Harder L. F. and Chung R. M. (1985), Influence of SPT procedures in soil liquefaction resistance evaluations. ASCE, Journal of the Geotechnical Engineering Division, V111, GT12, pp. 1425-1445.

Sharma S. and Moudud A. (1992), Interactive slope analysis using Spencer's method. Stability and Performance of Slopes and Embankments II: Proceeding of a Specialty Conference Sponsored by ASCE, Geotechnical Special Publication No. 31, ASCE, Volume 2, pp. 506-520.

Shimada K., Fujii H., Nishimura S., Nishiyama T. and Morii T. (1999), Slope instability due to rainfall and earthquake. Slope Stability Engineering, Yagi, Yamagami & Jiang, Balkema, Rotterdam, pp. 653-656.

Shioi Y. and Sutoh S. (1999), Collapse of high embankment in the 1994 far-off Sanriku Earthquake. Slope Stability Engineering, Yagi, Yamagami & Jiang, Balkema, Rotterdam, pp. 559-564.

Skempton A. W. (1964), Long-term stability of clay slopes. Geotechnique, 14, 77-

102.

Skempton A. W. (1977), Slope Stability of Cuttings in Brown London Clay. Proc. 9th Int. Conf. Soil Mech., Tokyo, 3, 261-270.

Skempton A. W. (1984), Selected Papers on Soil Mechanics. Thomas Telford Limited, London.

Skempton A. W. and Hutchinson J. N. (1969), Stability of natural slopes and embankment foundations. Proc. 7th Int. Conf. Soil Mech. and Found. Engng., Mexico City, State of the Art Volume, pp. 291-340.

Skempton A. W. and Brown J. D. (1961), A landslide in Boulder Clay at Selset, Yorkshire, Geotechnique, 11, 280-293.

Skempton A. W., and Golder H. Q. (1948), Practical examples of the $\phi = 0$ analysis of stability of clays. Proc. 2nd Int. Conf. SMFE, Rotterdam 1948, 2, 63-70.

Skrabl S. and Macuh B. (1998), Space stability of slopes: Kinematical approach. Geotechnical Hazards, Proc. of the 11th Danube-European Conference on Soil Mechanics and Geotechnical Engineering, Croatia.

Snitbahn H. and Chen W. F. (1976), Finite element analysis of large deformation in slopes. Proc. of the 2nd International Conference on Numerical Methods in Geomechanics, Blacksburg, VII.

Snitbahn N. and Chen W. F. (1978), Elastic plastic large deformation analysis of soil slopes. Computers and Structures, V9, pp. 567-577.

Song L. Y. and Chang X. (1995), Finite element model used for determination of sliding surface. Proc. of 5th Symp. on Soil Mech. and Found. Engrg., National College and University Research Council of Soil Mech. And Fund. Engrg., pp. 102-115.

Spencer E. (1967), A method of analysis of the stability of embankments assuming parallel interslice forces. Geotechnique., London, 17(1), 11-26.

Spencer E. (1968), Effect of tension on the stability of embankments. ASCE, Journal of the Soil Mechanics and Foundations Division, V94, SM5, pp. 1159-1173.

Spencer E. (1973), Thrust line criterion in embankment stability analysis. Geotechnique, V23, 1, pp. 85-100.

Talesnick M. and Baker R. (1984), Comparison of observed and calculated slip surface in slope stability calculations. Canadian Geotechnical Journal, V21, pp. 713-719.

Tavenas F., Trak B., and Leroueil S. (1980), "Remarks on the validity of stability analyses." Can. Geotech. J., 17(1), 61-73.

Taylor D. W. (1937), Stability of earth slopes. Journal of the Boston Society of Civil Engineers, V24, pp. 197.

Taylor D. W. (1948), Fundamentals of Soil Mechanics. John Wiley, New York.

Terado Y., Hazarika H., Yamazaki T. and Hayamizu H. (1999), Slope stability analysis considering the deformation of slices. Slope Stability Engineering, Yagi, Yamagami & Jiang, Balkema, Rotterdam, pp. 265-269.

Terzaghi K. (1950). Mechanisms of landslides. In Application of Geology to Engineering Practice, Berkley Volume, The Geological Society of America, pp. 83-123.

Ting J. M. (1983), Geometric concerns in slope stability analyses. ASCE, Journal of the Geotechnical Engineering Division, V109, GT11, pp. 1487-1491.

Tsuji K., Suzuki K. and Hanzawa H. (1999), Evaluation of the shear strength for stability analysis of a heavily weathered tertiary rock. Slope Stability Engineering, Yagi, Yamagami & Jiang, Balkema, Rotterdam, pp. 787-791.

Vogl T. P., Mangis J. K., Rigler A. K., Zink W. T. and Alkon D. L. (1988), Accelerating the convergence of the back propagation method. Biological Cybern., Vol. 59, pp. 257-263.

Von Neumann J. (1958), The Computer and the Brain. New Haven, Conn.: Yale University Press, 87.

Wakai A. and Ugai K. (1999), Dynamic analyses of slopes based on a simple strain-softening model of soil. Slope Stability Engineering, Yagi, Yamagami & Jiang, Balkema, Rotterdam, pp. 647-652.

Walker B. and Fell R. (1987), Soil Slope Instability and Stabilization, Rotterdam, Sydney.

Whitman R. V. and Bailey W. A. (1967), Use of computers for slope stability analysis. ASCE, Journal of the Soil Mechanics and Foundations Division, V93, SM4, July, pp. 475-498.

Widrow B. and Hoff M.E. Jr. (1960), Adaptive Switching Circuits. 1960 IRE Western Electric Show and Convention Record, part 4 (Aug. 23): 96-104.

Widrow B. (1962), Generalization and Information Storage in Networks of Adaline Neurons. Self-Organizing Systems 1962, ed. M. C. Jovitz, G. T. Jacobi, G. Goldstein. Washington, D. C.: Spartan Books, 435-461.

Wright S. G., Kulhawy F. G. and Duncan J. M. (1973), "Accuracy of equilibrium slope stability analysis." J. Soil Mech. and Found. Div., ASCE, 99(10), 783-791.

Yamagami T. and Ueta Y. (1986), Back analysis of average strength parameters for critical slip surfaces. Proc. of a Symposium on Computer Aided Design in Geotechnical Engineering, AIT, pp. 263-283.

Yamagami T., Jiang J. C. and Khan Y. A. (1999), Progressive failure analysis based on a method of non-vertical slices. Slope Stability Engineering, Yagi, Yamagami & Jiang, Balkema, Rotterdam, pp. 299-304.

Yamagami T., Yamabe S., Jiang J. C. and Khan Y. A. (1999), A promising approach for progressive failure analysis of reinforced slopes. Slope Stability Engineering, Yagi, Yamagami & Jiang, Balkema, Rotterdam, pp. 1043-1048.

Yang J. X, Zhang Y. F and Zhou S. H. (1994), Estimation on Initial Sliding of a Cut Slope near a Reservoir. Proc., 4th Symp. on Soil Mech. And Found. Engrg., National College and University Research Council of Soil Mech. And Fund. Engrg., pp. 169-182.

Young D. S. and Pumjan S. (1999), A localized probabilistic approach for slope stability analysis. Slope Stability Engineering, Yagi, Yamagami & Jiang, Balkema, Rotterdam, pp. 1085-1088.

Zaman M., Booker, J. R. and Gioda, G. (2000), Modeling in Geomechanics, John Wiley and Sons, U.K.

Zhang X. J. and Chen V. F. (1987), Stability analysis of slopes with general nonlinear failure criterion. International Journal for Numerical and Analytical Methods in Geomechanics, VII, pp. 33-50.

Zhang Y. J. (2001), A summary on the present advances of landslide studies. Journal of China Carsologica Sinica, Vol. 18, No. 3.

Zhou S. H. (1993), Method for determining the most risk slip-surface of slope and its application to stability analysis. Journal of the China Railway Society, 15(2); pp. 27-39.

Zienkiewicz O. C., Humpheson C. and Lewis R. V. (1975), Associated and non-associated viscoplasticity and plasticity in soil mechanics. Geotechnique, V25, 4, pp.671-689.

Zurada J. M. (1992), Introduction to Artificial Neural Systems. West Publishing Company, St. Paul, MN.

APPENDIX Slope Data for Developing the Proposed RNN Model

Slope	H	H_w	H_d	H_t	β	Layer	h_i	γ	c	φ	k_h	k_v	FEM				Bishop	Reference
(#)	(m)				(deg)	(#)	(m)	(kN/m³)	(kPa)	(deg)			(F_s)	(dim.)	(node)	(model)	(1962)	
1	10.00		10.00		33.69	1	10.00	20.00	10.00	20.00	0	0	1.14	2-D	4	M-C	1.32	Cai & Ugai, 1999b
2	15.20				71.60	1		18.00	20.00	20.00	0	0	1.00	2-D	4	M-C	0.94	Hunter & Schuster, 1968
3	50.00				21.80	1		11.00	15.00	21.00	0	0	1.13	2-D	4	M-C	0.97	Law & Lumb, 1978
4	10.00	9.00	0.00		26.57	1	10.00	19.61	31.70	13.00	0	0	1.44	3-D	8	M-C	1.61	Morii et al., 1999
5	10.50				26.57	1		20.27	31.70	13.00	0	0	1.82	2-D	4	D-P	1.64	Lovell, 1984
6	5.00		30.00		20.00	1		20.00	40.00	30.00	0	0	1.56	2-D	4	D-P	1.35	Atkinson, 1993
7	8.05		6.00		26.57	1		18.50	15.00	10.00	0	0	1.19	2-D	4	D-P	1.27	Huang & Yamasaki, 1993
8	23.75	6.30			29.20	1		17.65	0.00	37.00	0	0	0.92	2-D	4	D-P	1.06	Hansbo, 1994
						2		17.16	0.00	35.00								
9	10.00	9.00	2.00		30.00	1	10.00	18.00	25.00	10.00	0	0	1.54	2-D	4	M-C	1.55	Sangler at et al., 1985
10	6.00	6.00	0.00		33.69	1		19.80	4.00	32.00	0	0					1.40	Lee, 1968
11	44.20	12.00	0.00		19.98	1		22.76	16.76	37.50	0	0					1.18	Lee, 1968
12	20.00				33.69	1		19.65	4.31	32.00	0	0	1.00	2-D	4	M-C	1.31	Talesnick & Baker, 1984
13	6.20				16.72	1		18.80	0.00	20.00	0	0					0.75	Skempton, 1977
14	7.20				19.98	1		18.80	1.00	20.00	0	0					0.80	Skempton, 1977
15	7.00				18.43	1		18.80	1.00	20.00	0	0					0.77	Skempton, 1977
16	7.80		3.20		44.50	1	7.80	18.60	10.20	20.00	0	0	1.00	2-D	4	D-P	1.05	Zhou, 1993
17	12.20				17.10	1		18.80	1.50	20.00	0	0					0.98	Skempton, 1977
18	8.00				26.57	1		18.50	20.00	20.00	0	0	2.05	2-D	4	D-P	2.09	Huang & Yamasaki, 1993
19	20.00	0.00	0.00		22.00	1		20.00	0.00	20.00	0.035	0					1.00	Jurak et al., 1998
20	20.00	10.00	0.00		22.00	1		20.00	0.00	20.00	0.035	0					0.90	Jurak et al., 1998
21	11.50		10.80		27.60	1		17.71	9.09	20.35	0.2	0	1.09	3-D	8	M-C	1.10	Shioi & Sutoh, 1999
22	11.50		10.80		27.60	1		17.71	9.09	20.35	0.1	0	1.15	3-D	8	M-C	1.20	Shioi & Sutoh, 1999
23	8.00		6.00		45.00	1		18.50	15.00	20.00	0	0	1.46	2-D	4	D-P	1.29	Huang & Yamasaki, 1993
24	8.00	5.60	5.60		45.00	1	9.00	19.50	17.50	7.50	0	0	1.00	2-D	4	D-P	0.97	Zhou, 1993
						2	4.60	16.40	10.30	15.20								

APPENDIX Continued

Slope (#)	H (m)	H_w	H_b	H_t	β (deg)	Layer (#)	h_i (m)	γ (kN/m³)	c (kPa)	φ (deg)	k_h	k_v	FEM (F_s)	FEM (dim.)	FEM (node)	FEM (model)	Bishop (1952)	Reference
25	7.62	6.73	2.31	0.93	26.57	1	0.93	18.53	0.00	30.00	0	0	1.16	2-D	4	M-C	1.13	Skempton, 1984
						2	3.25	18.53	6.70	30.00								
						3	2.78	17.91	6.70	30.00								
						4	1.40	17.59	6.70	21.00								
						5	2.31	15.71	11.01	20.00								
26	32.80	26.90	164.00		18.16	1	32.80	17.00	12.00	16.30	0	0	0.94	3-D	8	M-C	0.86	Terado et al., 1999
27	20.40	20.00	0.00		22.00	1		20.00	20.00	20.00	0.035	0					1.12	Jurak et al., 1998
28	20.40	20.00	0.00		22.00	1		20.00	20.00	20.00	0.1	0					0.96	Jurak et al., 1998
29	44.20		0.00		19.98	1		22.80	16.80	37.50	0	0					1.00	Lambe & Silva, 1992
30	44.20		0.00		19.98	1		22.80	16.80	37.50	0	0					1.12	Lambe & Silva, 1992
31	4.90				18.43	1		18.80	1.20	20.00	0	0					1.10	Skempton, 1977
32	20.00		100.00		33.69	1		18.80	41.70	15.00	0	0					1.40	Arai & Tagyo, 1985
33	15.20				63.40	1		18.00	20.00	20.00	0	0	1.00	2-D	4	M-C		Hovland, 1977
34	46.00	0.00			41.01	1	46.00	9.00	25.00	20.00	0	0	1.03	2-D	4	D-P	0.99	Koda, 1999
35	45.50	0.00			41.01	1	45.50	12.00	23.00	25.00	0	0	1.08	2-D	4	M-C	1.03	Koda, 1999
36	8.00				45.00	1		18.50	20.00	15.00	0	0	1.45	2-D	4	D-P	1.32	Huang & Yamasaki, 1993
37	8.00				45.00	1		18.50	20.00	20.00	0	0	1.68	2-D	4	D-P	1.50	Huang & Yamasaki, 1993
38	30.00				20.56	1		19.61	14.71	20.00	0	0	1.75	2-D	4	M-C	1.52	Hardin & Hardin, 1984
39	32.80	26.90	164.00		18.16	1	32.80	17.00	12.00	16.30	0	0	1.08	2-D	3	M-C	1.11	Terado et al., 1999
40	17.00				33.69	1		18.80	1.00	20.00	0	0					0.97	Skempton, 1977
41	6.10		30.50		33.69	1	6.10	19.62	4.31	32.00	0	0	1.54	3-D	8	D-P	1.47	Mochizuki et al., 1999
42	10.00		5.00		26.57	1	10.00	16.00	10.00	15.00	0	0					0.93	Wakai & Ugai, 1999
43	9.10	4.00	5.00		26.60	1	3.30	16.50	8.50	10.60	0	0	1.00	2-D	4	D-P	0.99	Yang et al., 1994
						2	7.20	18.70	2.80	17.00								
						3	3.60	19.20	6.80	15.50								
44	8.00				45.00	1		18.50	25.00	10.00	0	0	1.42	2-D	4	D-P	1.35	Huang & Yamasaki, 1993
45	17.68	17.68	88.40		26.57	1	106.08	19.65	10.06	27.00	0	0	0.86	2-D	4	D-P	0.79	Larsson et al., 1998

APPENDIX Continued

Slope	H	H_w	H_d	H_t	β	Layer	h_t	γ	c	φ	k_h	k_v	FEM				Bishop	Reference
(#)	(m)				(deg)	(#)	(m)	(kN/m³)	(kPa)	(deg)			(F_s)	(dim.)	(node)	(model)	(1952)	
46	8.56				45.00	1		18.50	20.00	10.00	0	0	1.23	2-D	4	D-P	1.15	Huang & Yamasaki, 1993
47	44.00		0.00		19.98	1		22.80	16.80	37.50	0	0					1.50	Lambe & Silva, 1992
48	13.50				26.57	1		17.30	57.50	7.00	0	0	2.11	2-D	4	M-C	2.08	Liu, 1990
49	6.10		0.00		33.69	1		19.65	4.31	32.00	0	0	1.11	2-D	4	M-C	1.19	Cheng et al., 2000
50	6.00				23.96	1		18.80	1.00	20.00	0	0					0.93	Skempton, 1977
51	7.00				26.57	1		18.80	1.00	20.00	0	0					0.81	Skempton, 1977
52	10.00		0.00		26.57	1		18.93	11.97	32.00	0	0	1.22	2-D	4	M-C	1.05	Cheng et al., 2000
53	10.00		5.00		33.69	1	10.00	17.66	7.85	25.00	0	0	1.05	3-D	8	M-C	1.07	Cai & Ugai, 1999a
54	8.00				26.57	1		18.50	5.00	20.00	0	0	1.23	2-D	4	D-P	1.21	Huang & Yamasaki, 1993
55	8.00				26.57	1		18.50	15.00	20.00	0	0	1.85	2-D	4	D-P	1.82	Huang & Yamasaki, 1993
56	10.40				15.24	1		18.80	0.00	20.00	0	0					0.97	Skempton, 1977
57	5.10	3.27	25.50		25.25	1	1.55	18.84	0.00	34.00	0	0					0.62	Lee et al., 1983
						2	1.50	18.34	0.00	22.00								
						3	22.45	18.05	10.00	18.00								
58	4.00	0.00	6.00		20.00	1		17.95	5.00	15.00	0	0	0.89	3-D	8	M-C	0.78	Lee et al., 1983
59	20.00				20.00	1		19.72	30.00	30.00	0	0	1.25	3-D	8	M-C	1.54	Lee et al., 1983
60	4.50		1.30		20.00	1		15.92	2.16	17.33	0	0	0.88	3-D	8	M-C	0.93	Lee et al., 1983
61	12.19				33.69	1		19.24	22.80	35.00	0	0	1.78	2-D	4	M-C	1.62	Cheng et al., 2000
62	9.50				25.50	1	9.50	20.00	11.50	9.60	0	0	1.00	2-D	4	D-P	1.30	Yang et al.. 1994
						2	6.00	16.40	8.70	11.00								
63	8.00				26.57	1	8.00	18.50	20.00	15.00	0	0	1.72	2-D	4	D-P	1.78	Huang & Yamasaki, 1993
64	20.00				26.57	1		18.71	0.00	23.50	0.51	0.1					1.03	Chen, 1999
65	21.50				24.13	1		17.40	5.00	10.00	0	0					1.23	Chirica et al., 1998
66	44.20		0.00		20.00	1		22.00	16.80	37.50	0	0					1.25	Lambe & Silva, 1992
67	44.20		0.00		20.00	1		22.00	16.80	37.50	0	0					1.37	Lambe & Silva, 1992
68	13.70				26.57	1		18.71	0.00	14.00	0.05	0					1.28	Liu, 1990
69	8.20				45.00	1		18.50	15.00	15.00	0	0	1.24	2-D	4	D-P	1.11	Huang & Yamasaki, 1993
70	44.10		0.00		19.98	1		22.80	16.50	37.50	0	0	0.68	2-D	4	D-P		Lambe & Silva, 1992

APPENDIX Continued

Slope	H	H_w	H_t	H_l	β	Layer	h_l	γ	c	φ	k_h	k_v	FEM				Bishop	Reference
(#)	(m)				(deg)	(#)	(m)	(kN/m³)	(kPa)	(deg)			(F_s)	(dim.)	(node)	(model)	(1952)	
71	44.10		0.00		19.98	1		22.80	16.50	37.50	0	0	0.70	2-D	4	D-P		Lambe & Silva, 1992
72	12.19		7.62		27.15	1		18.87	0.00	33.00	0	0					1.20	Sharma & Moudud, 1992
73	12.19		7.62		27.15	1		18.87	67.00	0.00	0	0	2.13	2-D	4	D-P	2.15	Sharma & Moudud, 1992
74	12.19		7.62		27.15	1		18.87	28.70	20.00	0	0	1.76	2-D	4	D-P	1.35	Sharma & Moudud, 1992
75	8.45				45.00	1		18.50	10.00	15.00	0	0	1.00	2-D	4	D-P	0.89	Huang & Yamasaki, 1993
76	21.50				24.13	1		17.40	0.00	14.00	0	0					0.92	Chirica et al., 1998
77	21.50				24.13	1		17.40	0.00	17.20	0	0	1.06	2-D	4	D-P	0.64	Chirica et al., 1998
78	46.00	0.00			38.66	1	46.00	14.00	20.00	26.30	0	0	1.19	2-D	4	M-C	1.14	Koda, 1999
79	22.70				16.27	1		18.20	0.00	14.10	0	0					1.19	Chirica et al., 1998
80	22.70				16.27	1		18.20	0.00	17.20	0	0	1.00	3-D	8	M-C	0.87	Chirica et al., 1998
81	15.50				15.01	1		18.00	5.00	10.00	0	0	1.05	3-D	8	M-C		Chirica et al., 1998
82	15.50				15.01	1		18.00	0.00	14.00	0	0	1.11	3-D	8	M-C	1.17	Chirica et al., 1998
83	15.00				12.99	1	5.00	22.00	0.00	26.00	0	0	1.39	3-D	8	D-P	1.31	Skrabl & Macuh, 1998
						2	10.00	20.00	45.00	0.00								
						3	30.00	22.00	150.00	0.00								
84	15.00				12.99	1	5.00	22.00	0.00	26.00	0	0					1.05	Skrabl & Macuh, 1998
						2	10.00	20.00	21.00	17.00								
						3	30.00	22.00	150.00	0.00								
85	25.00	6.25	125.00		22.00	1	150.00	18.80	30.00	20.00	0	0					1.36	Chowdhury, 1985
86	8.00				45.00	1		18.50	25.00	15.00	0	0	1.65	2-D	4	D-P	1.53	Huang & Yamasaki, 1993
87	8.00				26.50	1		18.50	15.00	15.00	0	0	1.45	2-D	4	D-P	1.35	Huang & Yamasaki, 1993
88	10.06	30.38		2.62	21.80	1	10.06	18.44	0.96	24.50	0	0	1.06	2-D	4	D-P	1.00	Duncan & Stark, 1992
89	10.06	30.38		2.62	21.80	1	10.06	18.44	0.72	25.60	0	0	1.00	2-D	4	D-P	0.83	Duncan & Stark, 1992
90	6.00	6.00	30.00		33.69	1	36.00	19.65	1.50	30.00	0	0					0.79	Larsson et al., 1998

APPENDIX Continued

Slope	H	H_w	H_d	H_t	β	Layer	h_i	γ	c	φ	k_h	k_v	FEM				Bishop	Reference
(#)	(m)				(deg)	(#)	(m)	(kN/m³)	(kPa)	(deg)			(F_s)	(dim.)	(node)	(model)	(1962)	
91	12.80				27.76	1		21.85	8.62	32.00	0	0					1.03	Jiang et al., 1999
92	27.43				26.40	1		17.29	44.54	12.00	0	0	1.52	2-D	4	M-C	1.45	Byrne et al., 1992
93	14.33	15.14	3.05		36.53	1	6.00	20.47	68.00	0.00	0	0	1.65	2-D	4	M-C	1.64	Skempton, 1984
						2	6.10	20.47	39.26	0.00								
						3	3.04	20.47	50.75	0.00								
94	8.00				26.57	1		18.50	10.00	15.00	0	0	1.29	2-D	4	D-P	1.29	Huang & Yamasaki, 1993
95	10.00	7.00			39.81	1		20.36	0.98	32.50	0	0	1.11	2-D	4	M-C	1.01	Skempton, 1984
96	18.00				26.57	1		19.50	9.81	27.00	0	0	1.02	2-D	4	M-C	1.07	Skempton, 1984
97	12.80		6.10		28.50	1		21.55	8.62	30.00	0	0	0.92	2-D	4	M-C	1.05	Skempton, 1984
98	10.06				21.80	1		18.01	15.33	20.00	0	0					0.73	Jiang et al., 1999
99	10.06				21.80	1		18.84	0.00	20.00	0	0	1.43	2-D	4	M-C		Skempton, 1984
100	7.01				18.43	1		21.29	0.00	20.00	0	0	1.05	2-D	4	M-C		Skempton, 1984
101	7.01				18.43	1		19.79	0.96	13.00	0	0	1.03	2-D	4	M-C	1.00	Skempton, 1984
102	18.29				11.00	1		22.32	15.33	21.00	0	0	1.00	2-D	4	M-C	1.28	Skempton, 1984
103	12.10	10.00			24.38	1	12.10	16.10	25.00	20.00	0	0	1.18	3-D	8	D-P	1.00	Ayalew & Vernier, 1999
104	30.00		20.00		30.00	1	30.00	21.00	22.11	18.29	0	0	1.22	3-D	8	D-P	0.86	Young & Pumjan, 1999
105	5.00		30.00		33.69	1	5.00	19.60	2.56	27.60	0	0	1.06	3-D	8	D-P	0.98	Yamagami et al., 1999
106	67.80				29.05	1		19.00	33.00	29.50	0	0	1.01	2-D	4	M-C	1.21	Dai et al., 2000
107	67.80	45.00	0.00		29.05	1	32.80	16.00	25.00	20.00	0	0					1.31	Tsuji et al., 1999
						2	35.00	19.00	25.00	24.00								
108	14.30	13.30	0.00	0.00	27.00	1	14.30	19.60	9.60	25.00	0	0	1.00	2-D	4	D-P	0.97	Huang & Yamasaki, 1993
109	8.00				45.00	1		18.50	30.00	15.00	0	0	1.85	2-D	4	D-P	1.75	Huang & Yamasaki, 1993
110	8.00				26.57	1		18.50	25.00	15.00	0	0	1.87	2-D	4	D-P	2.05	Huang & Yamasaki, 1993
111	11.50		10.80		27.60	1		17.71	9.09	20.35	0	0	0.99	2-D	4	M-C	0.82	Shioi & Sutoh, 1999
112	5.00	1.00	3.00		26.57	1	5.00	17.64	4.90	10.00	0	0					1.00	Jiang et al., 1999

APPENDIX Continued

Slope (#)	H (m)	H_w	H_u	H_t	β (deg)	Layer (#)	h_i (m)	γ (kN/m³)	c (kPa)	φ (deg)	k_h	k_v	FEM (F_s)	FEM (dim.)	FEM (node)	FEM (model)	Bishop (1952)	Reference
113	12.80	8.09	8.09	1.56	28.00	1	2.74	21.67	7.82	32.00	0	0	1.19	2-D	4	M-C	0.98	Skempton & Brown, 1961
						2	4.88	21.67	6.70	33.00								
						3	5.18	21.60	6.46	31.50								
						4	8.09	21.05	9.10	29.00								
114	10.00				14.04	1	10.00	20.00	10.00	25.00	0	0					0.67	Baker & Tanaka, 1999
115	6.00		30.00		45.00	1	6.00	18.00	10.00	37.00	0	0	1.15	2-D	4	M-C	1.76	Babu & Bijoy, 1999
116	6.00		30.00		33.69	1	6.00	18.00	10.00	37.00	0	0	1.19	2-D	4	M-C	1.20	Babu & Bijoy, 1999
117	20.15	10.00	0.00		22.00	1		20.00	20.00	20.00	0.035	0.25					1.12	Jurak et al., 1998
118	20.15	10.00	0.00		22.00	1		20.00	20.00	20.00	0.1	0.05					0.96	Jurak et al., 1998
119	8.00		6.00		45.00	1		18.50	25.00	20.00	0	0	1.87	2-D	4	D-P	1.74	Huang & Yamasaki, 1993
120	8.30		6.00		26.57	1		18.50	10.00	20.00	0	0	1.60	2-D	4	D-P	1.54	Huang & Yamasaki, 1993
121	11.50		10.80		27.60	1		17.71	9.09	20.36	0.05	0	1.21	2-D	4	M-C	1.25	Shiei & Sutoh, 1999
122	11.50		10.80		27.60	1		17.71	9.09	20.36	0	0.1	1.16	2-D	4	M-C	1.00	Shiei & Sutoh, 1999
123	11.50		10.80		27.60	1		17.71	9.09	20.36	0	0.2	0.90	2-D	4	M-C	0.87	Shiei & Sutoh, 1999
124	10.20		5.00		45.00	1		19.60	11.80	30.00	0.2	0	1.23	3-D	8	M-C	1.00	Shimada et al., 1999

Note: D-P indicates Drucker-Prager failure critirion and M-C indicates Mohr-Coulomb failure critirion.